Microfluidics for Investigation of Electric-Induced Behaviors of Zebrafish Larvae

Arezoo Khalili

A DISSERTATION SUBMITTED TO

THE FACULTY OF GRADUATE STUDIES

IN PARTIAL FULFILLMENT OF THE REQUIREMENTS

FOR THE DEGREE OF DOCTOR OF PHILOSOPHY

GRADUATE PROGRAM IN MECHANICAL ENGINEERING

YORK UNIVERSITY

TORONTO, ONTARIO

May 2022

Abstract

Zebrafish has emerged as a model organism for studying the genetic, neuronal and behavioral bases of diseases and for drug screening. Being a vertebrate, they are phylogenetically closer to humans than invertebrates, possess complex organs and the overall organization of their brain shows structural similarities with human. They are small at larval stages, optically transparent and easy to culture. In addition, zebrafish models of human diseases and genetic mutants are widely available. These characteristics make this vertebrate model an ideal organism for neurodegeneration study and drug screening from the molecule to whole organism level. Despite these attractive features, the conventional zebrafish screening methods used for movement-based behavioral tests are mostly time-consuming, uncontrollable, qualitative, low-throughput and inaccurate. Zebrafish larvae behavioral response to various stimulations including optical and chemical stimuli, have been already investigated. However, zebrafish sensory-motor responses to electrical signals, a controllable stimulus which its potential in inducing locomotion response was proven in research done before, have not been broadly studied. Examples of research questions remaining to be answered are if zebrafish electric induced response is sensitive to different electric

current intensities, voltage drops, multiple electrical stimulation, and the electric field direction. The involvement of different pathways and genes in this response and its potential for utilization in disease studies and chemical screening, and drug discovery can also be investigated. This research aims to enhance our understanding of zebrafish electric-induced response via presenting novel microfluidic devices that address the challenges associated with monitoring the behavioral activities of zebrafish larvae in response to various electrical signals. In Objective 1 of the thesis, we designed a microfluidic device to deliver electrical stimuli to the awake and partially immobilized zebrafish larvae, screen and study their phenotypic behavioral responses and analyze the outputs. Behavioral response was characterized in terms of response duration and tail beat frequency. A multi-phenotypic microfluidic device was also developed to study the effect of electric stimulation on the heartrate. In Objective 2, attention was given to investigate the effect of electric current, voltage, and field direction on the zebrafish larvae's response to find an optimized setting which can induce a traceable response in zebrafish. Using different habituation-dishabituation strategies, we also investigated if the zebrafish larvae show adaptation towards repeated exposures to electric stimuli. In Objective 3, we developed a quadruple-fish device to enhance the behavioral throughput of our microfluidic platform and showed the technique's effectiveness for larger sample size and faster behavioral assay. In Objective 4, our quadruple-fish device was employed to investigate the involvement of dopaminergic neurons in electric-induced movement response of zebrafish larvae. Lastly, since we could monitor the electric-induced behavioral responses of zebrafish larvae, in Objective 5, the applicability of our proposed technique in chemical toxicity and gene screening assays was investigated.

This study is expected to introduce a microfluidic platform for on-demand and phenotypic behavioral screening of zebrafish larvae with applications in chemical screening and drug discovery.

Acknowledgements

Performing this research and then writing this thesis was, undoubtably, one of the most difficult tasks that I have undertaken. However, one of the joys of having completed the thesis is looking back and thank everyone who has helped me over the past years.

I would like to start by expressing my special gratitude and thanks to my supervisor Professor Pouya Rezai. It is no overstatement to say that without his continued guidance, support, encouragement, and insights in this field, this thesis would never have been existed. I would like to thank Professor Georg R. Zoidl for his guidance, support, willingness to help and generous collaboration in this thesis. I am also grateful for Professor Terry Sachlos for his valuable advices during my annual committee meetings and comprehensive exam. I wish them all the best in their future careers.

Special thanks go to my colleague and friend, Ellen van Wijngaarden for her great dedication and contribution to this research during her undergraduate studies at York University. My appreciation also goes to my colleagues in the ACUTE lab who have willingly helped me out during the running of this project.

Above all, I would like to express my deepest gratitude to the persons who are the only reasons that I live and survive all of the difficult situations; My husband, Iman, for his continued love and constant support, for all the late nights and early mornings, for keeping me sane over the past years, for being my proofreader, editor and sounding board, but most of all, for being my best friend. My parents, my brother Sadegh and my sister Ladan who are pillars of support, guidance, and love in my life. I owe you everything. Without you, I would not be the person I am today.

I would also like to thank Janet Fleites Medina and Veronica Scavo for the dedicated husbandry of the zebrafish colony and Christiane Zoidl and Nickie Safarian for their help during the course of my project.

I would also like to acknowledge all funding received throughout my PhD from Ontario Government for offering me the Ontario Graduate Scholarship for three consecutive years, Natural Sciences and Engineering Research Council (NSERC) of Canada for grants awarded to Professor Rezai, York University for offering me the Susan Mann Dissertation Scholarship, York Graduate Scholarship, Carswell Scholarship and The Roderick Guthrie Graduate Scholarship.

Table of Contents

List of Tables

List of Figures

Abbreviations

3D: Three-dimensional

6-OHDA: 6-hydroxydopamine

AD: Alzheimer's disease

bpm: Beats per minute

CAD: Computer Aided Design

CCAC: Canadian Council for Animal Care

CFD: Computational fluid dynamics

CNS: Central nervous systems

CVD: Cardiovascular disease

DC: Direct Current

DI: Deionized

DMSO: Dimethyl sulfoxide

DOPAL: Dopamine aldehyde

dpf: Days post-fertilization

EEG: Electroencephalogram

EMG: Electromyography

ESEM: Environmental scanning electron microscopy

FOV: Field of view

fps: Frames per second

hpf: Hours post fertilization

HD: Huntington's disease

ISI: Interstimulus interval

KO: knockout

MEMS: Micro-Electro-Mechanical Systems

MPTP: 1-methyl-4-phenyl-1,2,3,6-tetrahydropyridine

ND: Neurological disorders

Panx1a: Pannexin1a

PD: Parkinson’s disease

PDMS: Polydimethylsiloxane

RD: Response duration

ROI: Region of interest

SEM: Standard Error of the Mean

TBF: Tail beat frequency

TL: Tupfel long fin strain

TR: Trapping region

WT: Wild type

Glossary of Terms

6-hydroxydopamine (6-OHDA): A neurotoxin that shares some **structural similarities** with dopamine and norepinephrineis and can enter dopaminergic and noradrenergic neurons through their normal reuptake mechanism and destroy the neuron terminals.

Agarose: A gelling agent with different biological applications such as fixation of various organisms (e.g., zebrafish larvae), cell culturing platform, etc.

Apomorphine: A non-selective dopamine agonist that activates D2-like and, to a much lesser extent, D1-like receptors.

Behavioral screening: Systematic and standardized behavioral evaluation of various organisms to, for instance, treat the behavioral diseases.

Biological pathway: A series of interactions among molecules inside a cell leading to a change in a cell or a specific product.

Bilateral Tail Turn: Lateral oscillation of the zebrafish tail to both sides of its body.

Butaclamol: A non-selective dopamine antagonist.

***Caenorhabditis elegans* (*C. elegans*):** A transparent free-living nematode that is extensively used as a model organism in various biological applications due to their genetic homology with humans.

***Danio rerio*:** Binomial name of the zebrafish, a freshwater fish used as a model organism for various biological studies such as human disease modelling and drug discovery.

Days post fertilization (dpf): An established term to show the zebrafish developmental stage by reporting the number of days after the zebrafish fertilization.

Dopamine: A neurotransmitter made by our body and used by the nervous system to send messages between nerve cells. It is involved in feeling pleasure, striving, focusing, thinking, and planning.

Dopamine antagonist: The chemical compounds that block the dopamine receptors. They are widely used in treating various neurological disorders such as bipolar disorder and schizophrenia.

Dopamine agonist: The chemical compounds that activate the dopamine receptors. They are widely used in treatment of various neurological disorders such as Parkinson's disease and depression.

Dopamine receptors: A class of G protein-coupled receptors in the vertebrate's central nervous system which are involved in different neurological states such as learning, motivation, pleasure, etc.

***Drosophila melanogaster*:** Binomial name of fruit fly used as model organisms in developmental biology due to their high genome similarity to humans.

Drug Discovery: The process of identifying potential new medicines.

E3 medium: Fish medium (a mixture of the distilled water and salt) used for raising the fish embryos and larvae.

Egg water: 1.5 mL stock salt solution added to 1 litre of RO water. This solution is used for topping up the petri dishes of eggs in the incubator.

Electroencephalogram (EEG): A non-invasive test detecting the electrical activities of the brain which is recorded by placing the electrodes along the sculp.

Electrotaxis: Directed motion of biological cells or organisms guided by electrical stimuli.

Embryonic development: Process of growing a living organism from the egg fertilization until the embryonic/larval stage.

G protein-coupled receptors: A large group of evolutionarily-related proteins that are cell surface receptors that detect molecules outside the cell and activate cellular responses. They are also called 7-transmembrane receptors because they pass through the cell membrane seven times.

Gene mutation: Permanent alteration of a gene in terms of the DNA sequences which induce different biological effects on the activities of the targeted gene.

Genetic screening: Monitoring the activities of a gene or protein and their changes for various biological applications.

GCaMP: Genetically encoded calcium indicator, which is a composite of the green fluorescent protein (GFP), calmodulin (CaM, i.e. a protein), and M13 (i.e. a synthetic peptide), that can act as a sensor to determine any neural activities of the living organisms such as the zebrafish.

Haloperidol: A selective D2-like dopamine antagonist.

Hatcher water: 25 grams salt added to 1 litre of RO water. This solution is used in the hatchers while growing the brine shrimp. It is also the same salt solution used for topping up the Conductivity dosing tanks on each fish rack system.

Hydrodynamic Force: Force imposed on an object immersed in a fluid due to the motions of surrounding fluid.

Hypoxia: Oxygen deprivation.

Kinovea: An open-source software for a semi-automated video analysis used in various applications such as targeted point tracking on a trajectory.

Knockout: Genetic disruption or modification of an organism to change their behaviors in response to a specific environmental cue. Gene knockout is a mutation that inactivates a gene function.

Larvae: Developmental stage of the zebrafish from 3 to 30 dpf.

Larvae water: 2.5 grams of salt per 1 Litre of RO water. This solution is used for the larva polyculture.

Lateral line: A system of sensory organs in fish to sense and detect the movements of their surrounding water.

Levodopa: A substance that is the precursor of dopamine. Dopamine cannot cross the blood-brain barrier, while levodopa can. Therefore, a synthetic form of levodopa is used as a common treatment of Parkinson's disease, which arises from a failure of dopamine production in the brain.

Model organism: Laboratorial non-human species including zebrafish that are appealing models for a variety of biological applications such as drug discovery as they offer many advantages such as easy handling and high genetic similarity to humans.

Mutant: New organism produced by alteration of a gene of a normal organism.

Neural circuit: A population of neurons interconnected by synapses to perform a particular function when activated.

Neural screening: Monitoring the activities of neurons in response to environmental cues using various imaging or electrical techniques.

Pannexin: A vertebrate protein family, consisting of the Panx1, Panx2, and Panx3, which are widely expressed in the brain and involved in different functions such as sensory processing in the nervous system.

Pectoral fin: An organ of a fish located on the sides of the fish helping them with respiration and swimming.

Phenotype: Observable physical properties of an organism including its appearance, development, and behavior.

Polydimethylsiloxane (PDMS): A transparent elastomeric polymer which is commonly used in fabrication of microfluidic devices.

Quinpirole: A selective D2-like dopamine agonist.

RO water: Reverse osmosis water. It must be made up into the proper salt solution before being used on live fish or larva or it will kill them.

Rheotaxis: A common behavior exhibited by the aquatic species, which is defined as turning, and swimming against an approaching flow.

Salt stock solution: 40 grams of "Instant Ocean" sea salts added to 1 litre of RO water. This solution is used for making up part of the egg water.

SCH-23390: A selective D1-like dopamine antagonist.

Sensory-motor system: The biological system whose role is to combine information from the sensory and motor systems to control the body movements.

SKF-81297: A selective D1-like dopamine agonist.

Tap water: It comes only from the taps with sinks.

Unilateral tail turn: The lateral oscillation of the zebrafish tail to either side of its body.

Visual system: Part of the organism's central nervous system (CNS) enabling them to process and respond to the visual cues properly.

Wilde type (WT): The most common zebrafish strain represented a normal (non-mutated) strain.

Chapter 1*

1. Motivation and Introduction

A wide variety of mammalian animals and small model organisms have been used to better understand human physiology and ontogeny and to study a variety of human diseases[1–7]. Model organisms are particularly useful for disease pathway discovery and evaluation of novel therapeutic agents[8–10], and to study the effect of different chemicals such as toxicants on molecular, cellular, and behavioural pathways and responses[11–13]. From an evolutionary point of view, mammals such as rats, mice and monkeys are closely related to humans. However, due to their complexity and difficulty of assays as well as financial and ethical concerns, laboratories prefer to start investigations with alternative models at initial stages of screening and where high throughput and high content fundamental investigations are needed[7]. Small model organisms such as

* Some content of this chapter has been published in "A. Khalili, and P. Rezai, "Microfluidic Devices for Embryonic and Larval Zebrafish Studies," *J. of Briefings in Functional Genomics*, vol. 18, no. 6, pp. 419-432, 2019". Permissions for the use of the text has been received from Oxford University Press.

Caenorhabditis elegans (roundworm)[14–16], *Drosophila melanogaster* (fruit fly)[17–19] and *Danio rerio* (*Zebrafish)*[7,20–22] have emerged as powerful models for biomedical research to overcome the difficulties associated with the use of mammalian models for early studies.

Caenorhabditis elegans and *Drosophila melanogaster* are the widely used invertebrate models in neurotoxicology[23,24], drug discovery[6,25] and other biological assessments[14,19]. They are inexpensive and have minor ethical limitations for research. However, from an evolutionary point of view, they are far from mammals and limited in recapitulating many functions of the cells, tissues and organs. Moreover, the lack of certain organs and genes make them less appropriate for some human disease studies[1,7,14,26].

Zebrafish have recently gained more attention as they are vertebrates and more similar to humans in terms of the physiological, genetic, anatomical, and behavioral characteristics[27]. Below, we provide a more thorough review on this model organism as the focus of this thesis.

1.1. Zebrafish as a Model Organism for Behavioral Studies

Zebrafish or *Danio rerio*, as shown in Fig. 1-1, are simple and low-cost vertebrate models that can bridge the gap between mammalian animals and invertebrate organisms. Being a vertebrate, they are phylogenetically closer to humans than invertebrates. The zebrafish nervous, cardiovascular and digestive systems are analogous to mammals[28]. The overall organization of their brain shows structural similarities with human and specific regions of the zebrafish brain can be related to their human counterparts [29,30]. For instance, the ventral telencephalon in zebrafish is considered to be similar to the striatum in humans[29]. The major dopaminergic pathways in zebrafish brain are analogous to mammals and similar receptors can be identified for most of the mammalian subtypes and zebrafish[30]. The small size of zebrafish facilitates cost-efficient

maintenance of embryos, larvae and even adult animals in abundance. Pharmacological manipulation of zebrafish is relatively easy since drugs are readily absorbed from the water into the skin[31]. This multiorgan vertebrate also possesses higher than 70% of human equivalent genes[28].

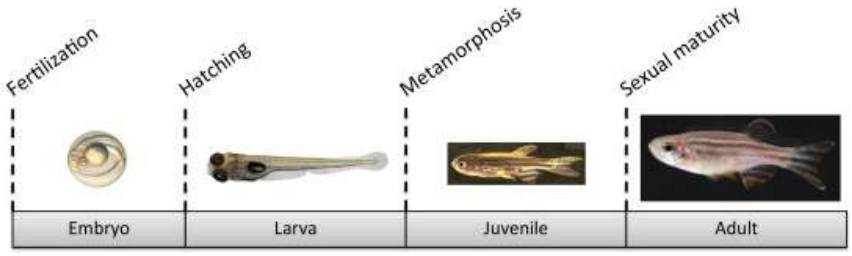

Fig. 1-1. Zebrafish life cycle[32]. Reprinted with permission from Elsevier.

Zebrafish have a mean and maximum life span of approximately 3.5 and 5 years, respectively[33]. Embryonic development takes 3-4 days at 28.5°C and after that, zebrafish hatch to begin the larval stage. Larval development also lasts about 6 weeks, during which the zebrafish experience various morphological changes to be transformed into juvenile stage at around 45 days post-fertilization (dpf) at 28.5°C. They finally reach the sexual maturity after 3 months and become adults[33,34]. Organogenesis is rapid in zebrafish. Most of the organs are developed within 5 to 6 dpf in the larvae. At 72 hours post fertilization (hpf), the zebrafish CNS development is well advanced[29]. Starting at 4-5 dpf, the zebrafish larvae fully develop many sensory-motor functions to perform complex behaviors such as swimming and feeding[35]. Once they arrive at 7 dpf, their visual system and brain are fully developed[25]. Moreover, their advantages over other vertebrate models including high fecundity, transparency and easy visualization which facilitate genetic and high-throughput functional studies[1,36].

The above features make zebrafish an interesting model for drug discovery[31,35,37–39], study of human disease such as neurodegeneration[29,30,40–43] and toxicology[11,25,44–49]. However, there are some challenges which should be addressed in the study of zebrafish. For instance, since they are

not mammals, they cannot be considered as closely related to human as mice or other higher organisms, therefore, all the new discoveries must later be verified in a mammal model. Yet, they are perfect models for fundamental research on molecular, cellular, and genetic bioprocesses and high throughput screening of chemicals.

Although zebrafish adults have been used in different biomedical research[31,50], many experiments on zebrafish embryos have also been performed for early developmental investigations. Embryos require less media, space and effort, which results in cost-efficient, rapid and high-throughput investigations[51]. Larval zebrafish are also ideal models for behavioral screening, and studies of their molecular and cellular basis, because of their maturity in terms of swimming capacity, functionality of the motor systems, and ability of doing simple motor tasks in response to relevant cues from the environment[52,53]. These factors have made zebrafish embryos and larvae perfect models for medium to high throughput *in-vivo* research. We will discuss various platforms and techniques employed to study the zebrafish behaviors at embryonic and larval stages in the next sections. The reason behind focusing on these developmental stages is the use of larval zebrafish in the microfluidic methods proposed in this thesis.

1.2. Conventional Methods for Zebrafish Behavioral Studies

Zebrafish behavioral assays require platforms to immobilize the larvae and external stimuli to evoke their behavioral responses. The most common conventional platforms used to study the zebrafish behavioral phenotypes are agarose gel substrates[54,55], multi-well plates[56,57] and petri dishes[58]. Different stimuli such as sound[59,60], chemical[59,60], light[61,62] and electricity[63] have been applied in these platforms to stimulate the behavioral responses. The mentioned techniques and platforms will be elaborated with some examples below.

Bianco et al.[61] investigated the behavioral responses of zebrafish larvae that were partially immobilized in a petri dish using agarose gel. The larvae responded to a moving optical stimulus by exhibiting eye convergence movements and J-bend pattern. Considering the involvement of J-bend pattern in the zebrafish prey-capturing behavior, they proposed that eye convergence might also help the larva to spot the prey.

In another study, Iron et al.[56] investigated the effect of different dopaminergic compounds on the larvae movement inside a 96-well plate. Dopamine antagonists and agonists are compounds that block and stimulate dopamine receptors, respectively. The authors identified the time and concentration of peak effect of each compound and reported a dose-dependent decrease in motion upon exposure of the larvae to dopamine antagonist and an increase in locomotor activity upon treatment with dopamine agonists. The data reported in this paper will be used in chapter 5 of this thesis to discuss the potential involvement of dopaminergic pathway in regulation of zebrafish electric-induced response.

Fajardo et al.[58] analyzed the behavior of zebrafish larvae inside a petri dish. They exposed the free wild type and ChR2 mutant larvae to the light stimulus and reported their backward motion upon activation of ChR2 protein. They also fluorescently imaged zebrafish brain activities and studied subtle behaviors and motor patterns of partially restrained larvae. For that, they embedded the head of zebrafish larva inside agarose gel while its tail and pectoral fins were free to move. They could classify zebrafish behaviors into several motor patterns such as J-bend, C-bend, struggling, and forward swimming (Fig. 1-2).

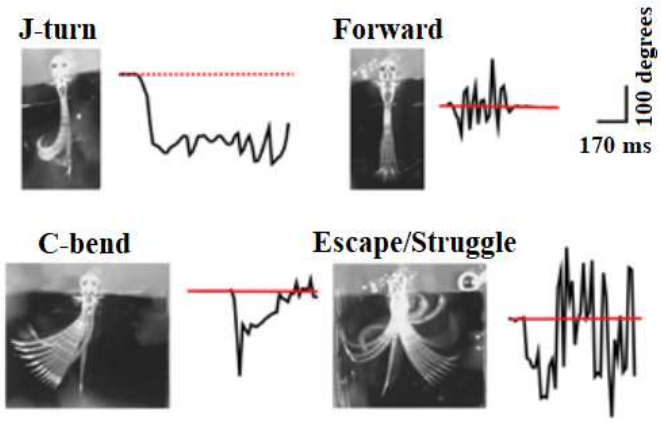

Fig. 1-2. Examples of four different behaviors observed in fish head-fixed in agar. Black traces and red lines show the tail curvature as a function of time and the straight tail, respectively[58]*. Reprinted under permission of Creative Commons License.*

Steenbergen[63] also exposed freely moving larvae to series of 20 electrical stimuli (5 V pulses lasting 100 ms) with interstimulus interval (ISI) of 10 or 2 s. Comparing the swimming activity of the larvae before and after exposure showed locomotion diminishing of zebrafish locomotor response to the repeated stimulus which depended on the ISI.

Despite noteworthy research on the zebrafish model organism and the advantages of the conventional screening assays, these techniques suffer from several shortcomings. Zebrafish immobilization in desirable orientations is commonly done using anesthetics[64]. Other uncontrollable and laborious techniques such as flipping zebrafish body with a superfine eyelash have also been used to orient the larvae[65]. These time consuming, irreversible and tedious manual processes can damage the fragile body of the zebrafish larva and prevent it from development under a normal condition, which in turn might jeopardize the validity of assay results. Covering the larva's body and specifically head with agarose might also lead to oxygen deprivation and morphological damages, making agarose inappropriate for assays. Furthermore, these platforms are often low in throughput and visualization of the organs of interest may be blocked in

uncontrollable orientations, making quantitative analysis of zebrafish behavior challenging. By exposing zebrafish to different external stimuli, some complex motor behaviors such as re-orientation, O-bends and avoidance responses can be investigated. However, there are difficulties in conventional assays for controlling the stimuli inside the three-dimensional (3D) environment of multi-well plates and petri dishes and monitoring the complex movement phenotypes of the zebrafish larvae.

The above limitations have motivated the application of microfluidics as an effective technology which provides accurate, repeatable, high throughput and multifunctional experimental tools to screen zebrafish behavior and perform quantitative analyses under controllable conditions[8,11,41,66,67]. For those who are unfamiliar with microfluidics, it is the science and technology of studying fluids and objects at sub-mm length scale using devices that are usually microfabricated using conventional microelectronic fabrication techniques. In the sections below, the current microfluidic approaches for investigation of behavior and neurobiology of zebrafish at embryonic and larval stages, due to their size match with microfluidics, will be reviewed. Our focus will be to provide an overview of the microfluidic methods used to manipulate (deliver and orient), immobilize, and expose or inject zebrafish embryos or larvae, followed by quantification of their responses in terms of neuron activities and movement. We will also provide our opinion in terms of the direction that the field of zebrafish microfluidics is heading towards in the area of biomedical engineering.

1.3. Zebrafish Assays on Microfluidic Platforms

Efficient entrapment of zebrafish in microfluidic devices enable precise control and favorable orientation of the target which plays a key role in high-resolution imaging. Although the gel-free

immobilization techniques are attractive in terms of prevention from probable developmental defects arising from oxygen and nutrient deprivation, there is still lots of work to be done to meet the ease-of-use by scientists and convince them to adopt these strategies. The larger size of zebrafish in comparison to other models like *C. elegans* or single cells precludes the use of most microfabrication methods. For instance, prototyping and fabrication of millimetre-scale devices through standard lithography are difficult and time consuming[68]. In addition, current microfabrication and replication techniques which utilize silicon wafer molds and biocompatible polymers such as polydimethylsiloxane (PDMS) cannot be used easily for developing 3D devices with complex designs required for zebrafish manipulation and assay[69,70]. Moreover, in PDMS and plastic molding techniques, bonding and assembly should be done manually, which are highly dependent on the operator[71]. Recent developments in 3D printing, access to Computer Aided Design (CAD) software and technologies such as advanced additive manufacturing have presented new fabrication strategies in bioengineering[69,72,73]. Considering the challenges mentioned above, a handful of microfluidic devices have been developed for manipulation of zebrafish embryos and larvae, which are reviewed in the next two sections.

1.3.1. Microfluidic Embryonic Assays

Microfluidic devices have provided non-invasive culture and development conditions with the ability to access and expose the embryos to chemicals at different developmental stages. Review of Micro-Electro-Mechanical Systems (MEMS) for embryo injection was outside the scope of this thesis and the readers are referred to papers published on this topic[74–77]. In this section, we will first review the microfluidic devices used to culture zebrafish embryos and examine the effect of different chemicals on their development. Then, the immobilization techniques employed to stabilize individual embryos inside microfluidic traps will be presented and a review will be

performed on microchips integrated with electronic interfaces to increase the efficiency of the specimen and stimulus manipulation in the device.

1.3.1.1. Embryo Culture and Development on a Chip

Yang et al.[78] used zebrafish embryos to evaluate the toxicity and teratogenicity of clinical drugs in a microfluidic chip (Fig. 1-3A). Their three-layer microfluidic device consisted of a microchannel network to generate and deliver a concentration gradient of different drugs to an array of culture chambers with zebrafish embryos pipetted into them. They used heartrate, tail detachment, body twisting, development of eyes, pigmentation, segmentation, and teratogenicity to assess the developmental differences between embryos treated with antiproliferating drugs and the normal ones. The tail, notochord and fin showed the highest sensitivity to the chemical compounds. The heartrate and pigmentation, as accessible and critical physiological indices, were also important parameters. Exposing 4 hpf zebrafish embryo to adriamycin and cisplatin, which impairs DNA structure, induced comparative teratogenicity and toxicity. However, the embryonic toxicity of 5-fluorouracil, which inhibits DNA synthesis, was significantly lower under the same conditions. Treating with Vitamin C ($0\sim100\mu M$) did not induce any apparent damage to the zebrafish embryos.

A microfluidic system proposed by Wielhouwer et al.[79], could facilitate on-chip culturing of more than 100 zebrafish embryos for real-time imaging. The device consisted of three borosilicate glass layers bonded together. Two sets of flow-through systems were designed for delivering buffer solutions and circulating warm water. The pre-heated water was also used to control the desired temperature for embryo growth. Although the embryos could successfully develop in the microfluidic chip for 5 days, some phenotypic effects such as body length reduction and yolk sac oedema were reported. Their acute exposure to ethanol in the biochip also replicated the same

results investigated in multi-well plates while consuming far less ethanol as an advantage offered by the use of microfluidics.

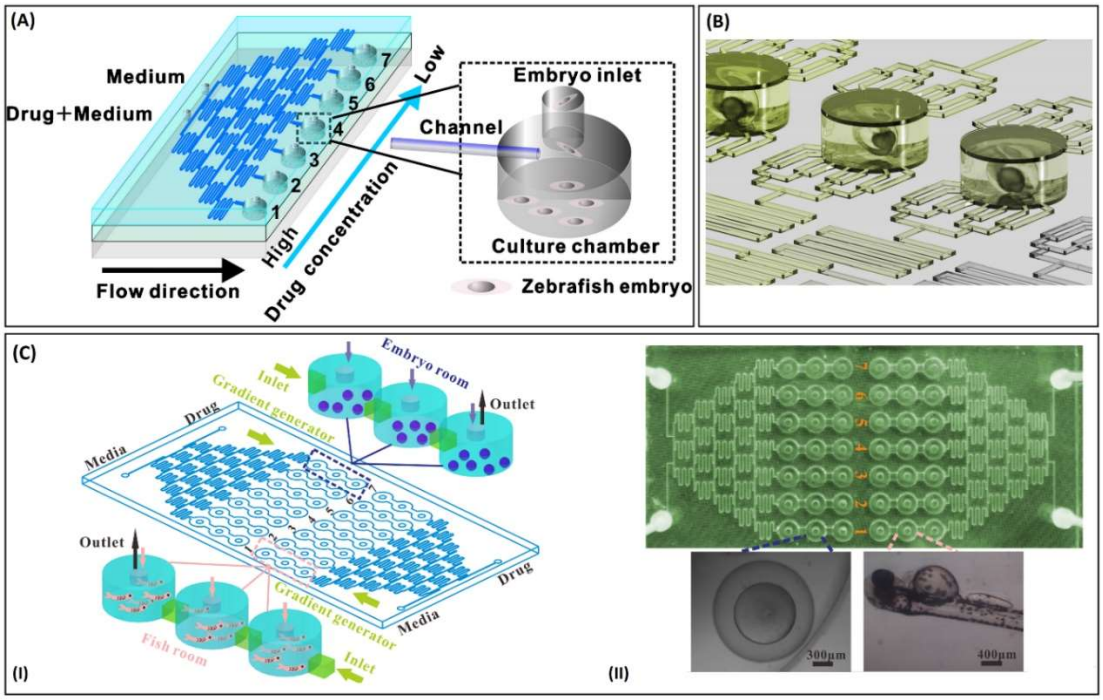

Fig. 1-3. Microfluidic devices for zebrafish embryonic assays. (A) A microfluidic device with two different inlets to generate drug concentration gradients in culture chambers 1 to 7 for exposure of zebrafish embryos trapped in them[78]*, Reprinted with permission from AIP Publishing, (B) A microfluidic perfusion device to monitor zebrafish development*[80]*, Reprinted with permission from Royal Society of Chemistry. (C) (I) Schematic of a microchip with two independent zones for embryonic and larvae drug toxicity assessment. Each zone included a drug inlet, a media inlet, a gradient generator and seven series of zebrafish chambers; (II) Images of the microfluidic chip and the embryo and larvae in the chip*[81]*, Reprinted under permission of Creative Commons License.*

Another microfluidic platform presented in Fig. 1-3B was used to culture zebrafish embryos and screen the development of their organs[80]. The device consisted of 8 fish tanks with independent outlets and inlets and a microfluidic gradient generator which ensured a uniform flow of chemicals with different concentrations into the fish tanks. Sealing the inlets and preventing from producing

air bubbles, they used an oxygen-permeable membrane to facilitate oxygen exchange and bubble removal. Although there were some problems associated with manual distribution of embryos for loading, the device was successfully used for high resolution imaging and chemical screening. They demonstrated the embryo developmental abnormalities upon exposure to valproic acid, a teratogen causing birth defects in human. Treating with valproic acid resulted in pigment perturbations, oedema and shortened tail. Their preliminary toxicity studies established the proof-of-concept evidence for a drug screening model.

A phenotype-based microfluidic device in Fig. 1-3C was proposed by Li et al.[81] to monitor immediate and long-term developmental toxicity and teratogenicity effects of an anti-asthmatic drug. The chip consisted of two independent units to assess zebrafish embryos and larvae. Each functional section was composed of 7 culture microchambers, solution inlets, a concentration gradient generator to deliver different doses of drugs to chambers (similar to Fig. 1-3A), and waste outlets. Ten zebrafish were accommodated per chamber and exposed to aminophylline. They used body length, survival, convulsion, heartrate and hatch rate as quantitative parameters to characterize zebrafish embryonic development via optical imaging. They demonstrated that persistent exposure to aminophylline resulted in cardiovascular toxicity and deformities such as tail and skeletal malformations, bent trunk and pericardial edema in both zebrafish larvae and embryos.

Huang et al.[82] introduced a PMMA microfluidic device to simultaneously measure the acid extrusion (PH) and oxygen consumption rates of zebrafish during embryonic development. Their device consisted of an array of microwells, containing dual sensors for oxygen and acid detection, which were sealed with glass lids. They used blue and UV LED together to excite pH-sensitive and O_2-sensitive probes, respectively. A photodetector was also used to detect the emission. They

could observe a significant decrease in the oxygen consumption rate and a rapid decrease in the acid extrusion rate after 20 min of acute hypoxia. They successfully monitored the transition between aerobic and anaerobic metabolism of 48 hpf zebrafish in normoxia and moderate and acute hypoxia. Their results also indicated the ability of zebrafish to regulate anaerobic and aerobic capacities to survive upon exposure to acute hypoxia.

An automated and programmable microfluidic device was also introduced to monitor the drug effects on zebrafish embryos precisely[83]. The device consisted of an array of culture chambers which were accessible from the top, control channels and fluidic channels. The crossover of these channels acted as microvalves which could control the fluid flow pneumatically. The small cross-section of fluidic channels prevented embryos from moving outside the wells. 24 embryos could be loaded in the culture chambers and screened simultaneously under a stereoscope. The proposed device offered an appropriate solution to study the effect of cyclopamine (a teratogen) on zebrafish blood vessels and somite development and monitor their real-time response to drug treatment. They showed that 70μM cyclopamine could block the Hedgehog signalling pathway, which transfers information required to form embryonic pattern to embryo's cells. Based on their results, 6-17 hpf and 17-24 hpf were confirmed as the critical periods of the effect of cyclopamine on intersegmental blood vessels and somite, respectively.

1.3.1.2. Embryo Immobilization on a Chip

Shen et al.[84] designed and tested a microfluidic bioreactor to immobilize and study zebrafish embryos. The device consisted of a two-layered PDMS chip, i.e., a thin layer containing a microfluidic channel to deliver chemicals and a thick layer with funnel-shaped holes to hold embryos stable. The funnel design was easy to fabricate and could protect the embryos from shear stress, helping to maintain their viability. The PDMS sticky surface, hydrostatic pressure and

gravity also prevented the embryos from rotating. The device was submerged in a petri dish filled with E3 medium to let embryos be exposed to different compounds which were flown underneath by a gravity-driven pump. The PDMS transparency also enabled automated screening and imaging. Using this microfluidic device, the effect of MIF, a cytokine growth factor which is known to affect the neural axis of embryos, on zebrafish development was examined. The experiments demonstrated that exposure to 30 nM MIF did not induce any developmental change on 53 embryos protected within chorion. However, all four dechorionated embryos exposed to the same MIF concentration either died or developed abnormality.

Using hydrodynamic forces to increase the docking efficiency, Akagi et al.[85,86] also designed a multi-layer PMMA microfluidic device for loading, trapping and developmental analysis of transgenic zebrafish embryos. The device shown in Fig. 1-4A consisted of loading and several suction channels, a U-shaped manifold to introduce warm water providing a desirable temperature for embryo culture, a piezoelectric micropump for chip actuation and 20 traps. The piezoelectric pump was used to create suction force at the outlet to deliver embryos along the loading channel. The gravitational force together with suction force from microchannels located under the traps caused the embryos to dock into the traps. A compound solution could then be delivered to each embryo. A 0.2 mM tricaine mesylate buffered solution was used to anesthetize the embryos temporarily and inhibit their movements during imaging. Using the proposed microfluidic system, the authors could manipulate developing zebrafish embryos in an autonomous manner without disturbing and repositioning them. They also could segregate embryos spatially to prevent adjacent embryos to be in touch with chemicals released from the others. This is a significant achievement in drug screening routines which eliminates the bystander effect present in conventional bulk embryo cultures.

A constrictive microchannel was developed by Huang et al.[87] to immobilize an un-anesthetized zebrafish embryo on its lateral side and investigate oxygen distribution in the cardiac tissue (Fig. 1-4B). The microchip consisted of input and output ports connected via a straight microchannel (1 mm × 0.5 mm cross-section) with a constriction trap region of 0.3 mm at the middle. A PDMS membrane was also sandwiched between a glass substrate and the PDMS microchannel. An air pressure of 2.5 psi was exerted on the membrane to slightly press the embryo and prevent it from moving after immobilization in the trap. An excitation light was projected to illuminate different regions of the tissue of interest for in-vivo oxygen measurements. Heartrate analysis showed no adverse effect of the membrane-based immobilization technique on the physiological state of the zebrafish embryos. Using the device, they could measure oxygen changes in the cardinal vein and the cardiac region of a 48 hpf zebrafish embryo that experienced 0-20% O_2 (hypoxia and normoxic conditions). Acute hypoxia increased cardiac activity to stimulate oxygen transport. However, transition from hypoxia to normoxia resulted in a gradual decrease in the heartrate.

To minimize the possible damages caused by direct contact during manipulation, Chen et al.[36] suggested to attach magnetic particles to the zebrafish embryo yolk surface and apply a homogeneous magnetic field to orient the embryos accurately. The magnetic field should be generated through assembling three pairs of magnetic coils along three orthogonal directions. The embryos then could follow the direction of the produced magnetic field to be oriented in favorable manner. Considering this hypothetical microfluidic method, it will no longer be necessary to use a physical wall to restrain the embryos. Therefore, time-lapse imaging will not be limited by the rapid growth of the embryos. However, the potential damage of the magnetic field and the magnetic particles toxicity on the developing embryos should be evaluated.

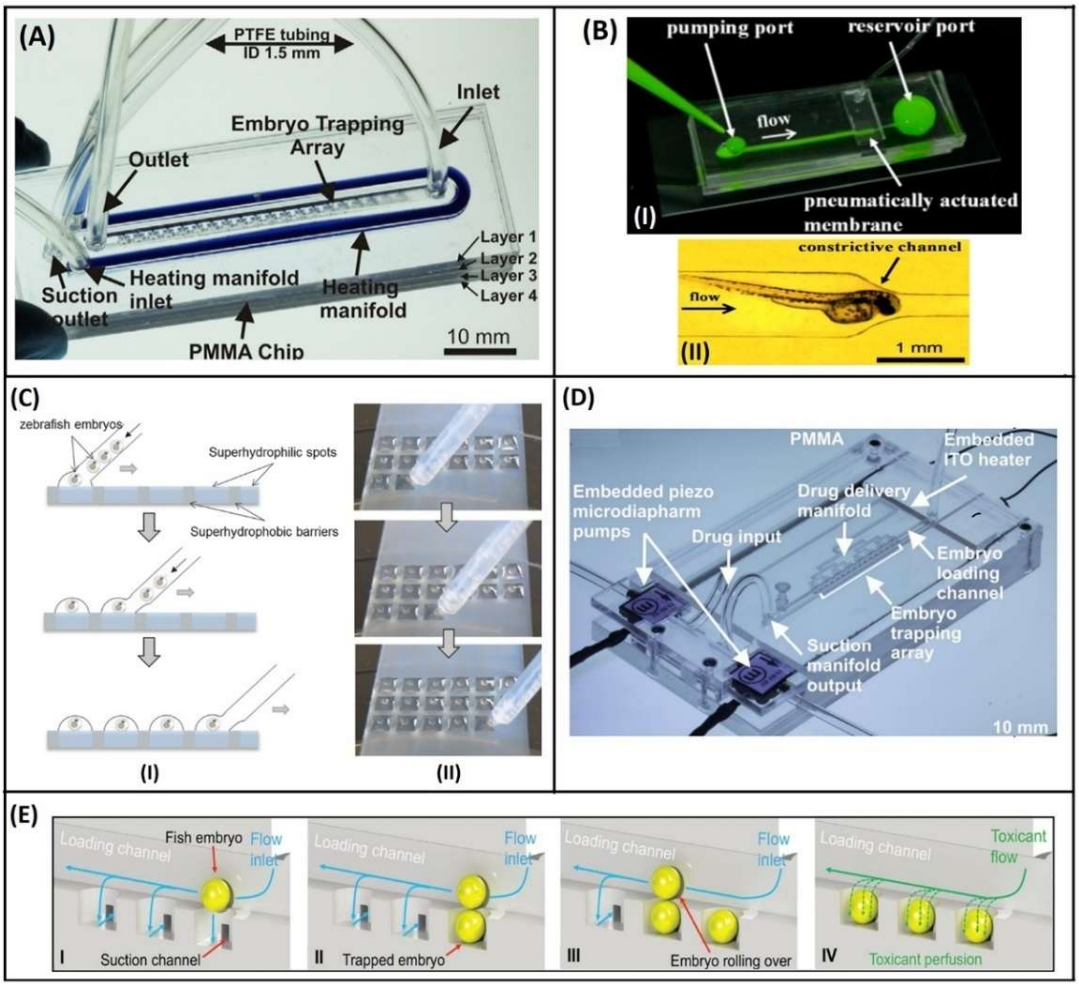

Fig. 1-4. Microfluidic devices for zebrafish embryo immobilization. (A) A microfluidic chip involving a main loading channel, a linear array of traps, and heating and suction manifolds for developmental analysis of transgenic zebrafish embryos[86]*, Reprinted with permission from Elsevier. (B) (I) A microfluidic chip with a constrictive microchannel and a pneumatically actuated membrane. (II) An un-anesthetized embryo pumped head-first and trapped in the microchannel*[87]*, Reprinted under permission of Creative Commons License. (C) (I) Schematic of microarray platform for toxicity screening assay. (II) The process of spreading zebrafish embryos based on the effect of discontinuous dewetting*[88]*, Reprinted with permission from John Wiley and Sons. (D) A multilayer microfluidic device for automatic culture and analysis of zebrafish embryo*[89]*, Reprinted with permission from SPIE. (E) The sequential process of automatic immobilization of zebrafish embryos inside a microfluidic chip*[90]*, Reprinted with permission from American Chemical Society.*

Popova et al.[88] developed a microchip to screen zebrafish embryos including arrays of highly hydrophilic regions separated by superhydrophobic walls. Using the effect of discontinuous dewetting, they could manually spread zebrafish embryos on droplet microarray platform (Fig. 1-4C). They investigated how the fluorescently labeled peptoids were localized in different organs. They also could evaluate the toxicity of different concentrations of ZnCl and AgNO and demonstrate the consistency of their results with those obtained in standard microtiter plates. Their high throughput microfluidic device had several advantages over the conventional microtiter plates. They could screen single embryos in small volumes as low as 5 μL to reduce the chemical consumption. The embryos were not affected by movements of their neighbors. Also, due to water surface tension, embryos were fixed in specific compartments, making the microscopic analysis more convenient.

Despite noticeable progress in fabrication of microfluidic devices for zebrafish embryonic studies, the manual loading and actuation can lead to reduction of the assay throughput. To overcome this issue, microfluidic chips can be integrated with electronic modules to provide higher levels of efficiency for automatic manipulation of stimuli and zebrafish embryos.

To prevent damage to fragile embryo bodies resulted from manual handling, Akagi et al.[91] presented a miniaturized chip to analyze zebrafish embryo development in-situ. Their device was used for autonomous trapping and immobilization of embryos, drug perfusion and time-lapse imaging at different developmental stages. A suction tube connected to a storage chamber was used to load zebrafish embryos onto the chip individually and about 5 s intervals were provided to prevent embryos from colliding. After loading, the embryos rolled on the channel surface due to the flow-induced drag force. A cross flow through the suction channels caused the embryos to dock inside the traps rapidly. They used a transgenic zebrafish line (fli1a:EGFP), which expresses

green fluorescent protein in the vasculature, to demonstrate the applicability of their device to analyse antiangiogenic compounds. The transgenic zebrafish embryos were loaded automatically and perfused with media containing 1 μM of selective VEGFR inhibitor, AV951, continuously. The non-stimulated embryos could develop normal vasculature, while intersegmental vessel inhibition was demonstrated in the exposed embryos.

Akagi et al. modified their previously presented chip[85], through adding a manifold for drug delivery and an extra piezoelectric pump to control the embryo loading and drug delivery steps separately[89]. The device comprised an array of 16 traps with suction channels, a drug delivery manifold, piezoelectric micro-diaphragm pumps and indium tin oxide heating elements to maintain an optimal temperature during embryo development (Fig. 1-4D). Gambit 2.3 and Fluent 6.3 software (Fluent Inc., USA) were used to simulate the device with virtual embryos inside it and solve the associated differential equations for conservation of mass, momentum and chemical species. The proposed device enabled trapping embryos efficiently, treating them and visualizing the vasculature patterns in response to drug treatment. The embryos were perfused with E3 media containing anti-angiogenic compounds such as VEGFR2/PDGFRβ inhibitor Sunitinib, VEGFR1-3 inhibitor AV951 and DMSO vehicle. Images of embryos at different developmental stages were used to evaluate the effect of these compounds on formation of intersegmental vessels. VEGFR1-3 was the most potent drug which resulted in 100% of intersegmental vessels growth inhibition at 1 μM concentration.

Based on Akagi's work[91], Wang et al.[92] proposed an integrated automatic microfluidic platform including a motor driven stage, an actuator, peristaltic pumps to provide a suction force to immobilize the zebrafish embryos in the traps, a heating module and an imaging unit. Their device was employed to automatically immobilize, culture and treat zebrafish embryos during toxicity

biotests. A field programmable gate array was also used to implement an embedded interface to provide real-time control over loading and immobilization processes, flow control, temperature stabilization and imaging. They could replace the conventional microscopes with a customizable cost- and power-efficient imaging system providing the same sensitivity and resolution. The proposed platform outlines the future path for developing a completely integrated lab-on-a-chip which can perform in-situ analysis of small model organisms like zebrafish. Such devices enable automated and fast biotests on developing embryos.

Another automated microfluidic chip with the exact well interspacing of a 96-well plate was also designed for entrapment, culturing and treatment of zebrafish embryos for toxicological study[90]. The chip composed of 12 microscale clusters, each consisting of a loading channel, an array of 21 embryo traps, inlet and outlet ports, and a suction channel which exerted suction force on embryos to immobilize them. The immobilized embryo blocked the trap and conducted the other embryos to the next traps (Fig. 1-4E). Many embryos were loaded and immobilized in the chip in a quick manner and exposed to a variety of chemicals such as copper sulfate, caffeine, ethanol and phenol. Comparing the experimental results obtained on the microfluidic chip with those performed in microwell plates provided evidence that the microchip could be considered as an alternative platform for aquatic toxicological studies. The device could also overcome the limitations of testing unstable or volatile compounds. For instance, nicotine, a light-sensitive organic toxicant, was shown to be more dose-effective in the proposed microfluidic chip when compared with the conventional wells.

1.3.2. Microfluidic Larval Assays

In contrast to the immobile embryo that has semi-uniform spherical geometry, a zebrafish larva features random orientation, active swimming, and a complex shape which poses difficulties for

immobilization and probing. Recently, microfluidic devices have been employed to address some of these challenges. Here, we will review different techniques employed for manipulation and assay of immobilized and freely moving zebrafish larvae in microfluidic devices. Immobilizing the larva is a technique required for performing cell- or organ-based assays such as neuronal imaging and organ-based microinjection, while the devices studying freely moving zebrafish are mostly focused on behavioral assays and dominantly larvae's locomotion. Some researchers have developed devices for partial immobilization of the larva which makes both cellular and behavioural investigations possible simultaneously.

1.3.2.1. Immobilized Zebrafish Larva Assays on a Chip

Bischel et al.[93] employed a microfluidic device with branching channels (Fig. 1-5AI) to manually load, position and orient 3-5 dpf larvae, allowing either dorsal or lateral views of the immobilized fish for drug treatment studies. These views could be achieved by the head-first or tail-first loading of the larvae into the main channel, respectively. The device had an oval input connected to a circular output via a network of straight branching channels that each had a 0.3 mm wide constriction trap at the end. These traps were used for immobilization of the larvae from their head (Fig. 1-5AII) or tail regions. Considering the differences in surface tension along the channel, water containing the larvae was passively transferred from the smaller input port to the larger output port. After loading the first zebrafish larva into a trap, flow was restricted causing the next larva to be transferred to one of the other three channels. This process was continued until all four larvae were loaded successfully. A micropipette was used to deliver a chemical to the larva through a small access port above each trap. Their device enabled screening the neutrophil migration from the caudal hematopoietic tissue to the fin. Three dpf zebrafish larvae were treated with LTB_4 (a

neutrophil attractant) or LTB_4 without and with LY294002 (a PI3K inhibitor). Their experiments confirmed the role of LY294002 in impairing neutrophil motility induced by LTB_4.

Fig. 1-5B shows another promising method for larva immobilization at favorable orientations in a repeatable and rapid manner[94,95]. The authors developed a gel-free, anesthetic free, high-throughput microfluidic fish-trap array to investigate the ethanol-induced response and neural activities in tens of 4-6 dpf zebrafish larvae. Their device consisted of two side-by-side horizontal channels bridged by a series of short, tapered channels. They tested three distinctive tapered channel designs for behavioral studies, brain function monitoring and cardiac screening. Hydrodynamic force was continuously applied for loading and immobilizing the larvae. As a larva flowed in a tail-forward format, it could dock into the first trapping channel acting as a plug and resulting in directing the other larvae towards the next empty channels in a sequential manner. In the motion chip, larva's head was fixed by a baffle partially blocking the outlet of the trapping channel while fins and tail could move freely to allow behavioral studies. In the lateral chip, larva's tail was trapped in a plane parallel to the horizontal plane to provide access to larva's heart. Using the dorsal chip to trap the larva's tail in a plane perpendicular to the horizontal plane, the dose-dependent effect of ethanol on neural activities was examined using imaging of genetically encoded calcium indicators. The pectoral fin beats, body and eye movements were used to quantify the behavior of larvae exposed to ethanol at different concentrations. Results suggested that ethanol may cause impairment in the motor coordination and vision function of zebrafish larvae. The cardiac function analysis also showed the abnormal cardiac cycles induced by ethanol treatment. They also showed that at low ethanol concentration (0.75%), neuron responses initiated from the caudal hindbrain, then gradually expanded to the cerebellum, ventral midbrain and even forebrain upon increasing the ethanol concentration to 1.5% or 3.0%.

Another design including two sets of zigzag microchannels (Fig. 1-5C) was used to control the oxygen level in the media surrounding a zebrafish larva and study the larva's behavioral responses under acute hypoxia[30]. Permeability of PDMS channel walls to the gases made it possible to manipulate the oxygen level in the exposure media. Using a micropipette, a larva was loaded into the microchannel inlet in a head-first orientation and pushed against a barrier located at the end of the channel. Their experiments demonstrated that the strongest hypoxia treatment ($[O_2]$ =1.8%) could increase the body movement rate and pectoral fin beats of 7 dpf zebrafish larvae significantly when compared to the control group. However, the eye saccade rate was not significantly affected by hypoxia. The proposed setup can be used to test the effect of different drugs and genetic modifications based on behavioral responses of larvae exposed to different concentration of O_2 and other dissolved gases, such as N_2O, NO and CO_2.

A microfluidic-based electrophysiology unit demonstrated in Fig. 1-5D was developed for neural study of zebrafish larvae[96]. The larvae were aligned autonomously and restrained at the head in twelve half-cylindrical narrow-ended microchannels. Multiple surface microelectrodes were in close contact with larvae head to capture different electrical episodes related to electroencephalography, electrooculography, electromyography and audiology. A reference electrode was also located in the front of larvae's mouth. The electrodes were used to monitor and record brain activities through electroencephalogram signals with high sensitivity. Using different chemicals as stimuli, the authors could demonstrate the applicability of the proposed device for long-term electrophysiological monitoring in epilepsy zebrafish models. Exposure to pentylenetetrazole (a convulsant agent) could evoke seizures in 5-7 dpf zebrafish larvae which were monitored via electroencephalogram signals. Topiramate and valproic acid (antiepileptic drugs) were also used as chemical stimuli to stimulate response in scn1lab mutant zebrafish larvae

which recapitulate Dravet syndrome in human. Treating with valproic acid decreased the seizure score. However, exposure to Topiramate induced positive response in the mutant larvae.

Our group also proposed a microfluidic chip to assess the behavioral responses of 5–7 dpf semi-mobile zebrafish larvae under exposure to chemical stimuli[97]. The microfluidic device (Fig. 1-5E) was used to immobilize zebrafish larva's head while its tail was free to move in an open chamber to perform C- and J-bend movements. A membrane valve was also designed in front of the trap to prevent the trapped larva from escaping. The design was optimized to quantify zebrafish tail, eye and mouth movements. The head region was stabilized for controllable exposure to L-arginine to evoke responses in the olfactory receptor neurons of the zebrafish larva. Exposing to $10^{-6}, 10^{-3}$ and 1 mM L-arginine induced higher tail tip frequencies in the zebrafish larvae trapped in the microfluidic device in comparison to mobile larvae in a droplet. However, since actuation of the valve confined the larvae and eliminated their delicate movements, lower eye and mouth movements were observed in the immobilized larvae compared to the freely moving zebrafish. Very recently, we demonstrated that this device can be used for investigating the response of zebrafish larvae to electrical signal[98,99].

In another approach, hydrodynamic forces were utilized for reversible trapping and immobilization of zebrafish larvae in the lateral position in a millifluidic chip, which was appropriate for imaging the internal organs[100]. The device was made of a main channel for zebrafish loading and drug delivery, an array of 10 microfluidic traps, an array of cross-flow channels to generate hydrodynamic forces, and an array of thrust channels providing hydrodynamic deflection to push the larvae toward the traps (Fig. 1-5.F). The larvae immobilized in the traps acted as plugs and conducted other larvae to subsequent cages. The larvae were introduced into the device with the head first orientation and positioned in the ventral or dorsal

configuration. Considering the design geometry, the larvae then were rotated to the lateral position forcing fluid to pass around the elongated shape of the zebrafish larvae. The system was also coupled with a miniaturized camera to monitor the perturbations induced in the cardiac function upon introducing and withdrawing cardio-active compounds. They evaluated the effects of 0.162 mM nicotine (a parasympathomimetic stimulant), 0.195 mM caffeine (a nervous system stimulant), 0.102 mM verapamil hydrochloride (a hypotensive medication) and 0.032 mM lead acetate (an environmental toxin) on zebrafish heart activity. A 10 min exposure to caffeine and nicotine resulted in a significant decrease and increase in zebrafish heartrate, respectively. Exposure to verapamil hydrochloride reduced heart contractions in zebrafish larvae by 20% and exposure to lead acetate also induced an immediate increase in the heartrate. The results were consistent with those observed in physiological reaction of human.

Candelier et al.[101] introduced an open-ended microfluidic chip made of transparent acrylic (PMMA) to record neural activities of zebrafish larvae partially immobilized in agarose and exposed to distinct flavors of L-proline, as an appetitive tastant, and critic acid, as a sour aversive chemical (Fig. 1-5G). Using two-photon microscopy and a high-speed camera, they monitored the gustatory neuronal responses and the tail movement behavior of a semi-immobile larva simultaneously. It was shown that most neurons in three different focal planes of the olfactory bulb (ventral, medial and dorsal) reacted to either L-proline or critic acid while a few responded to both. Monitoring tail movement and neural activity demonstrated a positive correlation between behavioral responses and neuronal firing induced by chemicals. Increasing the stimulus duration increased the average number of tail flips.

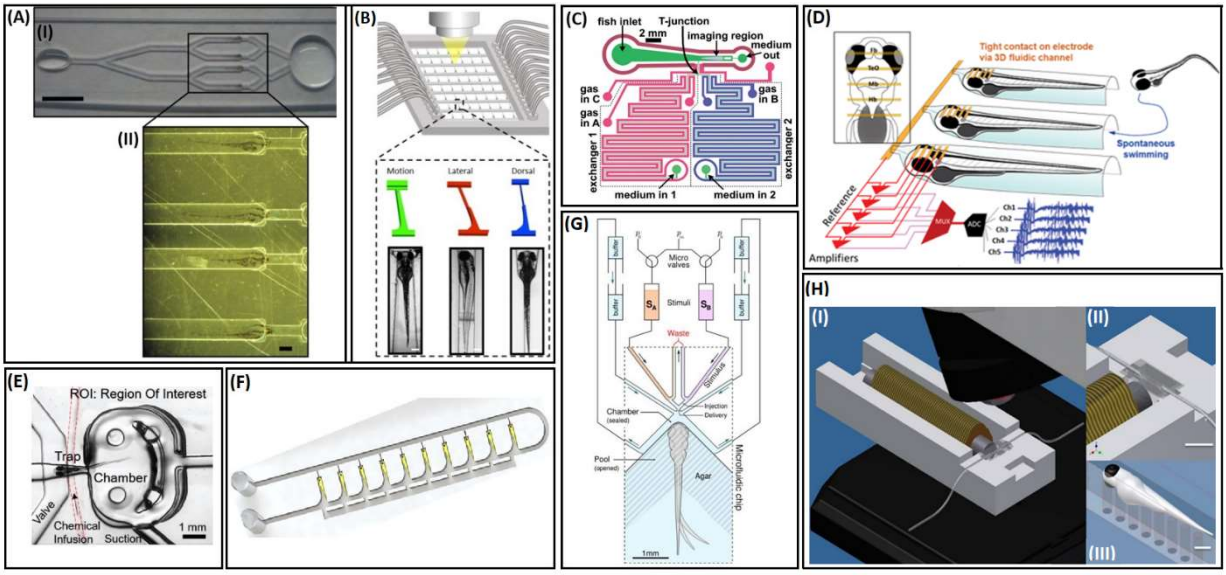

Fig. 1-5. Microfluidic devices for zebrafish larval studies. (A) Microdevice fabricated in polystyrene to position zebrafish larvae for imaging the lateral or dorsal views. (I) Scale bar: 5 mm, (II) Scale bar: 0.5 mm[93]*, Reprinted with the permission from Royal Society of Chemistry, (B) Scheme of the chip with the real images of immobilized zebrafish in the end-tapered channels of motion, lateral, and dorsal chips. Scale bar: 0.2 mm*[94,95]*, Reprinted with permission from AIP Publishing, (C) A microfluidic device to study oxygen deprivation in a zebrafish larva showing the schematic of the channels in which different types of gases were utilized to change the level of oxygen in the media*[30]*, Reprinted with the permission from Royal Society of Chemistry. (D) Zebrafish analysis microfluidic platform for long-term high-throughput electrophysiological monitoring*[96]*, Reprinted under permission of Creative Commons License. (E) A microfluidic device to trap a zebrafish larva from its head region, treat it chemically and track its tail movement*[97]*, Reprinted with the permission from Royal Society of Chemistry, (F) A millifluidic device for immobilization of zebrafish larvae using the concept of hydrodynamic trapping*[100]*, Reprinted with permission from Elsevier, (G) Microfluidic device for trapping a zebrafish larva from its head region while its tail is free to move*[101]*, Reprinted under permission of Creative Commons License (H) A microfluidic platform to control axial orientation of zebrafish larva. (I) Assembled platform integrated with a magnetic coil; (II), (III) Images of the platform with embedded artificial cilia. Scale bar: 11 mm (II) and 0.55 mm (III)* [102]*, Reprinted with permission from Springer Nature.*

Mondal et al.[103] developed a membrane based microfluidic device using compressed nitrogen gas to apply pressure required for deflection of the membrane and immobilization of different organisms including *Drosophila* larvae, *C. elegans* and zebrafish larvae. The immobilization device consisted of a flow layer and a control layer bonded together, with the deflectable membrane installed between them. The main trap was connected to a nitrogen gas cylinder through a three-way stop cock and a regulator to apply appropriate pressures, ranging from 3 to 14 psi for different microorganisms, onto the membrane. Using a 3 psi nitrogen gas flow, the deflected membrane could immobilize the zebrafish larvae in the flow channel to record time-lapse movies of their heartrate. The heartrate (136.8±1.6 /min) was shown to be similar to reports published before outside microfluidic devices.

Another microfluidic system was designed by Akagi et al.[104,105] to immobilize zebrafish larvae in a way that was appropriate for environmental scanning electron microscopy (ESEM). The bi-layered microfluidic device was composed of trapping and drain reservoirs located at the top layer and multiple microwells and channels engraved in the bottom layer, which contained the larvae. After loading the larvae, the excess medium was removed from the trapping reservoir with a paper filter to provide an open surface without any water around the larvae which was required for ESEM. In this way, 15 zebrafish were immobilized with their yolk fitted perfectly inside the microwell. No apparent morphological, cardiovascular and behavioral abnormalities were observed in the zebrafish immobilized on the chip and none of the parameters were statistically different from the control groups kept in a petri dish. The chip microchannels were designed to let the larvae be placed in different angles for imaging from multiple directions. Although some promising images were obtained using 4% paraformaldehyde to fix the larvae, ESEM imaging of live larvae was not performed successfully.

A new microfluidic concept was proposed by Chen et al.[102] which enabled precise and small-angle axial rotation of a larva inside the microchannel. They employed an array of artificial cilia which were integrated into the microchannel and actuated magnetically (Fig. 1-5H). After settling the larva on top of the cilia, a uniform magnetic field was applied to actuate the artificial cilia. The larva body which was in direct contact with the cilia was then forced to rotate axially in response to cilia movement. Space limitation inside the microchannel prevented the larva from translational motion. They could image the hemodynamics in a specific vessel during the larva rotation which was useful for cardiovascular assessments. Their proposed platform can facilitate zebrafish screening with a wide range of viewing angles.

Huemer et al.[106] developed a microfluidic device for high-resolution imaging which allowed application of different reagents, orientation and wounding of zebrafish larva. The device composed of three semi-open chambers for loading, trapping, wounding and imaging of 2 to 4 dpf larvae. They deposited one larva in the loading chamber and oriented it dorsally with its tail toward the restraining area. A suction from the tip of pipette held at the wounding chamber entrance was used to draw the larva into the tunnel and place it in appropriate orientation for imaging. Fluid was removed from the loading chamber and replaced by agarose to stabilize the larva's head. The process was then followed by caudal fin wounding and long-term imaging to monitor the tail development and regrowth.

Another microfluidic chip was presented to position the zebrafish larvae at a desirable orientation to facilitate microinjection[107]. Their experimental setup consisted of an imaging platform, an open-ended microfluidic channel to control the direction of zebrafish, three syringe pumps to apply pressure required for adjusting the flow inside the microchannel and an automatic stage to move the device controllably. Different micromanipulators were used to control an

injection pipette for chemical infusion and a holding pipette for rotating the larva to a desired orientation. Two syringes mounted on two different pumps were connected to the channel entrance to load the larva and control the water flow rate and direction inside the microchannel. An algorithm-based operation ensured zebrafish loading from the tail into the channel. When the larva approached the injection pipette, its tail was sucked into the holding pipette. The larva was then immobilized with the target organ positioned in front of the injection pipette. The exact location of the larva was determined through analyzing the binary image of the zebrafish. The injection pipette was then driven along the axis perpendicular to the body axis till its tip penetrated the larva's heart. Using a micro-syringe pump, a fluorometric solution was pumped out to complete the injection process. They could achieve a success rate of 94% for heart injection of 50 zebrafish larvae with a survival rate of 100%.

Ellett and Irimia[108] could immobilize 2 dpf zebrafish larvae in a micro-structured device to facilitate microinjection. Their device included a funnel shaped entrance and a straight microchannel with different traps to stabilize larvae laterally, ventrally or dorsally for injection. They put their microchip in a petri dish such that it was covered by a thin layer of zebrafish embryo medium (E3) to make larvae's manipulation easier. A hair loop was used to manipulate the anesthetized larvae in the head-first orientation towards the appropriate channel and slide them down the microchannel until they reached the trap. Adjusting the amount of surface tension through removing excess E3 from the reservoir could help them reduce the larva sliding during injection. Their device was particularly efficient for injection of particles or cells such as human cancer cells, which were prone to aggregation in the microneedles. They could also use their chip for post-injection rapid imaging of stabilized zebrafish.

Another microfluidic device was designed to culture, sort and trap zebrafish larvae using light cues and acoustic actuation[109]. An LCD light pattern was used to stimulate the optomotor behavioral response of the hatched larvae to facilitate their transportation to the trapping area. Upon reaching of the larvae to the trapping zone, a trapping sound was played to drive the larvae into the chamber. The results suggested a delayed hatching by sound treatment due to the disruption of the circadian clock chemistry of the embryos. The sound treatment damaged the mechanosensory hair cells of the larvae as well. The locomotor behavior of zebrafish larvae in microfluidic environments was more dominated by an acoustic response than the optical one. Overall, the importance of noise isolation during the embryonic stage of zebrafish was confirmed. The technique proposed for the larvae transportation can be integrated with an automated system to transfer the larvae and trap them in desired test zones on a device.

Lee et al. presented a hand-size agarose-free microfluidic chip for electroencephalogram (EEG) recording from multiple zebrafish larvae trapped in a device[110]. The design consisted of several PDMS-made microchannels where the larvae were trapped, aligned and exposed to continuous and uniform drug infusion during EEG. A reference electrode was located at the bottom of each trapping channel. For this, titanium/gold with thicknesses of 50/200 nm were sputtered on the glass. The PDMS layer and the gold-patterned glass were bonded to each other by aligning the gold ground electrodes and the trapping channels. In the trapping channels, guide columns were implemented to guide the needle electrodes to the head of zebrafish. Using pentylenetetrazole and valproic acid, they showed that their microfluidic system could contribute to the mass screening of EEG for drug development to treat neurological disorders such as epilepsy.

Cho et al proposed a microfluidic chip to examine the electrical and functional activity of 5 dpf larvae zebrafish muscles[111]. Electromyography (EMG) recording was performed to measure the

muscular activity of four larvae with high sensitivity and low electrical noise while they were inside water. Zebrafish larvae were trapped and retained in the designed chip without using anesthetic agents. The needle electrodes locked up with a micromanipulator, were then inserted into the skeletal muscles of larvae. As a proof-of-concept, EMG recordings were done in four different conditions with larvae preincubated in a drug-free solution and three different chemicals that manipulate muscle activities, i.e., tricaine, N-methyl-D-aspartate, and dizocilpine. The electrical signals of less than 200 μV were produced by control group which was consistent with the intramuscular signals of adult zebrafish reported previously. No muscle activities were reported in the tricaine group. The N-methyl-D-aspartate group showed a significant increase in locomotor frequencies and signal amplitudes while a significant decrease was detected in the frequency of bursts and amplitudes of dizocilpine group. Their technique presents away for high-throughput electrophysiological recording of zebrafish and can be considered as an effective tool in diagnosing and examining the effect of different therapeutics on neuromuscular disorders.

Another microfluidic device was developed to assess and quantify the toxicological effects of food additives on 3-9 dpf zebrafish larvae[112]. Wang et al. investigated zebrafish cardiovascular activity upon exposure to two different food additives of Cochineal Red and Brilliant Blue FCF. Zebrafish swimming behaviors were also further studied through observation of the induced fluid flow pattern disturbed by zebrafish pectoral fin beating using micro-particle image velocimetry. Their result showed that 0.2% concentration of both Cochineal Red and Brilliant Blue FCF additives significantly increased the average heartrates of zebrafish control group. Cochineal Red pigment at a concentration of 0.2% also significantly affected the pectoral fin swing behavior of zebrafish larvae. Their research can be further extended to the comprehensive hydrodynamic

analysis of zebrafish pectoral fins. The information obtained from this investigation can improve the drug discovery and screening technology.

Zhang et al. designed a microinjection platform for anesthetized zebrafish larva[113]. A customized auxiliary microfluidic chip was developed to position the larva at the channel exit and control its head's direction. A rotation micromanipulator was employed to rotate the larva and move it to align the organ of interest to the injecting pipette tip. The larva aspiration was also controlled by an adaptive robust controller in order to minimize the damage to the larva body. After injection, the injection pipette was retreated, and the micromanipulator was driven to remove the larva before the next larva entered the channel. Their presented strategy offered high success rate, low cost, stability and easy implementablity.

1.3.2.2. Freely Moving Zebrafish Larva Assays on a chip

A microfluidic chip was proposed to study the auditory function of zebrafish larvae by inducing hearing damage in their sensory hair cells located in the lateral line[114]. Using a $6mm \times 2mm \times 1mm$ main channel, which was suitable for a zebrafish larva with the head width of ~0.8mm, and twelve pairs of auxiliary side channels with $60°$ angle to the main channel, they could induce damage to the hair cells without affecting the internal organs of the larva. They utilized a 3D computational fluid dynamics (CFD) simulation to decrease the trial-and-error steps in their design and to determine the flow pattern inside the device in a more efficient manner. The flow inside the chip was accurately controlled to achieve a high velocity at the sides of larva's head to induce damage in the hair cells. The results obtained from simulation indicated that design parameters such as the channel size and the auxiliary channels angle could affect the shear stress on the fish lateral line and the pressure on the fish head.

We developed a simple and efficient microfluidic device to quantify rheotaxis (orientation against flow direction) among 5-7 dpf zebrafish larvae in an accurate and repeatable manner[115]. A semi-confined larva was positioned along a channel and exposed to a streamlined constant-velocity flow directed axially towards the larva. We used water flow as a stimulus to demonstrate how flow velocity and direction can affect the rheotaxis behavior. Zebrafish larvae were exposed to different flow velocities (9.5, 19 and 38 mm/s) in the tail to head direction and their response in terms of reorientation rate and location along the microchannel was investigated. A high rheotactic response at 9.5 and 19 mm/s flow velocities were observed. However, a significant decrease in the rheotactic response was detected upon exposure to a higher flow velocity of 38 mm/s. The response location was also affected by the flow velocity. At higher velocities, the larvae were more inclined to show rheotaxis at the posterior and anterior ends of the microchannel.

We also studied the effect of electric stimulus on the movement of 5-7 dpf wild type (WT) zebrafish larvae (electrotaxis[116–118]) in a fluidic channel with two electrodes at its ends (Fig. 1-6A)[99]. We exposed zebrafish larvae to electric currents in the range of 1-25 μA in the tail-to head direction (cathode at the head). Exposing to 3-9 μA electric current, the larvae displayed a strong tendency to orient towards the anode pole. However, electric currents lower than 3 μA and higher than 9 μA led to inconsistent response and spontaneous paralysis of the larvae, respectively. We also demonstrated a significant decline in zebrafish electrotaxis at night which could be rescued through exposure of the larvae to apomorphine, a dopamine agonist. We examined the role of D1 and D2-like receptors in electrotaxis regulation. Zebrafish larvae were treated with 16.7 μM Quinpirole (D2 receptor agonist) and 50 μM SKF-38393 (D1 receptor agonist) and exposed to an electric current of 3 μA in the device. The results demonstrated a significant improvement of electrotaxis response upon exposure to quinpirole suggesting the involvement of D2 receptors in

modulating elextrotaxis of zebrafish larvae. However, treatment with SKF-38393 was not effective on electrotaxis. These results showed the feasibility of applying the electric stimuli inside the microfluidic device to produce instantaneous and repeatable locomotor responses in zebrafish larvae in a simple, repeatable and controllable manner.

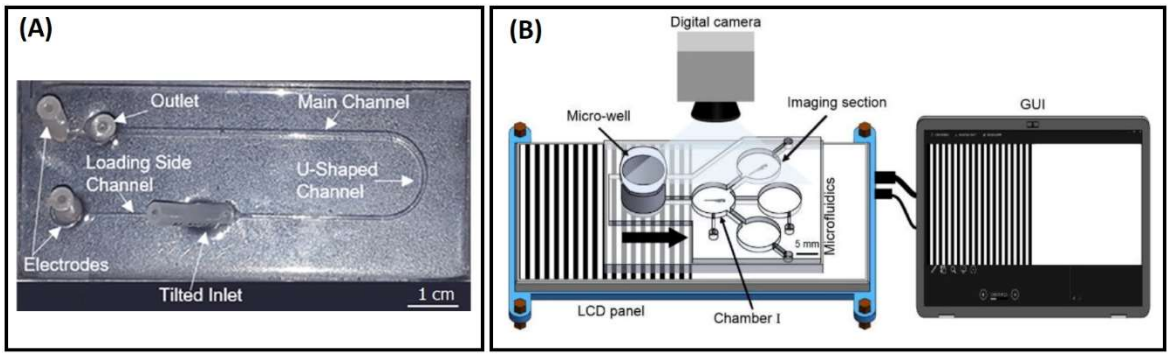

Fig. 1-6. Microfluidic devices for screening free to move zebrafish larvae (A) The top view of electrotactic-based microfluidic device[99]*. (B) The experimental setup including imaging section, micro-well and micro chambers to induce movement in zebrafish larvae using light stimuli*[119]*, Reprinted with permissions from AIP Publishing.*

A microfluidic device consisting of a chamber, a microwell and three imaging sections was also developed by Mani et al[119] to examine the feasibility of using a light driven method to induce guided movement in zebrafish larvae. A graphical user interface was used to generate an artificial visual stimulus at the bottom of the device. The larvae were transported from the breeding chamber into the three different imaging sections. As shown in Fig. 1-6B, three paths were designed to examine whether the larvae's response was resulted from the generated gratings, their nature or specific chip design. The results demonstrated that the moving grating could persuade the larvae to swim along the direction of the stimulus. Interestingly, larvae's response to the stimulus generated horizontally was weaker than those produced upon exposing them to sidewise signals.

Their presented platform can be employed for automatic transportation of larvae in different microfluidic devices.

Another study presented two microfluidic platforms in which zebrafish larvae transportation was guided by a combination of optical and hydromechanical cues[120]. The first microfluidic device consisted of one experimental chamber and two microwells, whereas the second device consisted of two additional test sections for potential drug testing with side ports to administer the fluidic requirements. Optical cues were generated by computer-animated gratings moving under the larvae to drive their optomotor response. Whereas different flow rates were used as hydromechanical cues. The results demonstrated that larvae transportation and orientation can be regulated by both modalities. The proposed platform can be utilized for drug screening and neurobehavioral studies.

Subendran et al. proposed a novel microfluidic chip coupled with a shape memory alloy actuator to immobilize the zebrafish larvae within the observation region[121]. They connected a flow visualization method with a biological experiment to quantify the influence of cochineal red food additives on zebrafish larvae behavioral responses. They analyzed the vorticity generated by zebrafish larvae tail-beating and hypothesized that the tail-beating might have been induced by the overdose of food additive exposure. Their findings can provide a protocol for new drug development and discovery.

In this section, we showed that microfluidic technology has led to the emergence of many useful tools for the analysis of zebrafish embryos and larvae in different biological applications including behavioral and neurobiological assays. Employing microfluidics, simple devices can be developed with high accuracy for applications in investigation of the zebrafish larvae behavior evoked by different stimuli.

1.4. Scientific and Technological Gaps

Animals can sense various stimuli and respond to them by producing nerve impulses travelling to the brain via sensory neurons. Upon detecting the stimulus, a response, which is often in the form of a behavior, will be produced by the animal. Exposing an awake organism like zebrafish larva to a controlled sensory stimulus, one can simultaneously screen the neural networks involved in sensing the stimulus and the behavioral dynamics involved in the consequent response. Among the sensory-motor studies presented in the previous section, electrical stimulus can be considered as one of the best candidates for evoking and studying locomotor behavior because it can be turned on and off quickly and manipulated on-demand in terms of magnitude, direction, and time. Moreover, mild electric signals have been shown not to affect small model organisms like *C. elegans* and zebrafish significantly[116,122]. As mentioned in the previous section and our review paper[123], there are a few studies that have employed electric current for conducting movement-based behavioural assays on zebrafish[63,122,124]. However, there are still several technological and scientific gaps related to zebrafish electric-induced behavior which should be addressed, with some scientific and applied questions that are listed below.

1. Are zebrafish sensitive to different amplitudes of electric currents and voltages, repeated electrical stimulation, and the field direction? How are the response phenotypes affected by these parameters?
2. Are any genes or neurons involved in zebrafish response to electric signal?
3. Can electric-induced response be utilized for disease studies, chemical screening, and drug discovery?

In addition to the questions above, several technological gaps can be found in studying zebrafish response to electric signals. There are some difficulties associated with manipulation of zebrafish larvae and electric signal as well as screening of zebrafish behavioral responses. When this research started in 2017, the first challenge was to partially immobilize zebrafish larvae to quantify a variety of their subtle behaviors induced by electrical signals such as response duration (RD), tail beat frequency (TBF) and heartrate. Establishing a suitable environment to deliver an on-demand, accurate and controllable electrical signal to the zebrafish larvae to evoke their response was another challenge. Beyond fundamental studies, exploiting the electric-induced locomotion response can lead to the development of application-driven microfluidic devices for quantitative chemical and gene screening assays on zebrafish models of neurodegenerative diseases like Parkinson's disease (PD). Moreover, simple and easy to use electrofluidic-based chips were yet to be developed for testing of multiple larvae to enhance the throughput of behavioral assays.

1.5. Thesis Goals and Objectives

Considering the abovementioned gaps, this thesis aimed to enhance our understanding of the electric-induced response of zebrafish larvae and the effects of electric field on various phenotypes using novel electrofluidic screening techniques with enhanced efficiency and behavioral throughputs. Multiple microfluidic devices were developed and progressively improved for this purpose and their applications for chemical and gene screening with quantitative behavioral readouts were exploited. To achieve our goal, different objectives were pursued during this research as follows (objectives are not presented in a chronological manner):

Obj. 1- Phenotypically investigate behavioral organ-based responses of zebrafish larvae upon exposure to electric stimulus.

Obj. 2- Investigate the effect of electric current, voltage, field direction and repeated electric stimulation on zebrafish larva's response to electricity.

Obj. 3- Increase the throughput of the electrofluidic screening technique.

Obj. 4- Investigate if dopaminergic pathway is involved in electric-induced movement response of zebrafish larvae.

Obj. 5- Investigate the application of zebrafish electric-induced response in chemical toxicity and gene screening assays.

The phrase "enhanced throughput" used in this thesis for behavioral assays refers to a range of tens of larvae per hour. Behaviours take time to be evoked, and timelapse studies are needed for transient and mean response evaluations, so such experiments are slow in nature which lowers the assay throughput. We acknowledge that the throughput of molecular and cellular screening assays of zebrafish can be substantially higher than the behavioral studies.

To address the scientific and technological gaps in this thesis, we developed novel microfluidic techniques to phenotypically investigate behavioral responses of zebrafish larvae upon exposure to electric stimulus and assess these responses (Obj. 1). Larvae were head-trapped individually and laterally restricted in the microfluidic device so that only longitudinal orientation and movement was allowed. As such, the 1-dimensional tail movement of larva upon exposure to the electrical stimulus could be easily monitored within a screening region and quantified. We then modified the microfluidic device and added a novel technical functionality to our chip to monitor the organ-based response of zebrafish larva. The core component of this system was an optical prism integrated into the microfluidic device to enable side imaging of the larvae to monitor their heart activity. Our technique facilitated cardiac screening and behavioral study of awake larval zebrafish in the same chip in their physiologically natural orientation, for the first time.

To achieve Obj. 2, some pilot experiments were then designed to interrogate the zebrafish response to different electric currents and voltages to determine how the electric-induced response was sensitive towards the voltage difference across larva's body and the flow of current. The effect of electric field direction on the electric response was also investigated. Finally, zebrafish larvae were exposed to multiple electric stimuli to investigate if they show habituation towards repetitive exposures to electricity.

At this stage, the device design was modified to monitor the behavioral responses of multiple zebrafish larvae simultaneously (Obj. 3). Multiple microfluidic traps were positioned beside each other with the possibility of loading, immobilizing, and behavioral screening of a group of larvae at the same time. Such opportunity could increase the throughput of our behavioral assay while maintaining its simplicity, making it more attractive for biologists to use and expediting the data analysis process.

To approach Obj. 4, and considering the similarities between major dopaminergic pathways in zebrafish and mammalian subtypes, we learned that compounds that target the dopaminergic system have similar effects on zebrafish and mammals[30]. Generally, dopaminergic receptor agonists enhance locomotor activity, while antagonists block the dopamine receptors and decrease locomotor activity. In our research, zebrafish larvae were exposed to different drugs that target dopaminergic receptors in mammals to investigate if they could affect zebrafish response to electric signal. The test results have shed light on the potential involvement of dopaminergic neurons in zebrafish electric-induced response.

Finally, in Obj. 5, for proof of concept of the use of our electrofluidic device in chemical screening, we investigated if 6-hydroxydopamine (6-OHDA), a neurotoxin, and Levodopa, a PD modifying drug, could affect the zebrafish larvae electric-induced locomotor responses. The

electric-induced response of Pannexin1a (Panx1a) knockout (KO) larvae was also monitored and compared with the WT group to investigate the application of our electrofluidic device in gene screening assay and shed some light on the possible involvement of this gene in the electric response.

1.6. Thesis Outline

This thesis consists of 7 chapters, starting with an introduction to the zebrafish model organism in the first chapter followed by a review of the conventional and microfluidic platforms used for behavioral screening. Second chapter reports on the methodologies and materials utilized to fabricate the microfluidic devices, chemicals used in our chemical screening assays, data and statistical analysis and viability tests conducted to evaluate the performance of our proposed devices. Third chapter elaborates on our single-fish microfluidic devices for studying electric-induced and organ-based behavioral responses of semi-mobile zebrafish larvae (Obj. 1). The sensitivity of zebrafish electric-induced response towards the electric current intensity, voltage drop, field direction and multiple exposure to electric stimuli is also investigated (Obj. 2). In forth chapter, a new design is proposed to increase the throughput of our electric-induced behavioral assay (Obj. 3). Then, in chapter five, zebrafish larvae are exposed to different drugs that target dopaminergic receptors in mammals to investigate if they could affect zebrafish response to electric signal (Obj. 4). Sixth chapter discusses the application of zebrafish electric-induced response in chemical toxicity and gene screening assays (Obj. 5). Finally, in chapter seven, we provide a summary of the thesis with a focus on its limitations and propose the future directions of our research.

1.7. Publication Contributions

This thesis has been written based on the papers co-authored by the PhD candidate (See list of thesis publications section). The following describes my contribution to the mentioned articles. Chapter 1 is based on a review paper[123] that was originally drafted by me and revised by my supervisor, Prof. Pouya Rezai. The contents of chapters 2-6 have been extracted from seven journal papers[125–130] (one under preparation). For all papers, I designed and performed the experiments, from device design and implementation to data analysis in collaboration with Ellen van Wijngaarden. I wrote the original drafts and the initial responses to reviewers, and they were revised by Prof. Pouya Rezai and Prof. Georg R. Zoidl. Prof. Pouya Rezai and Prof. Georg R. Zoidl helped with conceptualization and device design enhancement and provided constructive feedback to guide my research. They also helped with reviewing original drafts of the conference and journal papers. Khaled Youssef, Nickie Safarian, Alireza Zabihihesari and Amir Reza Peimani have also contributed to the code development, numerical analysis and molecular tests in different papers.

Chapter 2[†]

2. Materials and Methods

In this chapter, we introduce the chemicals used in our experiments and explain the zebrafish larvae generation and maintenance procedure and methodologies common between our various experiments. The chapter will be continued with the viability tests, behavioral phenotyping and data analysis, and ended with statistical tests performed in this thesis.

[†] Some content of this chapter has been published in:

1. Khalili, A. R. Peimani, N. Safarian, Kh. Youssef, G. Zoidl, P. Rezai, "Phenotypic Chemical and Mutant Screening of Zebrafish Larvae using an On-Demand Response to Electric Stimulation", *J. of Integrative Biology,* vol. 11, no. 10, pp. 373–383, 2019. Permissions for the use of the text has been received from Oxford University Press.
2. Khalili, E. van Wijngaarden, G. Zoidl, P. Rezai, "Multi-Phenotypic and Bi-Directional Behavioral Screening of Zebrafish Larvae", *J. of Integrative Biology,* vol. 12, no. 8, pp. 211–220, 2020. Permissions for the use of the text has been received from Oxford University Press.
3. A. Khalili, E. van Wijngaarden, G. Zoidl, P. Rezai, "Zebrafish Larva's Response to Electric Signal: Effects of Voltage, Current and Pulsation for Habituation Studies", *J. of Sensors and Actuators: A. Physical,* vol. 332, 113070, 2021. Permissions for the use of the text has been received from Elsevier.
4. Khalili, E. van Wijngaarden, Kh. Youssef, G. Zoidl, P. Rezai, "Designing Microfluidic Devices for Behavioral Screening of Multiple Zebrafish Larvae", *Biotechnology J.,* e2100076, 2021. Permissions for the use of the text has been received from John Wiley and Sons.
5. Khalili, E. van Wijngaarden, G. Zoidl, P. Rezai, "Dopaminergic signaling regulates zebrafish larvae's response to electricity", *Biotechnology J.,* 2100561, 2022. Permissions for the use of the text has been received from John Wiley and Sons.

2.1. Zebrafish Larvae Generation and Maintenance

Adult WT Tupfel long fin strain (TL) and Panx1a KO zebrafish were maintained and raised at 28°C with a 14:10 hours of light:dark cycle inside a recirculation system (Aquaneering, USA). Fish were fed ad libitum with brine shrimps (Brine Shrimp Direct, Odgen, Utah, USA) twice a day. Eggs from natural spawning were collected, rinsed and maintained in the egg water, containing 60 mg/ml of instant ocean sea salt (Instant Ocean, Blacksburg, USA) and 0.1% methylene blue (M291-100 Fisher Scientific, USA). Embryos were maintained in the egg water inside an incubator (28°C). After hatching, the larvae were collected and used for experiments at 5-7 dpf. The Panx1a KO zebrafish were generated by transcription activator-like effector nucleases (TALEN) technology using the procedures outlined by Bedell et al.[131]. In this study, the larvae of the F3 generation were tested. These larvae have a 4pb frame shift mutation in the exon 4 of the Panx1a gene generating a truncated channel protein with a premature stop codon at amino acid position 191. The instructions and specifications outlined in the Canadian Council for Animal Care (CCAC) and ACC protocol *GZ 2020-7* were diligently followed. The number of experiments and the zebrafish larvae were kept to the minimum required, following guidelines approved by York University biosafety permit *PR 02-19*.

2.2. Chemical Exposure

We have used ethanol, 6-OHDA and levodopa for our chemical toxicity assays. Three dopamine agonists of apomorphine, SKF-81297, quinpirole and dopamine antagonists of butaclamol, SCH-23390, and haloperidol were also used to investigate the involvement of dopaminergic neurons in electric-induced locomotor response of zebrafish larvae. All chemicals were purchased from

Sigma-Aldrich (St. Louis, MO, USA). The concentration and preparation method of each chemical will be elaborated in the next section.

2.2.1. 6-OHDA and Levodopa Exposure

Two mM 6-OHDA was prepared and stored in single-use Eppendorf reaction tubes at -20 °C. It was thawed, diluted to reach the suitable concentration of 50, 100 or 250 µM and applied to the swimming medium of the growing zebrafish when required. A total of 15 embryos per well were placed in a 12-well plate and 6-OHDA was administered in the swimming media starting at 2 dpf. Each well contained 3 mL of prepared solution. Considering the light sensitivity of 6-OHDA, the multi-well plates were covered with aluminum foil to avoid light exposure. To keep consistent condition, the control groups not exposed to 6-OHDA were also kept in well plates and shielded from light in parallel with the test group. Levodopa at 0.5 mM, 1 mM or 2 mM concentration was prepared daily in swimming medium. Concentration of 6-OHDA was selected following previous studies[40,41], while different concentrations of levodopa (except 1 mM[40,132]) were tested for the first time.

2.2.2. Dopamine Antagonist and Agonist Exposure

Six dpf TL zebrafish larvae were divided into several groups to generate sample sizes of 45 fish per condition to study the effects of dopamine agonists and antagonists presented in Table 2-1. All exposures were done off-chip, with all larvae in each category exposed to a specific test chemical and washed off at the same time. The concentrations and exposure times presented by Iron et al.[56] were used for each drug and the desired compounds were administered in the swimming media. A total of 15 embryos per well were placed in a 12-well plate, with each well containing 3 ml of the prepared solution.

Table 2-1. Dopamine agonists and antagonists used in our chemical screening assays along with their concentrations and exposure times which were selected based on the literature[56].

	Non-selective		D1-like selective		D2-like selective	
	Agonist	**Antagonist**	**Agonist**	**Antagonist**	**Agonist**	**Antagonist**
Chemical	Apomorphine	Butaclamol	SKF-81297	SCH-23390	Quinpirole	Haloperidol
Concentration	0.2 μM	16.7 μM	50 μM	0.6 μM	16.7 μM	16.7 μM
Exposure time	20 min	20 min	140 min	260 min	80 min	200 min

All chemical compounds were mixed with egg water to produce the desired stock concentration with one exception. Haloperidol was the only drug that required dimethyl sulfoxide (DMSO) as a solvent due to its low solubility. The solutions were then diluted with egg water to reach the desired concentrations ranging between 0.2–50 μM. In contrast, Haloperidol was diluted with 0.4% DMSO to make the stock solution and further diluted with egg water to form the desired concentration.

Prior to conducting an experiment, larvae were divided into groups and exposed to the desired chemicals as reported in Table 2-1. A total of 12 groups of larvae were tested, i.e., 1 control group with no electric and chemical exposure, 1 control group with no chemical exposure, 3 groups for dopamine non-selective antagonists and agonists, 6 groups for D1- and D2-like selective antagonists and agonists, and 1 group for DMSO (as Haloperidol solvent) control.

2.3. Microfluidic Device Fabrication

In this thesis, different microfluidic devices were designed and progressively improved to investigate behavioral responses of zebrafish larvae to electric signals, and each chip required a specific design.

All devices were fabricated by replica molding of PDMS prepolymer against plastic master molds. The master molds for PDMS casting were designed using the SolidWorks software

(SolidWorks Corp., USA) and printed using an Objet260 Connex3 printer (Stratasys Ltd., USA). Printed molds were first thoroughly cleaned with soap and water to remove any support material.

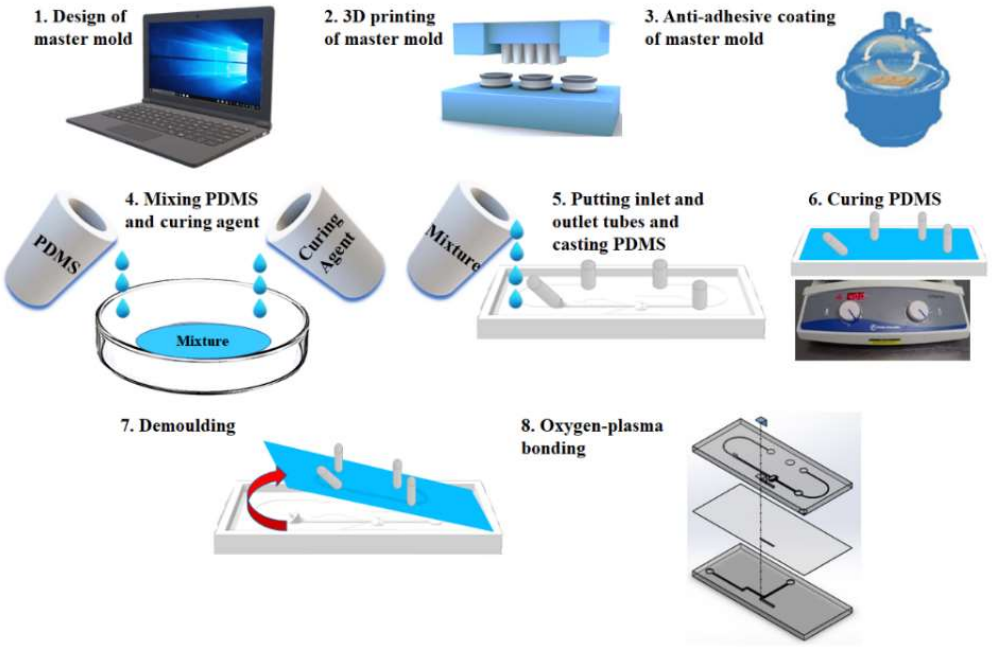

Fig. 2-1. Microfabrication process for the development of PDMS-based microfluidic devices in this thesis.

A 10:1 ratio of PDMS base to curing agent (Sylgard 184 kit from Dow Corning, MI, USA) was thoroughly mixed and air bubbles were removed using a vacuum chamber for 30 minutes at room temperature. After positioning the inlet and outlet tubes (Cole-Parmer Canada. QC, Canada) with an inner diameter of 1.6 mm in their respective reservoirs, the PDMS pre-polymer was poured into the mold. The device was then allowed to be cured on a hotplate at 50 °C for 6 hrs[103]. Once fully cured, the PDMS layer was removed from the mold and oxygen-plasma treated at 870 mTorr pressure and 30W for 30s to glass or additional layers of PDMS (more details are provided in the following chapters) to produce the final device. This final step was completed using a plasma bonder (PDC-001-HP, Harrick Plasma, USA) for surface activation and bonding of the layers. Using this method, our microfluidic devices could be fabricated with good reproducibility. Therefore, it was not required to fabricate several devices to check for technical errors in our

experiments. However, the errors associated with the operator, experimental setup and variability among tested larvae remained inevitable. The designs and operations of our proposed devices will be elaborated later in more details.

2.4. Design of Microfluidic Devices

Three main types of microfluidic devices were developed in this thesis which are described in the next sub-sections. Briefly speaking, we started with a *single-fish device* in which one zebrafish larva at a time could be immobilized from the head region and screened from the tail region. This device was then improved into a version in which not only the tail, but also the heart function of the same larva could be studied quantitatively (called *multi-phenotypic single-fish device*). Finally, we offered a device in which multiple fish could be head trapped and tail monitored (called *multiple-fish device*), noting that beyond the scope of this thesis, we have also successfully implemented another multiple-fish device to monitor the heart and fin functionality.

2.4.1. Single-Fish Microfluidic Device

A microfluidic device shown in Fig. 2-2 was used for electrical stimulation and phenotypic behavioral screening of 5-7 dpf semi-mobile zebrafish larvae. It was made of three separate PDMS layers that were plasma-bonded together. The top main layer consisted of a 45º-angled inlet tube, a loading channel, 2 side U-shaped channels, a funnel-shaped TR and a screening pool (adopted from the work in our group by Nady et al.[97] (Fig. 1-5D) on chemical screening, and an outlet tube. The middle layer was a ~200 µm thick PDMS membrane sandwiched between the top and bottom layers. The bottom valve layer consisted of a L-shaped channel, called the valve actuation channel, which was designed underneath the TR with a 1.5 mm offset from the screening pool, and used to

prevent larva's escape from the trap by deflecting the PDMS membrane into the main channel in front of the larva.

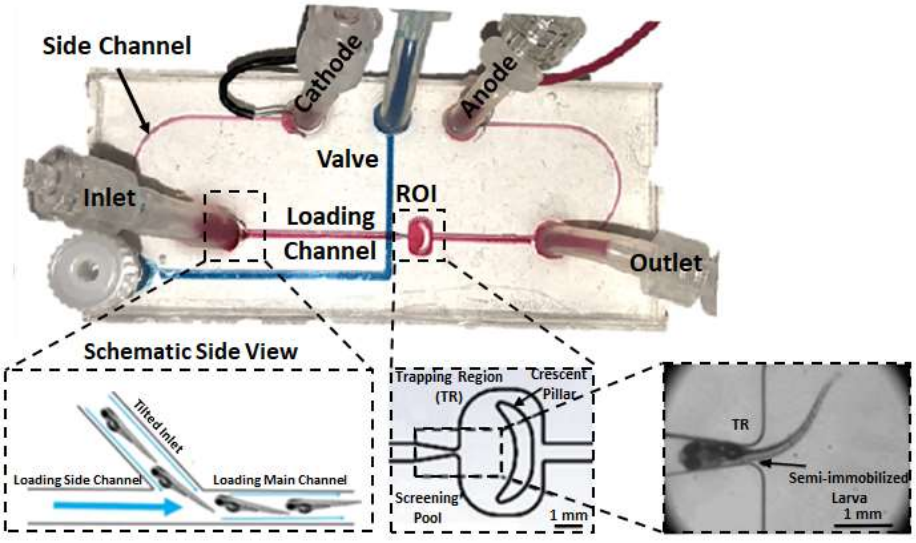

Fig. 2-2. Microfluidic device for screening the electric-induced response of semi-mobile 5-7 dpf zebrafish larva. The device consisted of three layers, i.e. a main (top) layer containing the TR and the screening pool, a valve (bottom) layer for maintaining the larva in the TR, and a PDMS membrane (middle) layer sandwiched between the top and bottom layers. The region of interest (ROI) is magnified to show more details about the TR, pool, and crescent-like pillar. The TR is magnified to display how a larva is partially immobilized. The tail tip-point shown by a black circle was tracked by a software for behavioral quantification. The main channel centerline and two lower and upper thresholds are also drawn manually which helped with quantifying the TBF[129]*. Reprinted with permission from Oxford University Press.*

The 45º-angled inlet tube was designed to facilitate a smooth loading of a larva into the device as schematically shown in Fig. 2-2 left inset. The loading channel with 0.9 mm width and 25.2 mm length was used for delivering the larva from the inlet reservoir into the TR hydrodynamically. Two U-shaped side channels with 0.5 mm width, 0.2 mm depth and 53 mm length were used to connect the inlet and outlet to the electrode reservoirs. These channels were implemented to (i) place the electrodes at their anterior ends for electric current application, (ii) maintain the electrical

resistance of the device at ~35 MΩ which is comparable to our previous screening device for freely moving larvae[99], (iii) provide a side flow to safely transfer the larva from the inlet into the loading channel, and (iv) save space for a cost- and size-effective design.

For efficient immobilization, the TR design mimicked the approximate shape and size of 5-7 dpf zebrafish larvae's head up to the yolk region, i.e., gradually narrowing from 0.9 mm to 0.25 mm, connecting the loading channel to the screening pool. The screening pool with 6.5 mm length and 4.35 mm width was added for monitoring the whole range of zebrafish's tail motions including the highest striking tail oscillations such as C-bend and struggling swimming motions[58], when the larva was exposed to an electric current in the TR. We added a crescent-shaped pillar inside the screening pool to preclude the middle-layer PDMS membrane from collapsing. The pillar also prevented disruptive bubbles from being trapped and aggregated at the pool corners. The outlet channel with 0.9 mm width and 17.9 mm length was used to remove the larva after each experiment. The depth of all channels except U-shaped side channels was 0.55 mm.

2.4.2. Multi-Phenotypic Single-Fish Microfluidic Device

The single-fish device introduced in the previous section was further modified to enable simultaneous screening of heart and tail activity of zebrafish larva in the same chip (Fig. 2-3A). The device contained two major components, i.e., a larva TR and an optical prism as shown in Fig. 2-3B and 3C, respectively. The previous design was improved by integrating a 5 mm optical right-angle prism (Edmund Optics, USA) to provide a lateral view of the larvae and enable cardiac screening, making the device applicable for bi-directional imaging of zebrafish larvae. The orientation of the prism beside the microchannel and the two imaging paths are shown in Fig. 2-3C. The path of the valve channel was selected to avoid interference with the prism when the device was bonded.

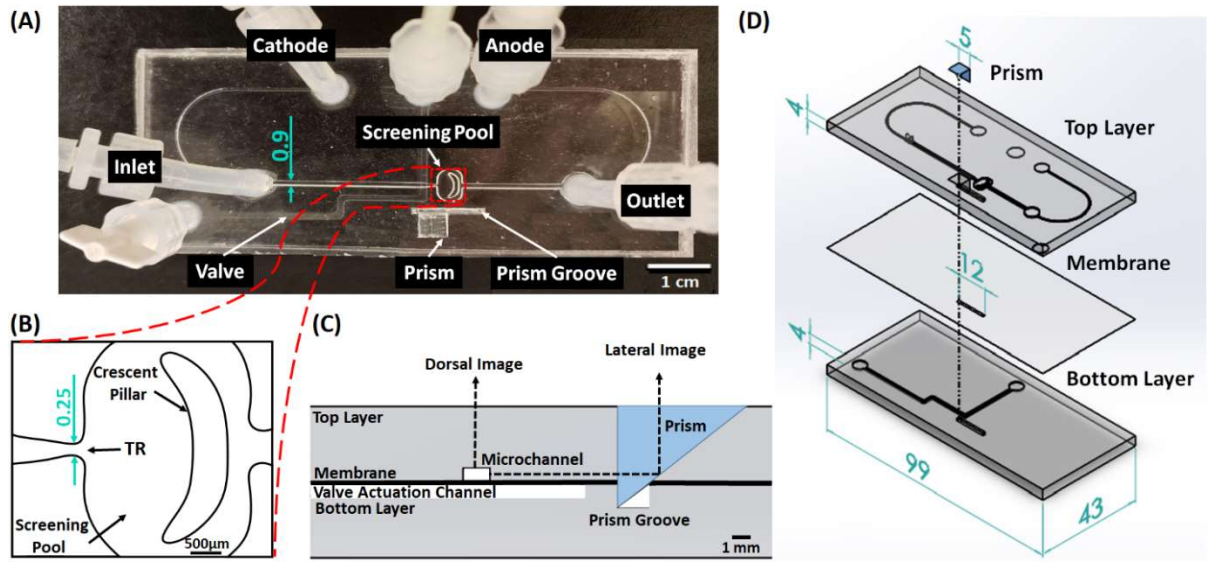

Fig. 2-3. The multi-phenotypic microfluidic device for multi-directional imaging and behavioral study of zebrafish larva. (A) The device consisted of an angled-inlet, two U-shaped side channels, a main channel, a TR, a screening pool, an outlet, two electrode reservoirs, a trapping valve channel and a prism set in a groove. (B) The magnified view of the TR and the screening pool. (C) Side cross-section view of the device (from left viewpoint) which shows the prism orientation and its position with respect to the channels. (D) Exploded view drawing of the device layers. All dimensions are in mm[126]*. Reprinted with permission from Oxford University Press.*

To integrate the prism into the device, a 1 mm deep, 1 mm wide and 12 mm long groove was designed 1.7 mm away from the screening pool on the top layer master mold. This allowed for the prism to be fixed in place as the top PDMS layer was being cured. It also positioned the bottom of the prism below the main channel, as shown in Fig. 2-3C, to obtain a clear lateral view of the fish. The top surface of the prism was left uncovered when pouring PDMS into the mold. During bonding, care was taken to align the prism in the top layer with a groove inside the bottom layer (Fig. 2-3D).

The tip of the prism was used to reflect the optical path of the side view, providing a shorter distance between the microchannel and the reflection point (Fig. 2-3C). The two dashed arrows in

Fig. 2-3C depict the optical paths of the lateral and dorsal views. To achieve simultaneous dual view imaging of a larva, the difference between the focal lengths of the lateral and dorsal optical paths should be compensated. This was achieved by addition of an optional PDMS compensating layer on top of the prism as shown in Fig. 2-4. The thickness of this layer was calculated based on Snell's law of refraction in Eq. 2-1[133].

$$n_0\, sin\theta_0 = n_1 sin\theta_1 \qquad \textit{Eq. 2-1}$$

The variables in Snell's equation refer to the incident index (n_0), refracted index (n_1), incident angle (θ_0) and refractive angle (θ_1) of a ray of light passing through a surface. Following the method outlined by Kazama et al.[133], Eq. 2-1 was rearranged as Eq. 2-2 and Eq. 2-3 to find the focal-length shift of paths 1 and 2 ($d_1$and d_2) in Fig. 2-4.

$$d_1 = l_1\left(1 - \frac{n_0}{n_{PDMS}}\right) \qquad \textit{Eq. 2-2}$$

$$d_2 = (l_2{+}l_c)\left(1 - \frac{n_0}{n_{PDMS}}\right) + l_p\left(1 - \frac{n_0}{n_{Prism}}\right) \qquad \textit{Eq. 2-3}$$

The parameters and refractive indices used in our study were summarized in Fig. 2-4. Substituting $d_1$and d_2 in Eq. 2-4, a thickness of 12 mm was determined for the compensating layer (l_c).

$$d_1 + l_2{+}l_3 = d_2 \qquad \textit{Eq. 2-4}$$

For the dorsal view of the tail, the larva was observed through the PDMS layer on top of the microchannel as shown by path 1 in Fig. 2-4. For the lateral view of the heart, the larva was observed through the compensating PDMS layer, the prism, and the PDMS layer between the microchannel and the prism, i.e. path 2 in Fig. 2-4.

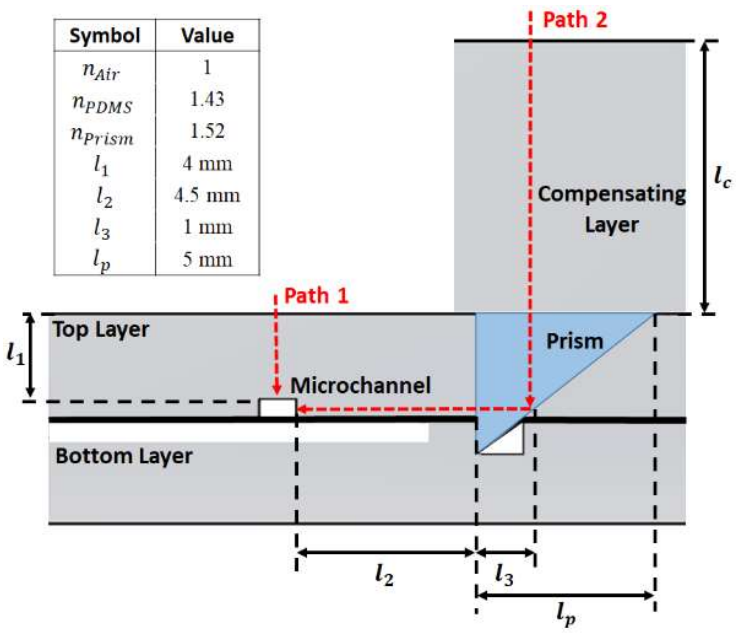

Fig. 2-4. Side view of the multi-phenotypic microfluidic device with a compensating PDMS layer added to facilitate simultaneous dorsal and lateral imaging of zebrafish larvae[126]*. Reprinted with permission from Oxford University Press.*

2.4.3. Multiple-Fish Microfluidic Device

Our single-fish design (Fig. 2-2) was used as a reference device and iteratively modified for multi-fish screening. Several modifications including altered trap dimensions and alternative loading and orientation techniques were considered to design a novel device, enabling simultaneous behavioral screening of two fish. Common components of the designs included an inlet, a main channel, larva TR, screening pool and outlet, as shown for our single-fish design in Fig. 2-2. Different loading and orientation strategies from addition of an orientation loop to indirect flow assisted loading were considered to increase the number of larvae tested at the same time which will be described in detail in chapter 4. The final design shown in Fig. 2-5 enabled behavioral screening of four larvae at the same time. We have successfully integrated 4 prisms

into this chip recently, for simultaneous monitoring of heart functions of the 4 larvae, but this will not be discussed in this thesis.

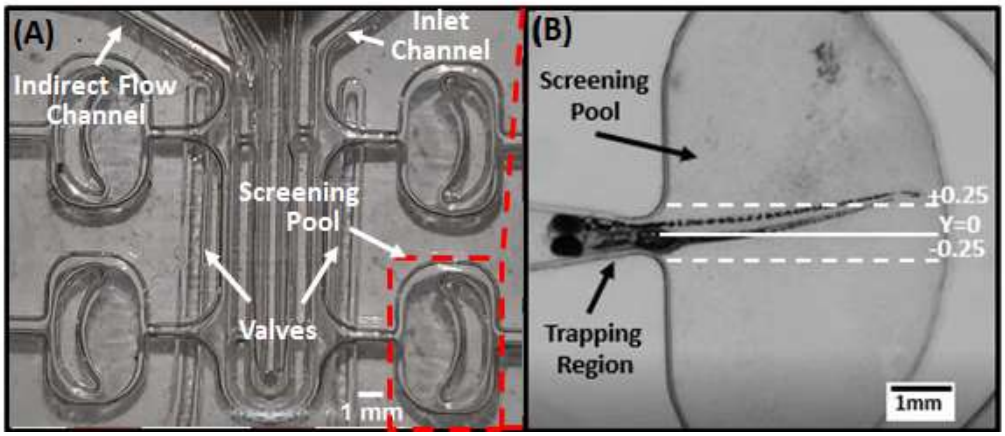

Fig. 2-5. The quadruple-fish microfluidic device for screening the electric-induced response of semi mobile 5-7 dpf zebrafish larvae. (A) The labelled device identifying the screening pools and valve channels. (B) A close-up view of the screening pool with a larva trapped in the TR with its tail free to move in the screening pool[130]*. Reprinted with permission from John Wiley and Sons.*

2.5. Experimental Setup

The experimental setup (Fig. 2-6) consisted of one of the designed microfluidic devices which was placed under a of a Leica upright microscope (Stereomicroscope Leica MZ10F, Singapore), equipped with digital C-mount camera (GS3-U3-23S6M-C, Point Grey Research Inc., Canada). An electric sourcemeter (Model 2410, Keithley, USA) was used to apply a Direct Current (DC) electric signal to electrodes of the device to supply electric stimulus during behavioural screening. The necessary number of syringe pumps (LEGATO 111 and 110, KD Scientific Inc., USA) based on the device design were used for loading and positioning a zebrafish larva inside the device.

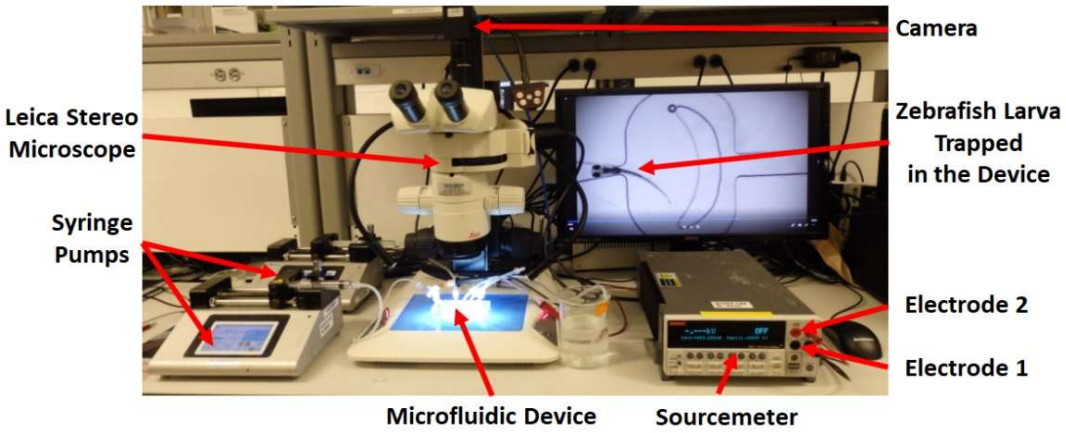

Fig. 2-6. The experimental setup to test microfluidic devices for behavioural screening of zebrafish larvae, with the main equipment including one or two syringe pumps, microscope, electrical sourcemeter, and a computer[127]*. Reprinted with permission from Elsevier.*

2.6. Experimental Procedures

2.6.1. Single-Fish Microfluidic Device

The first step in each experiment was loading zebrafish larvae into the device. To conduct the experiment, a 5-7 dpf zebrafish larva was pipetted into the device inlet (Fig. 2-2). Flow rates of 2, 0.2, and 1 ml/min in the tilted inlet, side, and main channels were used, respectively, to load the larva smoothly into the TR. The side channel assisted the loading process by providing a side flow around the larva's body to prevent it from colliding with the channel base and walls (Fig. 2-2 left inset). Rheotaxis response of the larvae[115] ensured loading them from the tail side into the TR for majority of the loading attempts.

Once the zebrafish larva was positioned in the TR, the valve actuation channel was pressurized with air to stabilize the larva inside the TR (Fig. 2-2). By running air through the valve actuation channel, the PDMS membrane inflated at the overlapping site of the valve and the main channels, creating a physical barrier in front of the fish head. Then, the larva was given 60 s to recover from

any loading and handling stresses and to acclimate to the new environment. During this time, the larvae started to move their tail randomly inside the screening pool till they become inactive and ready for screening. The electric-induced response of the semi-mobile larva was video-recorded at 2x magnification and a speed of 160 frames per second (fps) using the camera mounted on the microscope. Behavioral recording lasted until the larva stopped moving its tail, which occurred in a period of less than 20 s. After each experiment, the larva was removed through the outlet and the device was prepared for the next experiment with a new larva. The extracted larvae were sacrificed following the Zebrafish Humane Killing protocol[134].

2.6.2. Multi-Phenotypic Single-Fish Microfluidic Device

The microfluidic device shown in Fig. 2-3 was used to trap the larva's head inside the TR for multi-phenotypic screening. The experimental procedure explained in section 2.6.1 was followed to optimally position the larva inside the device. The larva was given 60 s to recover from any stress induced by loading and to acclimate to its new environment. This recovery time was observed to be sufficient for heartrate to return to baseline levels during off-chip tests. Although simultaneous tail and heart recording was possible at 2x magnification, videos of the heart were recorded at 8x magnification to achieve higher resolution images and facilitate heartrate counting.

2.6.3. Multiple-Fish Microfluidic Device

The loading procedure in quadruple-fish device was similar to single-fish device (described in section 2.6.1) except that here four larvae were loaded into the inlet channel in Fig. 2-5A. An indirect flow channel was also connected to the main channel through a series of short horizontal channels, through which water was pumped to the main channel to increase the hydrodynamic flow focusing on each of the TRs. As soon as the first fish reached the main channel, the bulk

stream carried it into the first TR with lower flow resistance. Then, the indirect flow channel was switched on to provide a volumetric flow rate of 0.8 ml/min to push the larvae into the empty TRs and position them with their head immobilized in the narrow TR and their tails free to move within the screening pools as shown in Fig. 2-5B. When any valve channels situated in the bottom layer were pressurized, the membrane deflected, creating a physical barrier in the intersecting upper layer channels. This provided a way to prevent the larvae from swimming out of the TR.

2.7. Viability Test

Finalizing each design, a viability test was done on larvae following procedures reported by Peimani et al.[122] to confirm that the fish were not injured by the loading technique, the device components and the electrical stimulus. The morphology and survival criteria were applied to examine the immediate and long-term impacts of the loading, immobilization and electric stimulation processes. Three groups of larvae were tested, including a reference group that was neither exposed to the device nor to any electric current, a control group with larvae trapped in the device but not exposed to any electric current, and a test group of larvae exposed to electric current inside the device. For gauging survival and morphological abnormalities, the fish were unloaded from the device through the tilted inlet tube, using the withdrawal function of the syringe pump and their viability and morphology was assessed each day. This approach reduced the chances of damaging the larvae as they were being removed from the device for the subsequent tests. The larvae were then delivered to a fish tank and placed inside a 28ºC incubator to be monitored for the survivability. For the survival assessment, we counted the number of days that the larvae remained alive under the controlled conditions. We used visual confirmation of the mortality in addition to the larvae's reaction to a gentle nudge. To evaluate morphological abnormalities, we visually monitored the fish inside the tank on a daily-basis and counted any spinal bends (e.g.,

lordosis, kyphosis and scoliosis) as an abnormality. Morphology criteria included craniofacial abnormalities and bending (i.e. scoliosis, kyphosis, and lordosis)[135,136] as described in Fig. 2-7.

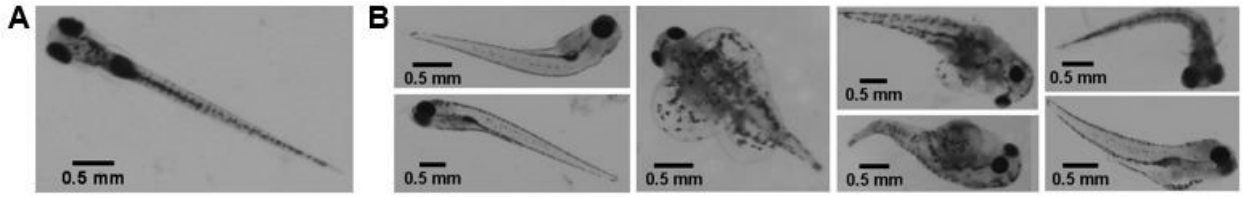

Fig. 2-7. Microscope images of A) an intact reference group larva and B) morphologically damaged zebrafish larvae[128]. Reprinted with permission from John Wiley and Sons.

2.8. Behavioral Phenotyping and Data Analysis

The electrically evoked tail movement of zebrafish larvae were characterized phenotypically in terms of RD and TBF (Eq. 2-5 and Eq. 2-6) in our devices.

The RD was measured from the beginning of tail motion until the larva ceased moving. Since no response latency was observed, the tail motion onset was defined as the time at which the electric current was applied.

$$RD = Movement\ End\ Time - Movement\ Start\ Time \qquad Eq.\ 2\text{-}5$$

The TBF was defined based on a recently published article[129,137] where any tail flicks (i.e. any small and negligible tail motion) were excluded. Based on experimental observations, we set a threshold of $\pm 0.25mm$ from centerline of the channel centerline as shown in Fig. 2-8. Every time that the tail tip passed over the threshold lines, we counted the movement as a quarter-strike cycle. A full cycle was defined as four quarter strikes, while bilateral and unilateral tail turns were counted as one-and-half full cycles, respectively[138]. TBF was calculated as the number of full cycles divided by the corresponding RD.

$$TBF = \frac{Number\ of\ full\ tail\ cycles}{RD} \qquad Eq.\ 2\text{-}6$$

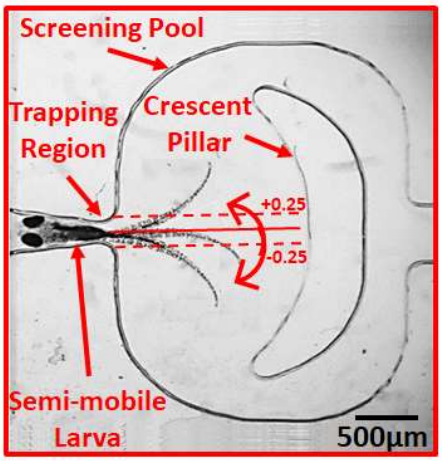

Fig. 2-8. A close-up view of the screening pool of a microfluidic device with a 5 dpf larva trapped in the TR and its tail free to move in the screening pool[127]*. Reprinted with permission from Elsevier.*

The open-source Kinovea software (www.kinovea.org, France) was used for analyzing the RD, TBF and heartrate of zebrafish larvae inside our microfluidic devices. The software automatically tracked the larva's tail tip point inside the screening pool of the microfluidic device in each video frame. In low-resolution frames where the tail tip was moving fast and blurred, we manually selected the tip position. Each frame of the videos was checked to ensure that the software was accurately tracing the tail activity. In order to rule out any possible errors in counting the tail stroke cycles with the Kinovea software, we randomly selected 10 videos and counted the strikes visually. Our manual assessment confirmed the same TBF obtained with the software. When required, heartrate was tabulated over a 20-s period directly from the Kinovea software and multiplied by a factor of 3 to obtain the number of beats per minute (bpm). For each larva, the heartrate was quantified three times, and the average value and standard error of mean were calculated for comparison between the groups. The raw data were saved in xml format, and the heartrate, TBF and RD phenotypes were analyzed using the Microsoft Excel (Microsoft Corp., WA, USA).

The tail position data was saved in an 'xml' format and further analyzed using Microsoft Excel (Microsoft Corp., WA, USA).

2.9. Statistical Analysis

Various statistical tools were applied during the analysis phase to aid with extracting meaningful information from the tests. Errors were described using the Standard Error of the Mean (SEM). Results were reported as mean±SEM. Wherever a clear depiction of the data distribution was required, box plots were provided with 25% and 75% percentiles, median, minimum and maximum data values. The data were tested for normality using Shapiro-Wilk test. Then, relying on Shapiro-Wilk test outcome, Mann–Whitney U test was used to ascertain if significant differences were present. The sample sizes were determined with power analysis conducted using open source GPower 3.1 software (https://gpower.software.informer.com/3.1/) with an upper limit of 0.05 for the significance level and a power of 80%. The star-based notation was used to identify the significance level as follows: * for p-value<0.05, ** for p-value <0.01 and *** for p-value <0.001.

Chapter 3‡

3. Electrofluidic Devices to Investigate Organ-based Electrical Responses of Zebrafish Larvae

As discussed in previous chapters, zebrafish are widely studied in biomedical research. Zebrafish behavioral screening is possible through accurate analysis of their movement in response to a stimulus. Considering difficulties associated with controlling the movement of zebrafish larvae and quantitative assessment of their complex response, new microfluidic techniques are introduced in this chapter that uses electrical stimulus to stimulate, control and characterize zebrafish

‡ Some content of this chapter has been published in:

1. Khalili, A. R. Peimani, N. Safarian, Kh. Youssef, G. Zoidl, P. Rezai, "Phenotypic Chemical and Mutant Screening of Zebrafish Larvae using an On-Demand Response to Electric Stimulation", *J. of Integrative Biology,* vol. 11, no. 10, pp. 373–383, 2019. Permissions for the use of the text has been received from Oxford University Press.
2. A. Khalili, E. van Wijngaarden, G. Zoidl, P. Rezai, "Zebrafish Larva's Response to Electric Signal: Effects of Voltage, Current and Pulsation for Habituation Studies", *J. of Sensors and Actuators: A. Physical,* vol. 332, 113070, 2021. Permissions for the use of the text has been received from Elsevier.
3. A. Khalili, A. R. Peimani, N. Safarian, Kh. Youssef, G. Zoidl, P. Rezai, "Phenotypic Chemical and Mutant Screening of Zebrafish Larvae using an On-Demand Response to Electric Stimulation", *J. of Integrative Biology,* vol. 11, no. 10, pp. 373–383, 2019. Permissions for the use of the text has been received from Oxford University Press.

movement in a quantitative manner to facilitate behavioral screening assays (Obj. 1 of the thesis). The next focus of this chapter would be on the assessment of the electric-induced behavioral responses of zebrafish larvae to the electric stimulus intensity, electric field direction and repetition of stimuli (Obj. 2 of the thesis).

3.1. Introduction

Sensing of electric signal and subsequent movement response of zebrafish was recently reported by us and others[63,122,124,129]. Tabor et al.[124] experimented with exposing zebrafish between the ages of 4 and 60 dpf to electric field providing insight into escape responses of the larvae. The work highlighted the larval preference to orient toward the anode with maximum responsiveness observed for electric fields aligned with the rostro-caudal axis of the fish. Fields administered with other orientations, including lateral and vertical alignments, elicited a low reaction. The stimulated responses were additionally linked to the intensity of the voltage applied. The group also discussed the involvement of Mauthner cells, a class of giant reticulospinal neurons, in the generation and regulation of the escape response behaviour. The role of Mauthner cells was similarly discussed by Featherstone et al.[139] and Prugh et al.[140], specifically outlining the events that comprise the startle response observed during initial electric stimulation. Behaviours relating to the electric-induced response have been discussed in several other papers with focus on learning and memory[141,142].

Our lab also recently demonstrated zebrafish larvae's response to electric current inside a microfluidic channel in which the larva was allowed to move longitudinally (Fig. 1-6A)[99]. Once exposed to electric current of 3 μA with the anode electrode positioned at the tail side, the zebrafish larvae showed a preference to orient and swim towards the anode. However, due to larvae's rapid movement, it was not possible to quantify the response phenotypically. This is required for future

development of sensitive and medium-to-high throughput phenotyping tools involving zebrafish larvae's response to electric signals. In this chapter, we introduce a microfluidic device (Fig. 2-2) for on-demand electrical stimulation and phenotypic movement response assessment of 5-7 dpf semi-mobile zebrafish larvae. TBF and RD phenotypes of the semi-mobile larvae in response to various electric stimuli were examined quantitatively.

Despite the aforementioned efforts, many aspects of zebrafish larvae's response to electric field remains ununderstood. Our proposed device will be used to shed some light on some aspects of the electric-induced response. Here, for the first time, we asked whether zebrafish larvae are sensitive to electric current and voltage magnitude as well as the direction of the electric current in a microchannel (i.e., anode at head vs tail). Moreover, using different habituation-dishabituation strategies, we investigated if the zebrafish larvae showed adaptation towards multiple exposures to electric stimuli.

Another challenge is multi-phenotypic screening of heart and movement, especially when anesthetic treatment and orientation of the larva in the abnormal dorsal direction should be avoided. Current microfluidic devices, developed for zebrafish larvae studies, only provide a single view of the larva at a time[93–95]. The heartrate of a zebrafish larva is best observed from a lateral view while monitoring the tail movement requires the larva to be visible from its dorsal side. Here, we introduce a gel-free and anesthetic-free prism-integrated multi-phenotypic microfluidic device (Fig. 2-3) for bi-directional imaging of zebrafish larva in the same chip.

3.2. Methods

Zebrafish larvae were loaded in the single-fish device following procedures explained in section 2.6.1 and 2.6.2.

3.2.1. Electric Current and Electric Field Conditions

Different DC electric currents were applied across the channel alongside the fish body axis to evoke zebrafish locomotor response. Using the sourcemeter controls, the anode pole was positioned at the larva's tail side for the electric current experiments. Electric field direction studies were performed with anode either at the tail or at the head side (Fig. 3-1B).

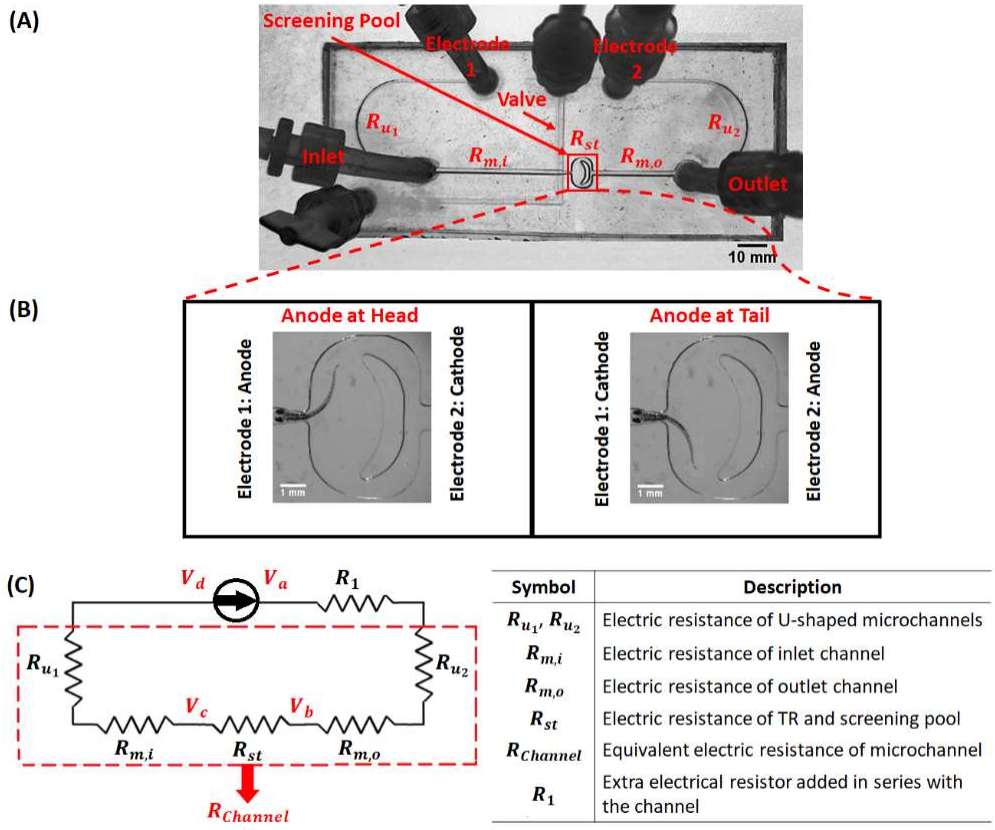

Symbol	Description
R_{u_1}, R_{u_2}	Electric resistance of U-shaped microchannels
$R_{m,i}$	Electric resistance of inlet channel
$R_{m,o}$	Electric resistance of outlet channel
R_{st}	Electric resistance of TR and screening pool
$R_{Channel}$	Equivalent electric resistance of microchannel
R_1	Extra electrical resistor added in series with the channel

Fig. 3-1. The microfluidic technique for behavioral study of semi-mobile zebrafish larvae in response to electric signals. (A) The microfluidic device with labels corresponding to different electric resistances. (B) Close-up view of TR and screening pool with a trapped 5 dpf larva showing the arrangement of electrodes to provide different electric field directions. (C) Equivalent electric circuit of the device and an external resistor[127]*. Reprinted with permission from Elsevier.*

3.2.2. Electrical Circuit of the Microfluidic Device and Voltage Conditions

The equivalent electric circuit of the microfluidic device is shown in Fig. 3-1C. The main channel resistance ($R_{Channel}$) consisted of five series electric resistances including two U-shaped microchannels (R_{u1}, R_{u2}), inlet and outlet main channels ($R_{m,i}$, $R_{m,o}$), and the TR and screening pool resistances together (R_{st}). The extra resistor R_1 was added externally in series to the channel to alter the voltage conditions in the device as described later in this section. The total electric resistance of the setup (R_T) can be expressed by Eq. 3-1.

$$R_T = R_{Channel} + R_1 \qquad \textit{Eq. 3-1}$$

The electric resistance of an object depends primarily on its shape and material characteristics and can be calculated using Eq. 3-2.

$$R = \frac{L}{\sigma A} \qquad \textit{Eq. 3-2}$$

where L, A and σ are the length (m), cross-sectional area (m^2) and electrical conductivity (S/m) of the conductor, respectively. Considering the low electrical conductivity of PDMS (1.71×10^{-8} µS/cm)[143] which is approximately ten orders of magnitude lower than the tap water electrical conductivity, the electrical resistance of the microfluidic device would be significantly higher than the microchannel. Therefore, for our studies, we excluded the electrical resistance of the microfluidic device from our calculations and assumed that the whole electric signal passed through the fluid in the microchannel.

To assess the effect of electric voltage on zebrafish response in our device, we exposed the larvae to different voltage drops across the whole channel ($V_{ad}=V_a-V_d$) and their body ($V_{bc}=V_b-V_c$). Considering the Ohm's law ($V=RI$), different V_{ad} under a fixed electric current could be obtained by varying the electric resistance of our setup. Electric resistance modulation could be achieved

using three approaches, i.e. (i) introducing an additional series resistance to the device (R_1), (ii) changing the media and altering the electrical conductivity σ, and (iii) changing the microchannel dimensions L and A. Here, we followed the first two approaches to evaluate the sensitivity of zebrafish to electric voltage. In method (i), addition of R_1 resulted in increasing the voltage drop across the channel (V_{ad}) while not affecting the voltage drop across the fish body (V_{bc}). Method (ii) resulted in changes in both V_{ad} and V_{bc}. Method (iii) was not pursued as our device was designed for efficient immobilization of 5-7 dpf zebrafish larvae and trap dimensions could not be modified.

Two sets of experiments were designed based on methods (i) and (ii) above, to examine the effect of electric voltage on the zebrafish locomotor response. Using the sourcemeter, the total voltage drop across the channel (V_{ad}) and the total resistance of the device (R_T) were measured. For the first set of experiments, the external electrical resistor R_1 was added to the channel while electric current was kept constant at 3 μA. Substituting the dimensions of different channel sections in Eq. 3-2, all electrical resistances except R_{st} were calculated. Then, Eq. 3-3 was used to calculate R_{st}.

$$R_{st} = R_T - \left(R_1 + R_{u1} + R_{u2} + R_{m,i} + R_{m,o}\right) \qquad \textit{Eq. 3-3}$$

Eq. 3-4 was then used to calculate the voltage drop across the fish body (V_{bc}).

$$V_{bc} = V_b - V_c = IR_{st} \qquad \textit{Eq. 3-4}$$

Table 3-1 shows the values of the external resistance R_1 and the corresponding voltage drops obtained across the channel (V_{ad}). In these experiments, voltage drop across the larva TR and screening pool, V_{bc}, remained constant at 5.6 V.

Table 3-1. Electrical characteristics of the microfluidic device by using different external resistances R1

I (μA)	R_1 ($M\Omega$)	R_T ($M\Omega$)	V_{ad} (V)	V_{bc} (V)
3	0	35	105	5.6
3	30	65	195	5.6
3	60	95	285	5.6

For the second set of voltage changes, V_{ad} and V_{bc} were altered simultaneously through introducing various solutions into the microchannel. This enabled investigation of the effect of V_{bc} since our studies showed that V_{ad} had no effect on the zebrafish response (see Results). We chose four media commonly used for zebrafish, i.e. egg water, tap water, larvae water and hatcher water, each containing different salt concentrations. As shown in Table 3-2, the solutions covered a wide range of conductivities, from egg water at 220 µS/cm to hatcher water at 1500 µS/cm, which can be tolerated by zebrafish[144].

To investigate the possible effects of electrolysis, the device was filled with four different solutions mentioned in Table 3-2, i.e., hatcher, larvae, tap and egg waters. An electric current of 3 µA was applied through each solution in our microfluidic device for 5 min with the electric voltage measured every 30 s**.** Ohm's law was then used to calculate the correspondent electric resistances. Using Eq. 3-5, the maximum deviation from the electrical resistance of the microfluidic device at t=0 (R_0) was obtained.

$$R^* = Max\left|\frac{R-R_0}{R_0}\right| \qquad \textit{Eq. 3-5}$$

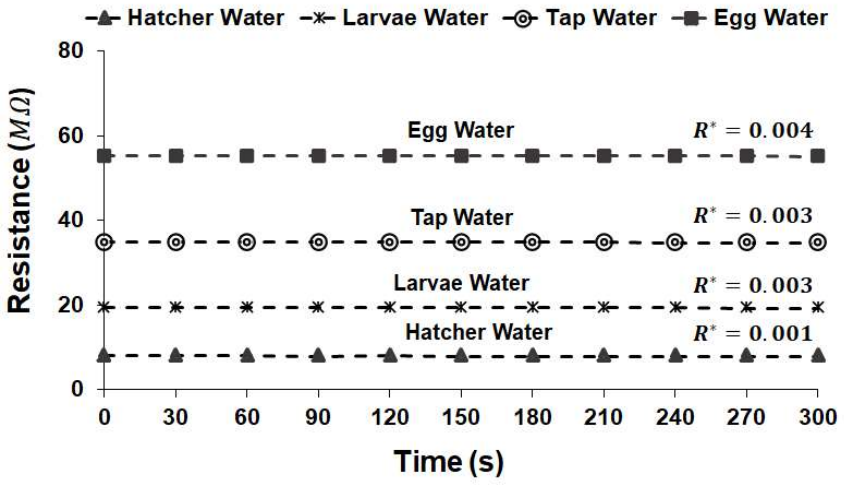

Fig. 3-2. Electrical resistance of the device using hatcher, larvae, tap and egg waters when tested at an electric current of 3 μA for 5 min at 30 s interval. All the experiments were done at room temperature ($25 \pm 2°C$*) and were repeated 3 times each*[127]*. Reprinted with permission from Elsevier.*

As shown in Fig. 3-2, for all four different media, the electric resistance of the device was constant during a 5 min exposure to an electric current of 3 μA ($0.001<R^*<0.004$), suggesting that electrolysis was not significant and the electrochemical composition of the solutions remained constant during the zebrafish experiments which lasted for less than 30 s at the electric current of 3 μA. Table 3-2 also shows the voltage drops across the channel and the trap using the abovementioned types of water.

Table 3-2. Electrical characteristics of the microfluidic device by using different media

Media	I (μA)	$\sigma\ (\mu S/cm)$	$R_T\ (M\Omega)$	$V_{ad}\ (V)$	$V_{bc}\ (V)$
Hatcher water	3	1500	8.1	24.4	1.3
Larvae water	3	625	19.5	58.5	3.2
Tap Water	3	348	35	105	5.6
Egg Water	3	220	55.4	166.1	9

Before testing, the larvae were incubated overnight in the same media which minimized their sudden exposure to different ionic environments and ensured that the behavioral alterations were the result of exposure to different electric voltage conditions in Table 3-2.

3.2.3. Habituation to Electric Current

To investigate the effect of repeated exposure to electrical stimuli on zebrafish locomotor response, the larvae were exposed to a series of 10 electrical pulses at I=3 μA in our device, for a pulse duration of 20 s. Anode was positioned at the larvae's tail side and electric current pulses with various Interstimulus intervals (ISIs) were used. Given that shorter ISI lead to faster habituation[63,145], the pulses were given at ISI of 20, 10 or 5 s. To determine whether zebrafish habituate to these electrical pulses, two scenarios were proposed. First, two series of electrical pulses, separated by a 5 min rest period, were administered to forty-five zebrafish larvae at 5-7 dpf to evaluate if the fish response could be spontaneously recovered. Each series included 10 pulses at I=3 μA with a pulse duration of 20 s and an ISI of 5 s. For the second approach, a group of forty-five zebrafish larvae at 5-7 dpf were exposed to 6 electrical pulses at I=3 μA with a pulse duration of 20 s and an ISI of 5 s (till habituation happened), followed by a 2 s light pulse (white LED light: 560 lux, 465–700 nm)[146] and 7 more electric pulses. The 2 s light pulse was interspersed between the 6th and 7th electric pulses without affecting the ISI to investigate if a response still occurred when a novel stimulus was introduced[147]. In all scenarios above, the microfluidic device was filled with tap water while no extra resistor R_1 added to the channel.

3.2.4. Simultaneous Movement and Heartrate Monitoring of Zebrafish Larvae in the Multi-Phenotypic Microfluidic Device

Using our prism-integrated multi-phenotypic microfluidic device (Fig. 2-3) and the setup shown in Fig. 2-6, we could monitor a semi-immobilized larva from two different directions under a microscope (Fig. 3-3). More details about this chip was provided in Section 2.4.2 of this thesis. For the dorsal view, the fish was observed at 2x magnification from the top of the microchannel (Fig. 3-3A). For the lateral view, imaging was done at 8x magnification through the prism (Fig. 3-3B).

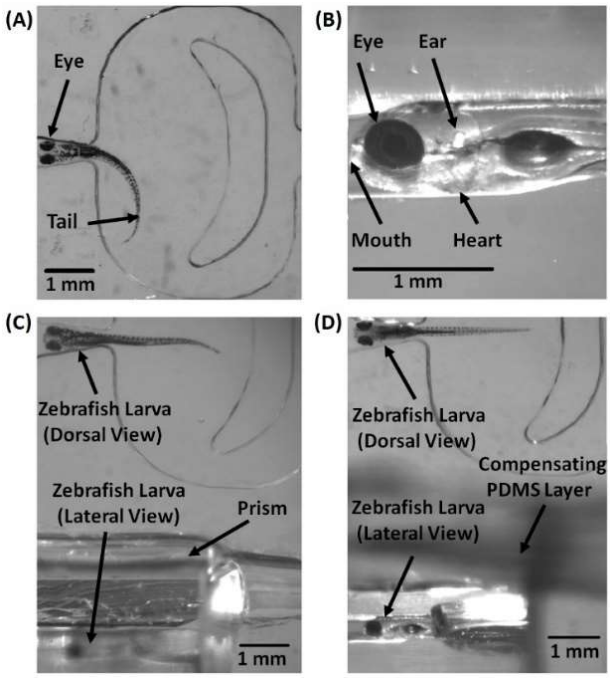

Fig. 3-3. Bi-directional imaging of a zebrafish larva in the multi-phenotypic microfluidic device. (A) Dorsal and (B) lateral (through prism) views of a 7 dpf zebrafish larva trapped in the microfluidic device and imaged at 2x and 8x magnifications, respectively, under the microscope. Dual view images of a 7 dpf zebrafish larva are shown at 2x magnification (C) without and (D) with a 12 mm thick PDMS layer compensating for the optical focal length mismatch between the dorsal and lateral views[126]*. Reprinted with permission from Oxford University Press.*

As shown in Fig. 3-3A and 3B, the quality of the images obtained from our chip was satisfactory, and multiple organs of interest could be imaged from two directions, allowing for visualization of the tail, eye, mouth, ears, and the heart of the same zebrafish larva in one device. The dorsal view of the zebrafish was used to track their tail movement, while the lateral view allowed examination of the organs of the same larva such as the heart and the mouth that would otherwise be unseen in the dorsal view. On average, an experiment for a single zebrafish larva took approximately 2.5 min including 30±3.7 s for loading, 60 s for recovery from any stress induced by loading, 30 s for heart screening, and 20 s for monitoring the tail movement.

Due to the difference between the focal lengths of the lateral and dorsal optical paths, simultaneous side- and top-view images could be obtained only when using a 12 mm thick compensating PDMS layer on top of the prism (Fig. 2-4). Fig. 3-3C and 3D show simultaneous dual views of 7 dpf zebrafish larvae obtained with a single objective lens at 2x magnification without and with the compensating PDMS layer, respectively. The quality of the images was satisfactory for heartrate and RD and TBF monitoring (data not shown) and dependent on the precise fabrication of the compensating layer. Simultaneous dual view imaging was not used in our experiments because we wanted to perform heart imaging at 8x magnification (compared to 2x for movement monitoring) to obtain a better resolution image of the heart (Fig. 3-3B). In the future, a higher-magnification lens can be used to improve the dual view resolution. The gap between the prism and the microchannel prism should be shortened by designing a new master mold for PDMS replication. The thickness of the compensating layer required can also be reduced by moving the prism closer to the trapping region. Moreover, other materials with better optical properties can be used for the compensating layer.

To examine whether the loading and test conditions in the multi-phenotypic microfluidic device had any adverse effects on the zebrafish heart activity, we compared the heartrate of 7 dpf larvae trapped on-chip with that of off-chip zebrafish, first without any chemical and electrical stimulation. In the off-chip assay, a larva was surrounded by a drop of water on a microscope slide. Favorable orientation and precise control of zebrafish larvae's position were prerequisites for off-chip heartrate screening, so a plastic pipette was used to orient the larvae sideways for heartrate recording[148].

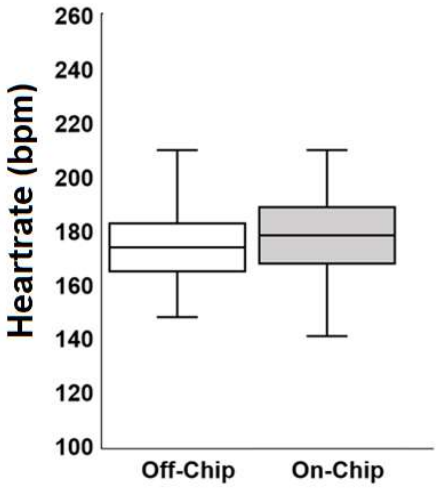

Fig. 3-4. Off-chip heartrate of WT zebrafish larvae compared to on-chip ones. The lines within the boxes mark the median heartrates, upper and lower boundaries are the 75th and 25th percentile heartrates, and whiskers are the maximum and minimum heartrates. (15 larvae per experimental condition in three independent trials, total N=45)[126]*. Reprinted with permission from Oxford University Press.*

As shown in Fig. 3-4, the mean heartrates of zebrafish larvae were 176.1±2.1 bpm and 177.8±2.7 bpm for the off- and on-chip assays, respectively. The results show that the device did not have a significant effect on the heartrate of zebrafish larvae. However, the active swimming and random orientation of the larvae tested off-chip presented a significant challenge to immobilize these zebrafish for heart imaging in a convenient and efficient manner. The results in Fig. 3-4 for unexposed larvae

also matched with the heartrate values previously reported for 7 dpf anesthetized larvae[149,150], verifying that our device did not affect the heart activity of the unexposed zebrafish larvae. The coefficient of variation of 9% and 8% was obtained for on- and off-chip results, respectively, verifying the small dispersion and high precision of our measurements. Calculating the relative difference, we ended up with an accuracy of ~99% for heartrates measured on-chip.

3.3. Results

The electric field induced tail movement of semi-mobile zebrafish larvae was thoroughly investigated in our single-fish microfluidic device (Fig. 2-2). Since zebrafish larvae at the age of 5 to 7 dpf displayed statistically similar electric-induced responses (Mann-Whitney U test, p-value>0.05)[122], the experiments in this chapter were performed using larvae between these ages. Here we asked, for the first time, whether the electric current, voltage and field direction have any effect on the response of zebrafish larvae, followed by the novel investigation of habituation to repetitive electric current pulses. Then, the multi-phenotypic single-fish microfluidic device (Fig. 2-3) was used to monitor the heartrate of zebrafish larvae and investigate the effect of electric stimulation on it.

3.3.1. Effect of Electric Current

Analyzing the response of a freely moving zebrafish larva to electric stimulation in a channel is complicated due to its rapid and long range of motion[99]. Phenotypic analysis has not been achieved because it requires medium-magnification imaging of the entire body while behavioral investigation requires allowing the larva to move in response to the electrical stimulation. To phenotypically examine zebrafish's response to electricity, the larvae were partially immobilized in the microfluidic device shown in Fig. 2-2 and their RD and TBF at various electric currents

were investigated (Fig. 3-5). For this, 5-7 dpf WT larvae were loaded individually into the device, fixed in the TR and given 60 seconds to adapt to the new situation. Within this timeframe, most larvae stayed immobile and rarely showed random, unpredicted, and inconsistent movements. Then, the trapped larva was exposed to a constant electric current in the range of 1-9 µA and its locomotor response was video-recorded for quantification of RD and TBF. The RD and TBF for unexposed control larvae were both zero.

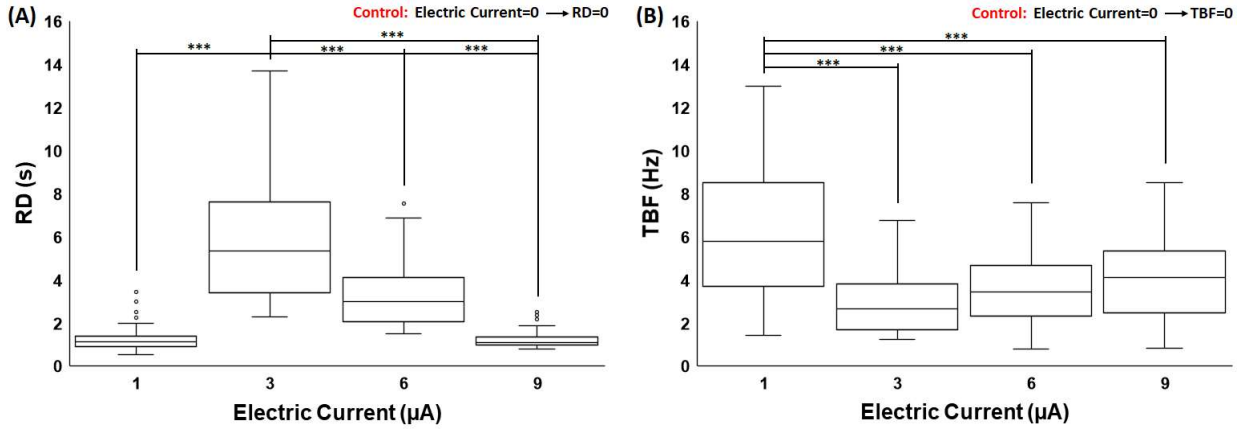

*Fig. 3-5. Electric-induced (A) RD and (B) TBF of WT zebrafish larvae at different electric currents. Control group RD and TBF were both zero. The lines within the boxes mark the median. Upper and lower boundaries are the 75th and 25th percentile and whiskers are the maximum and minimum. ***: p<0.001. (N=45 larvae per experimental condition in three independent trials)*[127]*. Reprinted with permission from Elsevier.*

Preliminary experiments on WT zebrafish larvae (N=45) determined the minimum threshold and optimum currents to which the larvae responded. WT larvae robustly responded to electric currents as low as 0.5-1 µA with >80% response rate. Currents lower than 0.5 µA resulted in no response in the device and the results for 0.5 and 1 µA were statistically similar, therefore not shown in Fig. 3-5. Further experiments were conducted at 3, 6 and 9 µA to monitor variations in the RD and TBF. As shown in Fig. 3-5A, a 3 µA electric current resulted in an average RD of

6.01±0.5 s which was the longest RD compared to the rest of the currents (Mann-Whitney U test, p-value<0.001). At 6 μA, RD was reduced to 3.4±0.2 s which was statistically longer than 1 and 9 μA (Mann-Whitney U test, p-value<0.001 for both).

We also studied the TBF of WT zebrafish larvae under exposure to the same electric current range of 1-9 μA (Fig. 3-5B). The highest TBF was 6.2±0.4 Hz at 1 μA, which was significantly different from all other currents of 3, 6, and 9 μA (Mann-Whitney U test, p-value<0.001). Increasing the electric current from 3 to 6 and 6 to 9 μA did not result in any statistical difference in the TBF of the WT larvae (Mann-Whitney U test, p-value>0.05).

3.3.2. Effect of Electric Signal Direction

Experiments were designed to evaluate the sensitivity of zebrafish response to the electric field direction, by positioning the anode at the head versus the tail of the larvae (Fig. 3-1B). As demonstrated in Fig. 3-6, for N=45 larvae in each group exposed to a 3 μA current, positioning the anode at the head resulted in a short RD of 0.34±0.03 s. Further analysis of zebrafish locomotor response demonstrated that although fewer bouts were carried out for this group, those executed were done with larger angle changes and body bending, indicative of an increased TBF of 13.5±1 Hz. However, reversing the electric field direction significantly increased the RD to 6.8±0.7 s and decreased the TBF to 3.9±0.4 Hz, displaying the sensitivity of zebrafish response to the direction of the electric field. It is worth mentioning that the control group of larvae tested with no electric current in the device demonstrated zero RD and TBF in this assay.

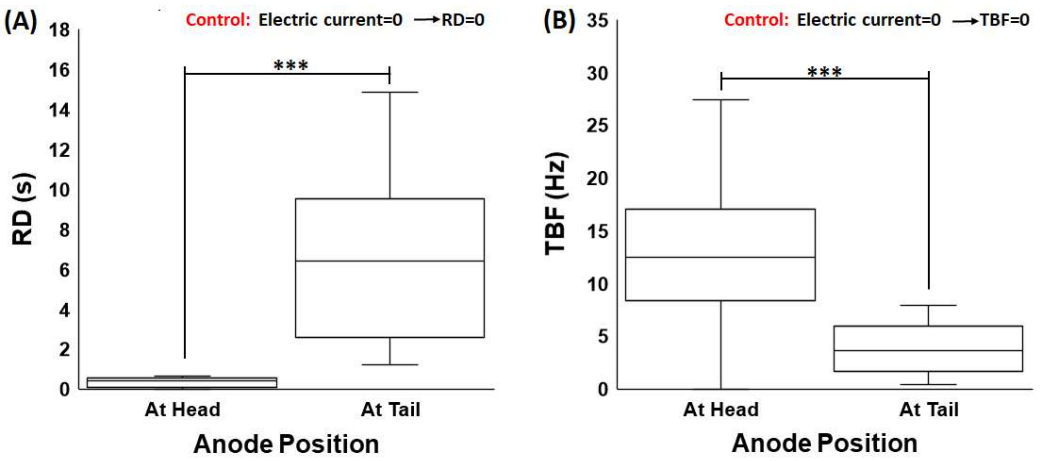

*Fig. 3-6. Electric-induced (A) RD and (B) TBF of WT zebrafish larvae upon exposure to different electric current directions (I=3 μA). Control group RD and TBF were both zero. The lines within the boxes mark the median. Upper and lower boundaries are the 75th and 25th percentile and whiskers are the maximum and minimum. ***: p<0.001. (N=45 larvae per experimental condition in three independent trials)*[127]*. Reprinted with permission from Elsevier.*

3.3.3. Effect of Electric Voltage

After demonstrating the sensitivity of zebrafish response to different electric currents[129] and longitudinal directions in the previous sections, we became interested in knowing whether this response is also dependant on the electric voltage magnitude across the microfluidic device and the larva. Accordingly, the effects of voltage drop in the whole device V_{ad}, and in the trap V_{bc} were examined, respectively, by introducing an additional series electric resistance R_1 to the circuit (Fig. 3-1C and Table 3-1) or by changing the media in the device (Table 3-2) as thoroughly discussed in the Methods section.

3.3.3.1. Effect of Device Voltage Drop V_{ad}

Introducing the new series resistance R_1 to the main circuit increases the total electric resistance which translates into an increase in the equivalent potential difference of the circuit (V_{ad}). Table

3-1 shows the various magnitudes of R_1 and the corresponding voltages across the channel and the trap at a constant applied electric current of 3 µA. In these conditions, the voltage drop across the zebrafish body (V_{bc}) remained constant at 5.6 V. As shown in Fig. 3-7A and 6B, the RD and TBF of zebrafish larvae obtained for the three voltage drops in the device were statistically similar (Mann-Whitney U test, p-value>0.05), verifying that the electrically induced response of zebrafish did not depend on the voltage drop across the device.

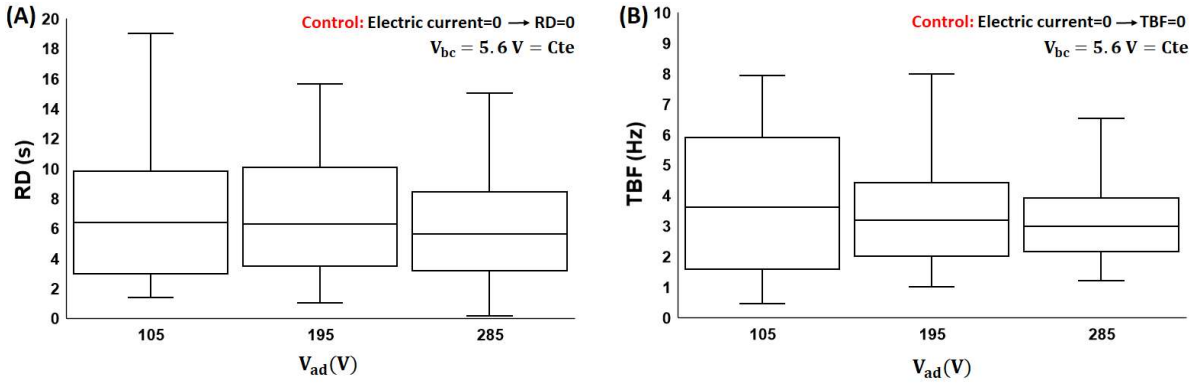

Fig. 3-7. Electrically induced (A) RD and (B) TBF of WT zebrafish larvae at different voltage drops across the device, V_{ad}, obtained with various external electrical resistances, R_1, added in series to the main circuit (I=3 µA). Control group RD and TBF were both zero. The lines within the boxes mark the median. Upper and lower boundaries are the 75th and 25th percentile and whiskers are the maximum and minimum. (N=45 larvae per experimental condition in three independent trials)[127]*. Reprinted with permission from Elsevier.*

3.3.3.2. Effect of Trap Voltage Drop V_{bc}

Having demonstrated that the voltage drop across the channel had no effect on zebrafish electrical response, here we asked whether the voltage drop across the fish body plays a deterministic role. At a constant current value of 3 µA, this required changing the electric resistance of the trap (R_{st} in Fig. 3-1C) which was achieved by replacing the tap water with three

different media described in Table 3-2. The zebrafish specimens were pre-exposed to the four media overnight before the experiments to ensure independency of the response from the change in the media. Since each medium had a different electric conductivity, using Eq. 3-1, we ended up with four different electric resistances, translating into various voltage drops, V_{bc}, across the trap and hence the zebrafish body (Table 3-2). It is true that the voltage drop in the whole channel was also changed in these experiments, but the effect of V_{ad} was already ruled out in the previous section, attributing any potential changes in response solely to V_{bc}. The results are shown in Fig. 3-8.

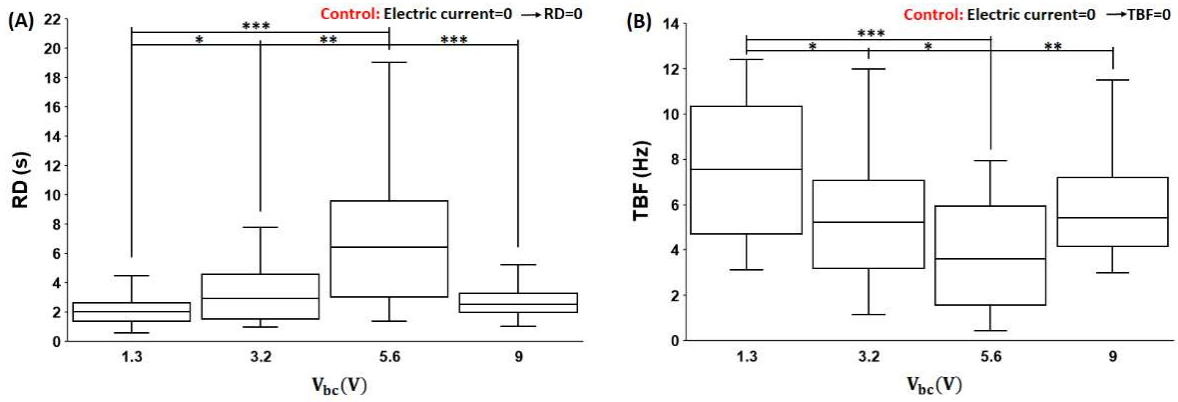

*Fig. 3-8. Electrically induced (A) RD and (B) TBF of WT zebrafish larvae at different voltage drops across the trap, V_{bc}, produced by changing the channel media (I=3 μA). Control group RD and TBF were both zero. The lines within the boxes mark the median. Upper and lower boundaries are the 75th and 25th percentile and whiskers are the maximum and minimum. *: p<0.05 **: p<0.01 ***: p<0.001. (N=45 larvae per experimental condition in three independent trials)*[127]*. Reprinted with permission from Elsevier.*

As demonstrated in Fig. 3-8, the RD and TBF obtained at different V_{bc} values were not statistically similar. A voltage drop of V_{bc} =5.6 V across the fish resulted in an average RD of 6.8±0.9 s which was the longest RD compared to the rest of the voltage drops (Fig. 3-8A). Increase in V_{bc} from 1.3 to 5.6 V resulted in an upward trend in RD, showing that a low voltage drop of 1.3

V across fish body led to an earlier end in response as compared to the intermediate voltage drops of 3.2 and 5.6 V. At the highest voltage drop of 9 V, we observed a significant reduction in the RD.

We also studied the TBF of WT zebrafish larvae under exposure to the same electric voltage drops of 1.3-9 V (Fig. 3-8B). The lowest TBF of 3.8±0.5 Hz was again associated with V_{bc} =5.6 V which was significantly lower than TBFs at other voltage drops. Increase in V_{bc} from 1.3 to 5.6 V resulted in a gradual decrease in TBF, showing that zebrafish larvae responded to a weak electric voltage with fewer bouts but with increased velocity and larger angle changes. The highest voltage drop of 9 V caused a significant increase in TBF which might be an indication of a short shock response with increased intensity and a large initial body bending.

3.3.4. Habituation of Semi-Mobile Zebrafish Larvae to Electric Current

Given that a specific stimulus elicits a response, repeated presentation of the same stimulus may intensify or suppress the response. The reduction in response may be one of the simplest forms of learning, known as habituation[151,152]. Zebrafish larvae exposed to multiple visual or auditory signals have been shown to demonstrate suppressed behavioral responses to these repeated stimuli[145,153]. The response reduction can last from minutes to hours depending on the stimulus type. Here, we asked if longitudinal electric current pulsation in our microfluidic device will result in habituation of semi-mobile zebrafish larvae.

Zebrafish larvae were exposed to a series of 10 mild electric pulses (I=3 μA, pulse duration=20 s) with ISI of 20, 10 or 5 s. Fig. 3-9 demonstrates the typical response of zebrafish larvae to electric pulses under these conditions. Exposure to the repeated stimuli resulted in a change in the locomotor activity which depended on the ISI as shown by alterations in the RD and TBF of the tested larvae. At ISI=20 s, RD and specially TBF responses were scattered with pulse numbers,

while reducing the ISI to 10 s resulted in orderly RDs but not TBFs. At ISI=5 s, RD and TBF steadily dropped with the sequential pulses, respectively decreasing from 6.9±1.3 s and 3.5±0.5 Hz to 0 by the fifth stimulus.

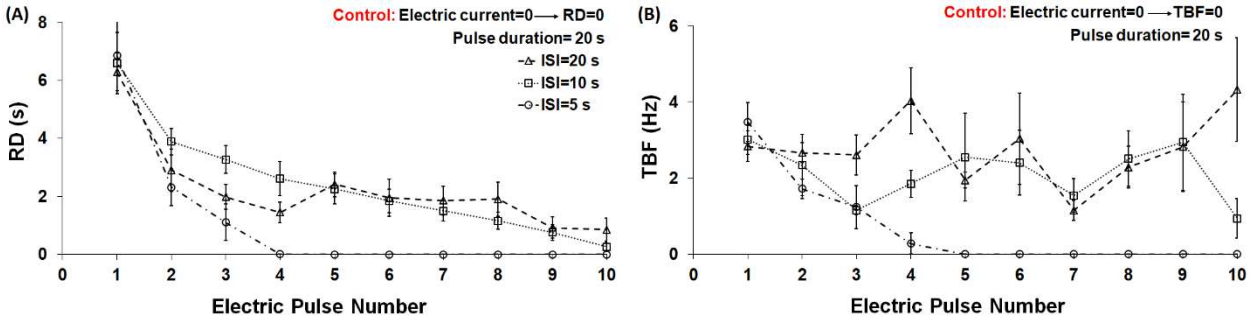

Fig. 3-9. Electrically induced (A) RD and (B) TBF of WT zebrafish larvae exposed to a series of 10 electric pulses (I=3 μA, pulse duration=20 s) with an ISI of 20, 10 and 5 s between the stimuli. Control group RD and TBF were both zero. Data points are mean values and error bars show standard error of means. (N=45 larvae per experimental condition in three independent trials)[127]*. Reprinted with permission from Elsevier.*

Two additional studies were conducted to determine if the attenuation seen in zebrafish locomotor RD and TBF in Fig. 3-9 were the result of habituation. In the first approach shown in Fig. 3-10, two series of 10 electric pulses (*I*=3 μA, pulse duration=20 s, ISI=5 s), separated by 5 min, were administered to forty-five zebrafish larvae to investigate if the response could be recovered after the 5 min rest time. For the first pulse series, the initial RD and TBF of 6.9±0.9 s and 3.1±0.2 Hz were obtained at pulse-1, while the values dropped to zero upon applying the fifth stimulus, with no further change during pulses 6 to 10. Interestingly, this attenuated locomotor activity was recovered upon introduction of the second stimuli series after the 5 min rest time. During the second pulse series, both RD and TBF values decayed to zero within 5 pulses, as observed in the first set of pulses.

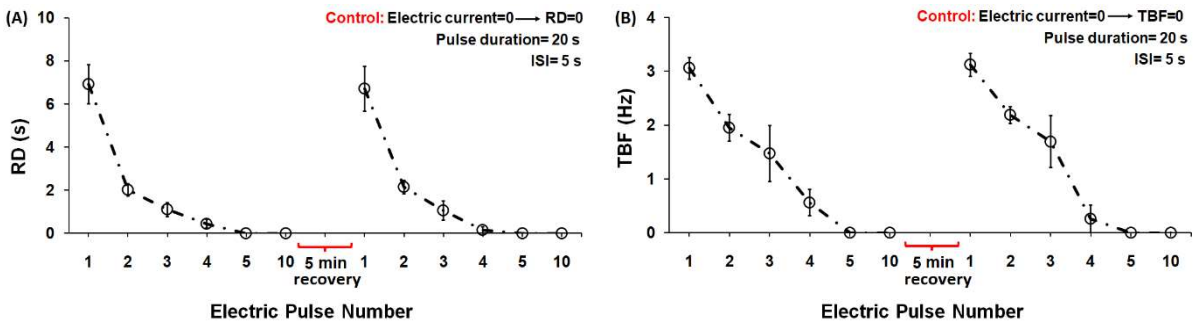

Fig. 3-10. Attenuation of the electrically induced (A) RD and (B) TBF of WT zebrafish larvae exposed to 10 electric current pulses (I=3 μA, pulse duration=20 s, ISI=5 s) in two series 5 min apart. Control group RD and TBF were both zero. Data points are mean values and error bars show standard error of means. (N=45 larvae per experimental condition in three independent trials)[127]*. Reprinted with permission from Elsevier.*

In the second approach, a light pulse (white LED 560 lux, 465–700 nm, pulse duration=2 s)[146] was applied between the two electric pulse series (*I*=3 μA, pulse duration=20 s, ISI=5 s). A group of forty-five zebrafish larvae were exposed to 6 electric pulses so that RD and TBF decays happened completely, then a 2 s light pulse was presented followed by another 7 electric pulses. The RD and TBF results are shown in Fig. 3-11.

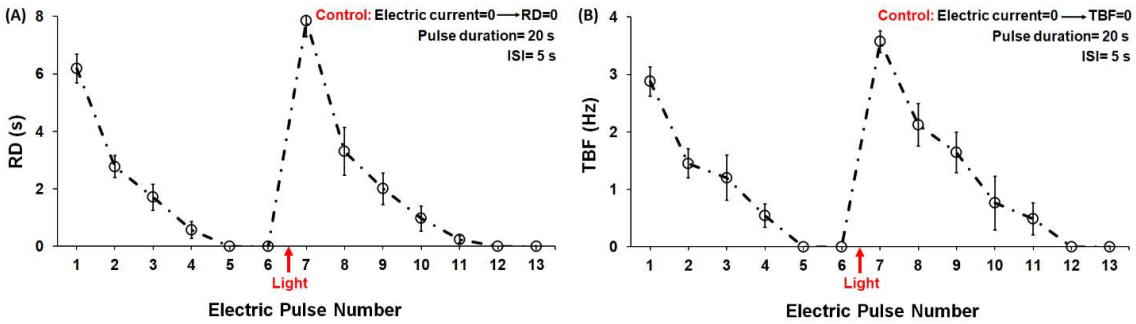

Fig. 3-11. Attenuation of the electrically induced (A) RD and (B) TBF of WT zebrafish larvae exposed to 13 electric current pulses (I=3 μA, pulse duration=20 s, ISI=5 s), when an alternate stimulus (2 s light pulse) was presented after pulse 6. Control group RD and TBF were both zero. Data points are mean values and error bars show standard error of means. (N=45 larvae per experimental condition in three independent trials)[127]*. Reprinted with permission from Elsevier.*

The first electric pulse caused the highest RD and TBF of 6.2±0.5 s and 2.9±0.3 Hz, respectively, which were statistically similar to those reported for the first pulse in Fig. 3-10 (Mann-Whitney U test, p-value>0.05). The RD and TBF decreased progressively to zero until presentation of the 5th electric pulse and remained unchanged in response to the 6th pulse (Fig. 3-11). Introducing the novel light stimulus after the 6th electric pulse could spontaneously recover zebrafish locomotor responses, leading to the RD of 7.8±0.6 s and TBF of 3.6±0.2 Hz which were slightly stronger than those obtained after the introduction of the first electric pulse (Mann-Whitney U test, p-value<0.05). During the second electric pulse series, both RD and TBF decayed to zero within 6 pulse repetitions.

3.3.5. Effect of Electric Stimulation on Heartrate of Zebrafish Larvae in the Multi-Phenotypic Microfluidic Device

Electric stimulus is being used increasingly for organism-based studies inside microfluidic devices[116,118,122,129]. Significant attention has been given to the effect of electric signals on the movement of organisms. To examine the unknown effect of electric current on the heart activity of zebrafish, the heartrate of 5-7 dpf larvae was measured in five different conditions before, during, and at 30 s, 1 min and 2 min after their exposure to a 3 μA electric current. The heartrate 30 s prior to presentation of the electric stimulus was used as the baseline heartrate. The results are shown in Fig. 3-12.

As shown in Fig. 3-12, exposure to electric stimulus resulted in a significant increase in zebrafish heartrate from 179.3±1.9 bpm baseline to 204.8±2.06 bpm (p-value<0.001). The impact was temporary since it took 30 s for the larvae to resume their baseline heartrate. The heartrate was also monitored for another 1.5 min to track its trend. The data showed no significant difference between the heartrates measured 30 s, 1 min, and 2 min after removal of the electric stimulus (p-

value>0.05), indicating that the heartrate had stabilized at baseline rate shortly after the disconnection of electricity. In addition, no significant difference was observed between the heartrates of 5 and 7 dpf zebrafish larvae before exposure to electric stimuli which was consistent with observations from literature not related to electric signals[154,155].

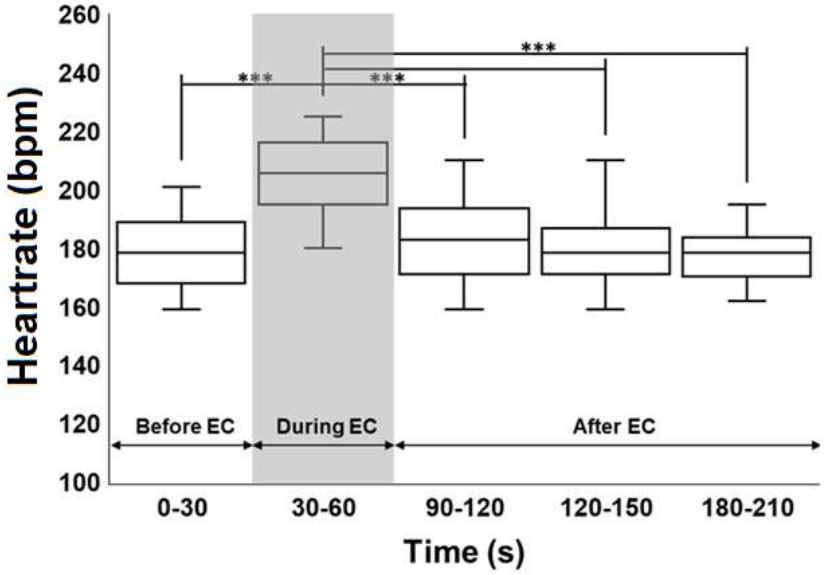

*Fig. 3-12. The heartrate of 5-7 dpf zebrafish larvae in the multi-phenotypic microfluidic device before, during, and after (30 s, 1 min, and 2 min) applying a 3 μA electric current (EC). The lines within the boxes mark the median heartrates, upper and lower boundaries are the 75th and 25th percentile heartrates, and whiskers are the maximum and minimum heartrates. ***: $p < 0.001$ (15 larvae per experimental condition in three independent trials, total N=45)*[126]*. Reprinted with permission from Oxford University Press.*

3.4. Discussion

The aim of this study was to enhance our knowledge about several aspects of zebrafish larvae's response to electric field. Using an efficient microfluidic device, with a larva head trap and two electrodes to induce tail movements on-demand in a chamber, the sensitivity of zebrafish larvae's response to electric field direction and current and voltage magnitude was assessed using RD and

TBF as quantitative behavioral readouts. Furthermore, zebrafish's response to multiple electrical stimuli with different ISI values was investigated, showing the applicability of our microfluidic device for habituation studies.

Positioning the anode at the tail resulted in a longer RD and lower TBF compared to the anode at the head (Fig. 3-6), verifying that semi-mobile zebrafish larvae can sense the electric field direction. The significant increase of RD for anode at the tail assay was consistent with our earlier findings on freely moving zebrafish larvae, showing immediate rotation and movement towards the anode[122]. Considering this tendency, zebrafish electric-induced response lasted longer (i.e. higher RD) but with a slower pace (i.e. lower TBF) when we put the anode at the tail side. We have also observed that the TBF and RD values are almost always inversely dependent on each other during electric responses. In other words, if the RD is long, the TBF is usually low, and vice versa. This phenomenon may be related to the amount of energy that the larvae spend during each response and their preference towards long and slow movements versus short strikes with fast tail oscillations. This requires further investigation in the future for which our device can be deployed for quantitative studies.

Our results showed that the electrically induced response of zebrafish larvae can be modulated with the electric current as well as the voltage drop across the larva's body (Fig. 3-5 and Fig. 3-8), but not the total voltage drop across the device (Fig. 3-7). A weak electrical signal of 1 μA led to an earlier end in response as compared to the intermediate currents of 3 and 6 μA (Fig. 3-5). Moreover, it potentially contended that a higher electric current of 9 μA resulted in partial paralysis of the larvae leading to a significant reduction in the RD. Comparing the RD and TBF results at 1 and 3 μA, it can be seen that the larvae responded with a high TBF for a short RD at 1 μA while the phenotypic behaviour was reversed at 3 μA. Using the proposed microfluidic device, we could

manipulate the electric stimulus to evoke the locomotor behavior of semi-mobile zebrafish larvae and introduce an on-demand, controllable and precise technique to study movement. Furthermore, comparing the RD and TBF results at 1.3 V and 5.6 V, one can see that the larvae responded with a high TBF for a short RD at 1.3 V, while the phenotypic behaviour was reversed at 5.6 V, suggesting that the larvae are expending their energy on either long responses or fast tail oscillations at a time (Fig. 3-8). At the highest voltage drop of 9 V, we observed a significant reduction in the RD and increase in the TBF, which may be attributed to partial shock and immediate paralysis of the larvae. This type of electrical paralysis was also observed in C. elegans at high-level electric field[116]. Our TBF and RD trends were in line with the recently published results showing that a stronger electrical stimulation of freely moving ~4 dpf zebrafish larvae resulted in reduction of their locomotor activities[63].

Habituation to multiple electrical stimuli was introduced as another novel example for the application of our microfluidic device in zebrafish behavioral studies. We concluded that habituation of the locomotor response to the electrical stimuli occurred when the ISI was 5 s, but not at 20 or 10 s (Fig. 3-9). Steenbergen exposed freely moving larvae to series of 20 stimuli (5 V pulses lasting 100 ms) with ISIs of 10 or 2 s[63]. Comparing the swimming activity of the larvae before and after exposure showed locomotion habituation of the larvae which depended on the ISI similar to our results. The significant dependence of habituation on ISI has also been reported for other behaviours, e.g. Best et al.[145] reporting the effect of acoustic stimulus on zebrafish larvae, showing that repeated exposure to acoustic pulses with an ISI of 20 or 5 s did not lead to habituation as contrary to an ISI of 1 s.

A behavioral response attenuation resulting from repeated stimulation may involve motor fatigue, sensory adaptation or habituation[147]. Generally, habituation is distinguished from motor

fatigue and sensory adaptation by the process of dishabituation. Dishabituation refers to the reappearance of a habituated response, commonly as a result of the application of a strong, novel or noxious stimulus[156]. We conducted two studies (Fig. 3-10 and Fig. 3-11) to determine if the attenuation seen in zebrafish locomotor RD and TBF were a result of habituation.

In the first approach in Fig. 3-10, two series of 10 electric pulses, separated by 5 min, were applied to the zebrafish larvae. For the first pulse series, the RD and TBF values dropped to zero upon applying the fifth stimulus, with no further change occurring after the 6th pulse. However, the 5 min rest time before introduction of the second stimuli series was sufficient to lead to response recovery. Zebrafish response to the second set of electrical stimuli was statistically similar to that in the first set (Mann-Whitney U test, p-value>0.05), verifying the recovery between the two sessions and habituation of the zebrafish larvae to electric pulses in our device.

Verification of habituation can also be made by demonstrating that the response still occurs with other types of stimuli[147]. In other words, following habituation to stimulus X, presentation of stimulus Y can rescue the response to stimulus X[145]. In our second assay in Fig. 3-11, repetitive electric pulses and an in-between light pulse were used as stimuli X and Y, respectively. The enhanced response after presentation of the light pulse suggested a potentiation effect, possibly resulting from increased alertness due to exposure to a novel stimulus[145,157]. It was concluded that the response was specific and consistent with the habituation phenomenon. Our results prove that the proposed microfluidic device and the electric assay can be used as a tool to study habituation under highly controlled experimental conditions. Moreover, testing zebrafish strains that express genetically encoded calcium indicators may help understand the cellular basis of habituation in our device.

Using our multi-phenotypic microfluidic device, we could monitor the heart and tail activity of zebrafish larva in the same chip. The addition of the prism to the microfluidic device eliminated the need for separate devices with different designs in order to orient the larva in the dorsal or lateral directions. The device had no adverse effect on the heartrate. We also showed a temporary increase in heartrate upon exposure to electric stimulus which was stabilized at baseline rate shortly after removing the electricity.

3.5. Conclusion

The goal of this study was to develop a novel platform in which the recently-introduced movement response of zebrafish larvae to electrical stimulation could be examined on-demand and phenotypically for applications in chemical screening and gene function studies. Thus, we developed a device in which 5-7 dpf larvae could be (i) partially immobilized and (ii) controllably exposed to electric stimulus to induce an on-demand tail oscillation which could be quantified in terms of RD and TBF. We aimed to enhance our understanding of the response of semi-mobile zebrafish larvae to electric field in a microchannel environment. The effects of electric field direction, current and voltage magnitude and repeated exposure to electric current pulses were investigated for the first time.

Exposing WT zebrafish larvae to 1-9 μA electric currents induced an amplitude-dependent behavior; that is, the longest RD was evoked at intermediate currents of 3 and 6 μA and the highest TBF was induced at the lowest current of 1 μA with a decreased plateau trend at higher currents, potentially resulted from paralysis in the larvae, and in line with previously published literature. Positioning the anode at the head of the larva resulted in few bouts with large angle changes and body bending (i.e. short RD and high TBF). However, reversing the electric field direction caused a significant increase in RD and decrease in TBF, confirming that zebrafish is able to sense the

direction of the electric field and modulate its response. In voltage studies, it was shown that zebrafish response was not sensitive to the voltage drop across the whole device if the current was kept constant. However, the voltage difference across the region where the larva was trapped significantly affected the RD and TBF. A slight increase in the trapping region voltage raised the RD while reducing the TBF, demonstrating that zebrafish larvae reacted to a low voltage drop with fewer bouts but larger angle changes. In contrast, the extreme increase in the trap voltage drop caused a significant decrease in RD, possibly as a result of partial paralysis.

In addition, we showed an ISI-dependent change in zebrafish responsiveness to multiple electric stimuli, demonstrating that the more rapid the frequency of stimulation (shorter ISI), the faster habituation was seen. Having demonstrated that the zebrafish RD and TBF consistently declined with subsequent pulses and ISI of 5 s, we aimed to identify whether this decrease fulfilled the habituation criteria. Two different habituation-dishabituation scenarios were used to distinguish habituation from motor fatigue and sensory adaption. First, a recovery time of 5 min between two series of 10 electrical pulses was proved to be sufficient for zebrafish larvae to regain the locomotor response, ruling out the possibility of motor fatigue. Second, introduction of a light pulse between electrical pulses could re-induce the locomotor responses, confirming that the observed iterative decrease was not a result of sensory adaption.

A new gel-free and anesthetic-free approach for immobilization and bi-directional imaging of 5-7 dpf zebrafish larvae in a single multi-phenotypic microfluidic device was also demonstrated. The proposed multi-phenotypic screening technique was shown to be applicable and sensitive enough for heart activity screening and behavioral studies of zebrafish larvae. The effect of an electric stimulus on zebrafish heartrate was investigated for the first time. The application of

electric stimulus resulted in a temporary increase in zebrafish heartrate during exposure. The heartrate returned to a baseline rate shortly after the disconnection of electricity.

The proposed platform opens broad areas of applications including on-demand behavioral investigations of chemical toxicity and gene functions using electric response as a versatile and on-demand readout. In combination with loss-of-function and gain-of-function zebrafish models, the versatile platform reported here will be instrumental for correlating the mechanism of electric-induced responses with the behavioral phenotypes. Our technique can be utilized to study different biological pathways involved in the habituation of zebrafish locomotor activity. The assay itself is also useful for behavioural investigation of movement disorders and to screen for toxic or therapeutic compounds. Further research opportunities may also involve designing a new device to improve the resolution of the dual-imaging and expanding the device capabilities to monitor multiple larvae in parallel and a more extensive range of phenotypes such as fin and mouth movement. The presented design is expected to contribute to a wide range of microfluidic applications such as multi-organ imaging on a chip and multi-phenotypic chemical screening assays.

Chapter 4[§]

4. Increase the Throughput of the Microfluidic Device for Zebrafish Electric Response Studies

In the previous chapter, we introduced single-fish electrofluidic platforms as a tool for screening zebrafish behavioural responses. Considering the potential of this technique in behavioural screening, there is a need for increasing the throughput of these assays to facilitate screening of multiple larvae in a shorter period of time. The focus of this chapter is on enhancing the throughput of our electrofluidic behavioral screening assay (Obj. 3 of the thesis).

[§] Some content of this chapter has been published in

1. Khalili, E. van Wijngaarden, Kh. Youssef, G. Zoidl, P. Rezai, "Designing Microfluidic Devices for Behavioral Screening of Multiple Zebrafish Larvae", *Biotechnology J.,* e2100076, 2021. Permissions for the use of the text has been received from John Wiley and Sons.
2. Khalili, E. van Wijngaarden, G. Zoidl, P. Rezai, "Dopaminergic signaling regulates zebrafish larvae's response to electricity", *Biotechnology J.,* 2100561, 2022. Permissions for the use of the text has been received from John Wiley and Sons.

4.1. Introduction

Despite of multiple microfluidic devices developed for monitoring the tail movement of individual zebrafish larvae in response to chemicals, fluid flow and electricity[97,115,122,129], the challenge of long time required for behavioral screening of one larva at a time and resulting low assay throughput still remains unaddressed in this method.

Testing zebrafish individually in our semi-mobile assay (Fig. 2-2) involves a rest period in addition to the stimulus exposure time, summing the total length of an experiment to more than 100 s per zebrafish larva[129]. In this respect, increasing the number of zebrafish on the chip can reduce both the resting and stimulation times per fish. However, locomotor response testing requires zebrafish larvae to be spaced out on a device to allow complete tail strokes, while preventing tail collisions with the device walls. In combination with restrictions associated with the microscope field of view (FOV), this limits the number of larvae that can be tested simultaneously under a microscope. Loading multiple active zebrafish larvae individually into designated locations on the device and preventing them from escaping the device during the loading process pose challenges.

In this chapter and through adapting experimental methods and modifying design components, we demonstrated that a multi-fish microfluidic device could be produced to reduce the time of behavioural screening and facilitate testing larger sample sizes with our electrical stimulation method. Much can be learned from the device design process described in this chapter. Various methods of trapping and orienting the fish were investigated. Using finite element method, the impacts of the design modifications on the electric field and fluid flow through the device were examined. Our final design allowed us to (i) load four larvae in parallel into the device (restricted by microscope FOV), (ii) partially immobilize all larvae with their heads trapped and tails moving

in chambers, (iii) expose the larvae to an on-demand electric stimulus and (iv) quantify the electric-induced tail movements in terms of RD and TBF. Responses to electric stimulation were compared between the previously developed single-larva device and the multi-fish design to ensure the new device was fit for future testing. Our multi-fish device can be used in the future genetic and chemical screening assays for faster and more efficient research involving behavioural phenotypes of zebrafish larvae with potential applications in toxicology and drug discovery.

4.2. Methods

4.2.1. Evaluation of Device Performance

To compare the functionality of different designs, the testing time per fish, loading efficiency and orientation efficiency of each design was calculated using Eq. 4-1, Eq. 4-2 and Eq. 4-3, respectively.

$$Testing\ time\ per\ fish = \frac{Loading\ time + 60\ s\ recovery\ period + 20\ s\ stimulation\ interval}{Number\ of\ fish\ successfully\ oriented\ in\ the\ device} \quad Eq.\ 4\text{-}1$$

$$Loading\ efficiency = \frac{Number\ of\ larvae\ trapped\ in\ the\ TRs}{Number\ of\ TRs\ in\ the\ device} \quad Eq.\ 4\text{-}2$$

$$Orientation\ efficiency = \frac{Number\ of\ fish\ correctly\ positioned\ in\ the\ TR\ (with\ tails\ in\ the\ screening\ pool)}{Total\ number\ of\ larvae\ trapped} \quad Eq.\ 4\text{-}3$$

The final successful design in loading was then modified to include electrodes to apply the required electrical stimulus for behavioural assays. Recordings were used to find the electric-induced RD and TBF of zebrafish larvae to characterize the tail movement.

4.2.2. Numerical Model

The numerical analysis was performed by a co-author (Ellen van Wijngaarden) of our paper[128] and is presented here for the sake of chapter completion. The model of the final device was created

using SolidWorks (SolidWorks Corp., USA) and imported into COMSOL Multiphysics (COMSOL Inc., Sweden) for 3D simulations of the device. The electric current module in COMSOL was applied to determine the required total electric current at the electrodes in the final device so that each fish was exposed to the electric current of 3 μA, for consistency with our single-fish device[129]. The electric field within a conductive media was modeled by solving Ohm's law (Eq. 4-4) using the steady-state direct-current electric module.

$$V = IR \qquad \textit{Eq. 4-4}$$

Where V is the voltage drop across the section, I is the electric current and R is the electrical resistance.

The electric resistance of the microchannel, R, can be calculated using Eq. 3-2.The electric conductivity of tap water was determined using the conductivity measurement kit (Combo meter (HI98129), HANNA instruments, Italy). The values of 293.15K and 0.034 S/m were defined for the temperature and electrical conductivity of tap water, respectively. The device outlets positioned downstream of the TRs were set as anodes while a central channel boundary upstream from TRs was set to cathode. All other channel boundaries were defined as electric insulation.

COMSOL was also used for flow field simulation to understand the flow patterns and fish loading sequence in the traps. The laminar flow module was applied and the relevant boundary, initial, and material conditions were defined. The Navier-Stokes (Eq. 4-6) and the continuity (Eq. 4-7) equations were used for the conservation of momentum and mass, respectively. The fluid was regarded as incompressible and Newtonian with gravity forces and viscous dissipation effects neglected in the equations.

$$\rho \frac{D\mathbf{u}}{Dt} = -\nabla \mathrm{p} + \rho \boldsymbol{g} + \mu \nabla^2 \mathbf{u} \qquad \textit{Eq. 4-5}$$

$$\rho \nabla \cdot \mathbf{u} = 0 \qquad \textit{Eq. 4-6}$$

The variables **u**, p, ρ, and μ are the velocity vector, pressure, density, and dynamic viscosity, respectively. An inlet flow rate of 1 ml/min and an indirect flow rate of 0.8 ml/min was inputted to reflect the values implemented during the experiments. While the inlets were described in terms of volumetric flow rates, the outlets were set to atmospheric pressure. The media was defined as water and a no-slip condition was added to all channel walls.

4.3. Results and Discussion

We first examined various designs for proper loading and orientation of two zebrafish larvae in parallel head-trapping regions in multiple microfluidic devices. The best double-fish design was assessed by examining the larvae's viability, then expanded to develop a device for behavioral screening of four zebrafish larvae in parallel. Using COMSOL simulation, numerical analysis was applied to understand the electric field and flow conditions in the device. We also examined the viability of the zebrafish larvae in our quadruple-fish device before quantitative comparison of devices in terms of loading time per fish, loading efficiency, orientation efficiency, testing time per fish, and last but not least, the RD and TBF of zebrafish larvae.

4.3.1. Orientation and Head-Trapping of Two Zebrafish Larvae in Multiple Microfluidic Device Designs

To achieve trapping of two zebrafish larvae from their heads in parallel TRs of a single device, our original design shown in Fig. 2-2 was modified in four designs as shown in Fig. 4-1, and each design was compared in terms of the proper loading and orientation of the larvae in the traps.

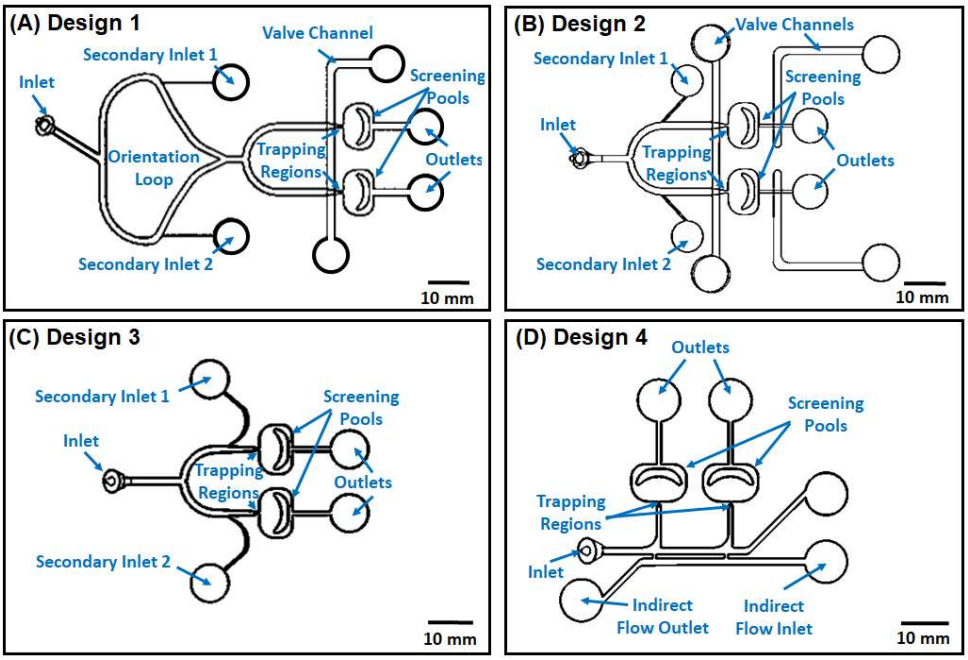

Fig. 4-1. Different designs tested for the development of the double-fish microfluidic device. (A) Design 1: double fish device with orientation loop, (B) Design 2: double fish device with valves, (C) Design 3: double fish device with modified trap, and (D) Design 4: double fish device with indirect flow assisted loading[128]*. Reprinted with permission from John Wiley and Sons.*

4.3.1.1. Design 1: Double-Fish Device with Orientation Loop

As the most obvious iteration, Design 1 in Fig. 4-1A was created to investigate if a trap similar to the one previously reported for single-larva studies[129] in Fig. 2-2 could be used twice in parallel to load two fish into the device. Therefore, some similar features including the trap, screening pool, valve layer, inlet and channel dimensions were applied in Design 1. The TR which is shown in Fig. 4-2A was gradually narrowed in width, from 0.9 to 0.25 mm, to mimic the ergonomic structure of 5-7 dpf zebrafish larvae from head to the yolk region. Considering the idea of direction-switching loop reported by Lin et al.[94], an orientation loop was added downstream of the inlets to allow for the fish to be directed by flow towards the TR with their tails facing the trap (tail-first). If a larva was loaded head-first, flow from the secondary inlet 2 would push the larva into the TR.

Otherwise (for a tail-first larva), the secondary inlet 1 would be involved to move the larva into the TR.

We fabricated the device and conducted 10 trials with 2 larvae per trial (N=20). This design was not successful in either orientation or trapping the larvae. Loading the first larva was easy but the trap size was not suitable to hold the fish in place while the second larva was being loaded. In most of the cases, the first larva was ejected from the device while the second larva was being loaded. Moreover, the fish were able to turn at different intersections, rendering the idea of orientation loop ineffective in our device. Due to these difficulties, this design was rejected in our studies.

4.3.1.2. Design 2: Double-Fish Device with Valves

Design 2 in Fig. 4-2B was developed to address the Design 1 issues of the fish being washed through the traps during loading and controlling the orientation of the larvae. In Design 2, we utilized a second deflectable PDMS membrane valve downstream from the screening pools to block the flow and prevent the fish from being washed through during the loading process. The orientation loop was also removed, and the secondary inlets were shifted to minimize the number of junctions and opportunities for the larvae to rotate in the channel. In this case, the secondary inlets were positioned as shown in Fig. 4-1B to direct the larvae into the proper trap based on their longitudinal orientation direction in the U-shaped channel. For example, for a larva loaded in the top branch with its head facing toward the TR, flow from secondary inlet 1 was used to send the larva into the bottom TR.

A total of N=20 zebrafish larvae were tested in 10 trials in this device. The additional valves could not completely cut off the channels, letting a small flow pass through the TR which was enough to push the zebrafish larva out of position. Moreover, actuating the additional valves added

to the difficulty of loading and consequentially increased the loading time. Removing the orientation channel shortened the inlet channel and decreased the user friendliness of the device as orientating the fish had to be done in a smaller section. Although the secondary inlets offered sufficient control to position the fish into the desired trap, it proved time consuming to operate and adjust the flow rate based on the position of the larvae. Accordingly, Design 2 was also abandoned in our studies.

4.3.1.3. Design 3: Double-Fish Device with Modified Traps

In the original device shown in Fig. 2-2 and in both Designs 1 and 2 of the double-fish devices, the trap design remained unaltered as shown in Fig. 4-2A. Preliminary experiments in the double-fish devices presented difficulties in maintaining the larvae in these traps as discussed above. Therefore, Design 3 in Fig. 4-1C specifically targeted the issue of the fish being washed through the device during loading. The valve layer in Design 2 was removed, and the focus of the design was put on shaping the traps to find the size that would hold the zebrafish larvae securely. The device used the same secondary inlet channels to reduce the number of factors that were changing from the previous design. However, we utilized longer channels to facilitate loading, with the secondary inlets pushed farther back along the U-shaped main channels.

The original trap shape in the single-larva device and Designs 1 and 2 had a rectangular cross-section with a width of 0.25 mm and a height of 0.55 mm (Fig. 4-2A). In Design 3, three trap shapes were tested consecutively, i.e. a half-oval shape (0.25 mm diameter by 0.25 mm height), a semicircular design ($r = 0.15$ mm) and a rectangular design (0.25 mm width by 0.4 mm height) as shown in Fig. 4-2B-D, respectively. The overall shape and dimensions were adjusted based on the average measurements of 5-7 dpf larvae's heights and widths.

Both the semicircular and ovular trap shapes in Fig. 4-2B and 3C were observed to trap the fish very tightly appearing to place undue stress on the fish. The rounded geometry resulted in the fish acting like a plug and blocking flow completely increasing the pressure drop experienced by the fish in the trap. The final rectangular shaped trap in Fig. 4-2D proved effective in holding the fish in the TR while allowing a small amount of flow around the fish.

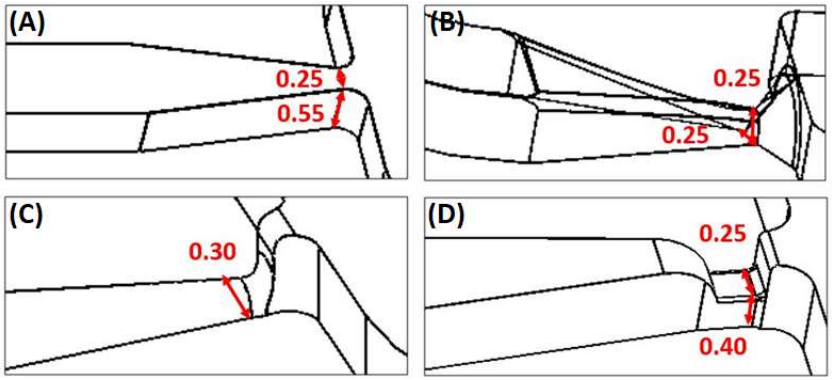

Fig. 4-2. Close up views of trap designs for (A) the original single-larva device and Designs 1-2, (B) Design 3 with oval trap, (C) Design 3 with semicircular trap, and (D) Design 3 with rectangular trap (which was the most successful design and also applied to Designs 4-5) [128]*. Reprinted with permission from John Wiley and Sons.*

A viability test was done to confirm that the fish were not affected by the loading technique and the device components in Design 3. During the 10 days of post-assay monitoring, the survival rates of the control (exposed to device flow) and the reference (not exposed to device) groups were similar (Fig. 4-3A, Mann-Whitney U test, p-value>0.05). More than 86% of the fish loaded into the device showed a normal morphology, demonstrating no significant difference with the reference group (Fig. 4-3B, Mann-Whitney U test, p-value>0.05). In summary, we concluded that the loading and trapping operations in Design 3 did not have a significant adverse effect on the zebrafish larvae.

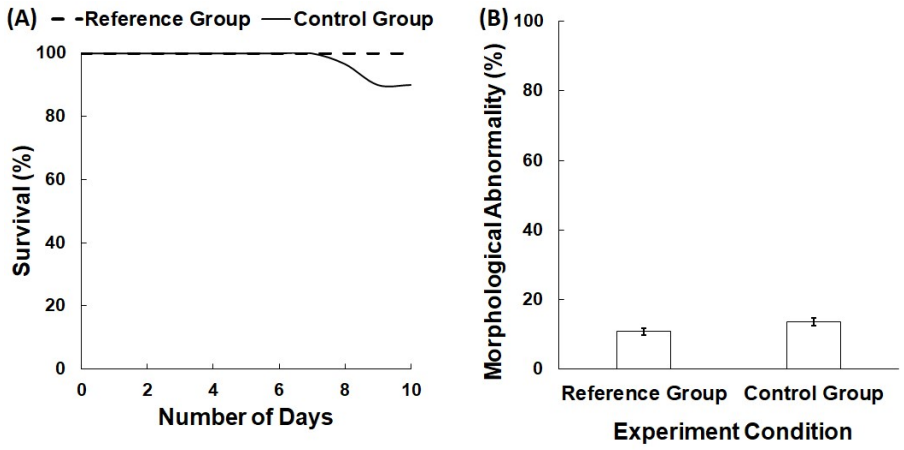

Fig. 4-3. Survival and morphological abnormality of 5 dpf zebrafish larvae tested in the double-fish device (Design 3) and then monitored off-chip for 10 days (N = 20 per condition in three different trials). (A) Survival of zebrafish larvae trapped in the device for 80 s but not exposed to any electric current (control group) compared to that of the fish that was neither exposed to the device nor to any electric current (reference group). (B) Morphological abnormality of the above-mentioned zebrafish larvae during 10 days of observation after experiments[128]*. Reprinted with permission from John Wiley and Sons.*

While the modified TR proved effective in trapping the fish, controlling the orientation remained challenging. Although secondary inlets enabled efficient trapping, sufficient time and expertise was required to adjust the flow rates from the main and secondary inlets to position the larvae in a tail-first orientation. The trap shape was deemed suitable for use in subsequent designs and the focus was shifted to addressing the fish orientation.

4.3.1.4. Design 4: Double-Fish Device with Indirect Flow Assisted Loading

To achieve tail-first orientation for the larvae, various methods were considered ranging from altering the previously unsuccessful orientation loop (Design 1) to the use of secondary inlets (Designs 2 and 3), and finally applying electric field for orientation before loading the larvae into the traps (results not reported). The challenges associated with Designs 1-3 were already discussed

in the previous sections. The use of electric stimulus to orient the fish was ruled out due to the possibility of adaptation to the electric field or altering the electrically induced movement response, which we aimed to test with the final design.

In Design 4, an indirect flow assisted loading technique inspired by the work of Lin et al.[94] was used. The indirect flow was used to facilitate the loading and trapping procedure (Fig. 4-1D). Once the larvae were loaded, the flow velocity was adjusted so that rheotaxis[115] ensured tail-first orientation for the majority of the trials. Additionally, the width of the main channel was decreased from 0.9 mm to 0.8 mm to decrease the possibility of larvae's turning at the junctions. The indirect flow was run in the opposite direction parallel to the main channel and was connected with the main channel through a series of short vertical channels (0.2 mm wide and 0.55 mm deep). Water was pumped into the main channel through these vertical channels to increase the hydrodynamic flow focusing on each trap and preventing the larva from swimming back. A trapped larva could act as a partial plug, raising the flow resistance in the first trap and directing the main flow to the second trap. Consequently, the second larva bypassed the occupied trap and was carried into the next TR.

Testing N=20 larvae, the advantages of Design 4 in regard to loading, orientation and trapping made it more appealing than Design 3. This design was modified further (see next section) to increase the number of fish being tested simultaneously, reduce the testing time per fish, and make full use of the microscope field of view.

4.3.2. Design 5: Quadruple-Fish Device with Indirect Flow Assisted Loading

Design 5 in Fig. 4-4 was created to investigate the possibility of expanding the indirect flow loading and trapping method in Design 4 (Fig. 4-2D) for testing of four zebrafish larvae simultaneously. Design 4 was expanded with screening pools and traps arranged to fit under our

microscope FOV of 12 mm by 18 mm. The main channel width was also further reduced to 0.7 mm to reduce the capability for the larvae to turn at the intersections. The new design consisted of three layers shown in Fig. 4-4A with various microchannels to enable loading and screening of four larvae simultaneously.

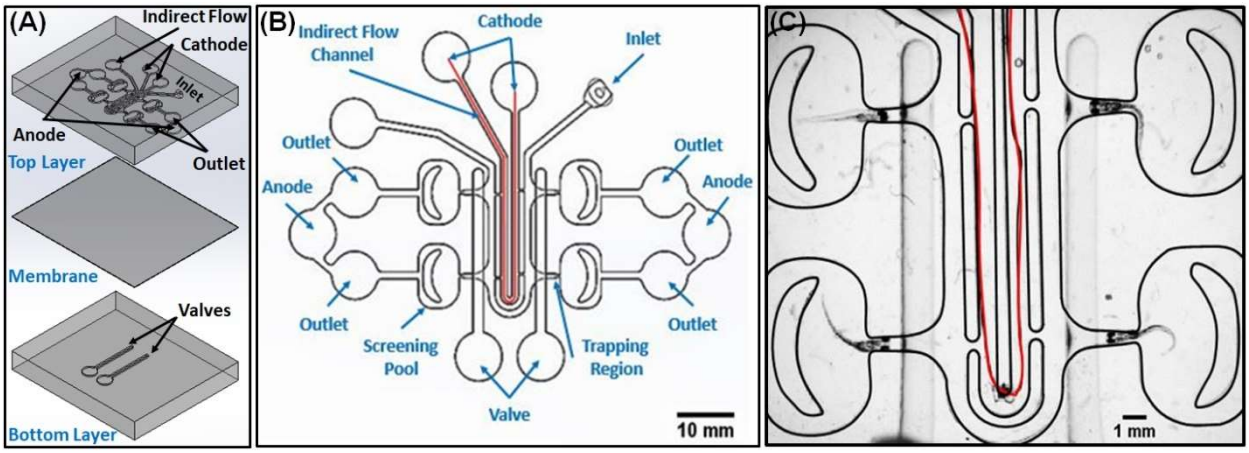

Fig. 4-4. Quadruple-fish device with indirect flow assisted loading (Design 5). (A) Exploded view drawing of the device layers. (B) Top schematic of the assembled device showing the inlets, outlets, screening pools, valve channels and electrodes. (C) The fabricated device with four zebrafish larvae loaded into the TRs. The cathode electrode running through the indirect flow channel is shown in red[128,130]*. Reprinted partially with permission from John Wiley and Sons.*

The top section of the three-layer device included the main inlet and outlets from which the fish entered and exited the device, the indirect flow inlet and outlet to help direct the fish into the TRs and the reverse flow to aid in positioning and orienting the fish. The screening pools provided enough space allowing complete tail strokes without any collision with the device walls. The bottom layer of the device included valve channels containing air. The middle layer consisted of a thin membrane, approximately 200 μm thick, separating the top and bottom layers. When the bottom valve was pressurized, the membrane deflected into the upper layer channel to prevent the fish from swimming out of the TR when the indirect flow was switched off. Two anodic copper

wire electrodes were attached to the outlets and a copper wire was run through the indirect flow channel (Fig. 4-4A and 4B), at the middle of the device, to function as the cathode.

Following loading procedure explained in section 2.6.3, four larvae are successfully oriented and trapped in the TRs as shown in Fig. 4-4C. The loading trials (N=40) proved that the design was ready to move to the viability test as well as the next stage of modifications for electrical stimulation and behavioral testing of the loaded larvae. The design was modified accordingly to include locations for the electrodes with a wire running through the indirect flow channel (shown in red in Fig. 4-4A and 4B) to act as the cathode and outlets being added for the anode wires.

Viability and morphological testing were repeated in our quadruple-fish device to ensure that electric stimulation would have no significant impact on the zebrafish. Three groups of larvae including a reference group (kept off-chip), a control group (exposed to device flow only) and a test group (exposed to device flow and electric field) were tested. During the 10 days of post-experimental monitoring, the survival rates of all three groups were similar (Fig. 4-5A, Mann-Whitney U test, p-value > 0.05). More than 85% of the fish exposed to the device or the electric current did not show any abnormal morphology, showing statistical similarity with the reference group (Fig. 4-5B, Mann-Whitney U test, p-value > 0.05). Therefore, we concluded that the device and electric stimulation did not have any significant effect on the zebrafish larvae in the quadruple-fish device.

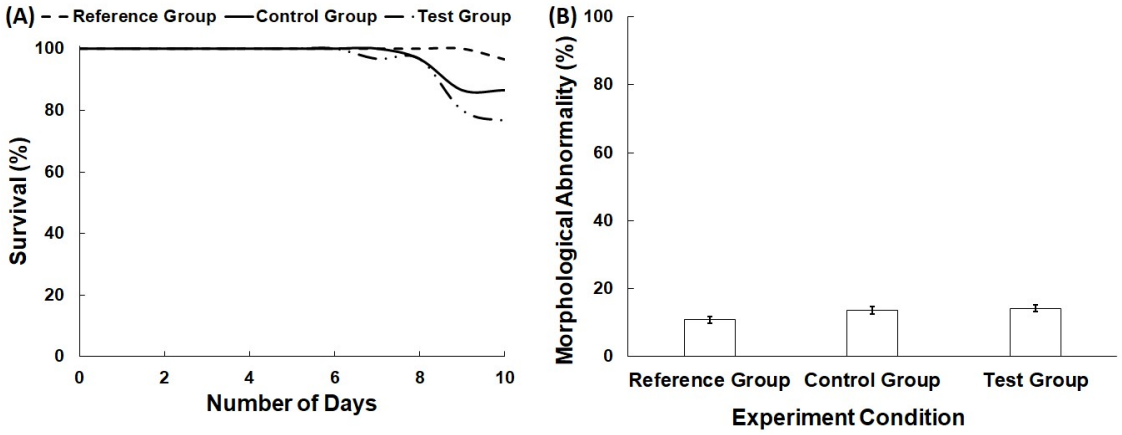

Fig. 4-5. Survival and morphological abnormality of 5 dpf zebrafish larvae tested in the quadruple-fish device (Design 5) and then monitored off-chip for 10 days (N = 20 per condition in three different trials). (A) Survival of zebrafish larvae exposed to electric current of 3 μA in the device (test group), compared to that of the fish not exposed to any electric current in the device as the control group and the fish tested off-chip as the reference group. (B) Morphological abnormality of the above-mentioned zebrafish larvae during 10 days of observation after experiments[128]*. Reprinted with permission from John Wiley and Sons.*

4.3.2.1. Numerical Analysis of the Quadruple-Fish Device

Design 5 was further analyzed using electric and flow simulations to ensure similar electro-fluidic conditions for all fish trapped in the TRs.

A mesh independency study was conducted for both the current density distribution and flow velocity to ensure the accuracy of the results. The model was meshed using tetrahedral elements through the built-in module in COMSOL with special focus on the size of the mesh to resolve high gradients and changes in dimensions along the channels. Fig. 4-6A shows the obtained current density along a zebrafish trap in the microfluidic device (line C-C') for various mesh sizes. For simplification, standard mesh size settings in COMSOL were applied. These settings were extra coarse, coarser, normal, fine, finer, and extra fine, with the corresponding number of elements in Fig. 4-6A. The graph exhibits small oscillations for Extra Coarse mesh setting when compared to

the smooth profile of the Extra Fine mesh. The mesh was refined until a smooth line, with values varying less than 1% was obtained, when using an Extra Fine mesh, to match a theoretical profile for current density, resulting in a suitable mesh for the required simulations.

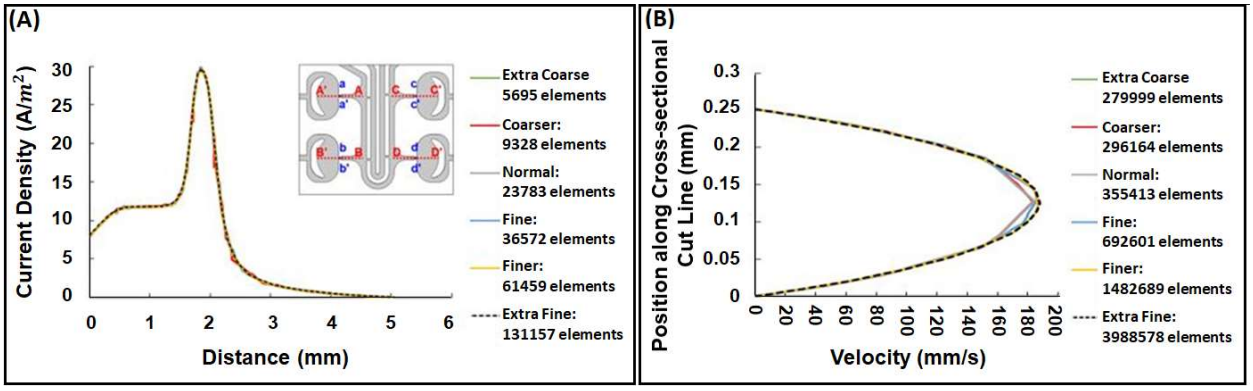

Fig. 4-6. Mesh independency study showing (A) the current density profile along the cut line C-C' for standard mesh sizes in COMSOL and (B) velocity profiles along the cross-sectional cut line c-c' for Trap C with the highest gradient[128]*. Reprinted with permission from John Wiley and Sons.*

The flow velocity mesh study followed a similar method. The required mesh was significantly finer than that used to study the current density. Therefore, a different mesh was used to maintain the low computational cost of the current simulation. The fluid velocity along the cross-section c-c' for trap C, where the velocity gradient was greatest, was examined using the same standard mesh size settings. However, the resulting meshes had a greater number of elements as the program automatically accounts for higher velocity gradients present compared to the electric field gradients. This automatically refined the mesh in conjunction with the automatic corner refinement tool. The mesh was refined until the reported velocities varied by less than 1% matching a theoretical parabolic profile characteristic of laminar flow through a channel. Fig. 4-6B displays the corresponding velocity profiles, with the higher element mesh curves approaching the correct parabolic shape achieved using the Extra Fine mesh.

Previous experiments in our single-fish device (Fig. 2-2) used an electric stimulus of 3 μA to induce tail movement[129]. As shown in Fig. 4-7A, we achieved a uniform voltage drop of 1.1 V in each trap along the cut lines A-A', B-B', C-C' and D-D' (displayed in the upper right corner of Fig. 4-7B) by applying a total electric current of 12 μA between the electrodes of the Design 5 device. Fig. 4-6B demonstrates the current density in traps A-D. Overlapping the four graphs confirmed that the current density across all traps was the same. An electric current of 3 μA, consistent with that used in our single-fish device, was obtained across each trap when the current density was multiplied by the area of the channel along the cutline at any given point[129]. The effects of ohmic heating were assumed to be negligible given the short stimulus. This assumption was supported with a simple calculation for the temperature change given the 20 s stimulus which resulted in a change of less than two hundredth of a degree.

Flow simulations were performed to understand the pressure, shear stress, and flow distribution in the channel and to predict the trap loading sequence. The pressure magnitude and shear stress were plotted to ensure uniform loading conditions in TRs (Fig. 4-7C and 8D).

Simulation results in Fig. 4-7C for the flow dynamics within the chip indicated a pressure drop and hence a hydrodynamic force pointing from the main channel towards the traps that was utilized to load and immobilize the zebrafish larvae. The change in pressure for traps A to D were found along the cut lines of A-A' to D-D'. The pressure drop magnitudes were 152 Pa, 145 Pa, 215 Pa and 160 Pa for Traps A, B, C and D, respectively, as shown in Fig. 4-8. This sequence was matched with the larvae loading patterns observed during experiments validating the simulation. Trap C displayed a pressure drop that is approximately 40% larger than the three other traps supporting the observation that fish preferred this TR most. Fish generally followed the order of the traps for

loading (C, D, A, B) but the occasional change in order was seen between traps B and A. This is likely due to the similar pressure drop values in these traps.

The water viscosity was multiplied by the velocity gradient at the wall to obtain the shear stress in the traps in Fig. 4-7D. Shear stress varied along the narrowing traps due to the altered flow velocity, which was compared to the levels of stress known to damage the larvae. Studies done by Ulanowicz and Morgan [158,159] examined the effects of shear stress due to fluid flow on various fish species at the egg, larval and fully developed stages. The maximum shear stress to avoid injury in larval fish was found to be approximately 45 Pa. This far exceeded the maximum shear stress of less than 10 Pa that the zebrafish experienced during loading in our device (Fig. 4-7D).

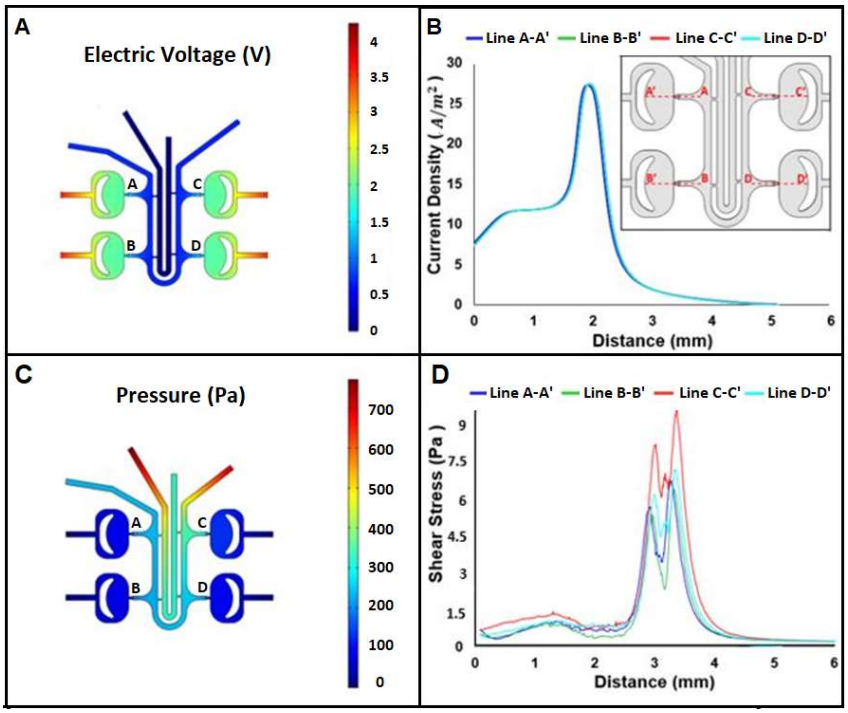

Fig. 4-7. COMSOL simulation results of (A) the electric voltage and (B) current density within the chip (Design 5) before larvae loading, indicating a uniform voltage and current in all four traps. (C) Fluid pressure magnitude and (D) shear stress magnitude within the chip during loading[128]*. Reprinted with permission from John Wiley and Sons.*

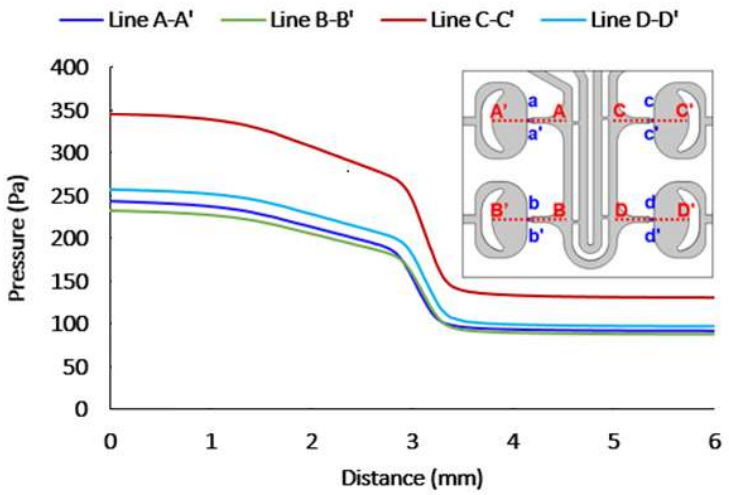

Fig. 4-8. Pressure drops across traps A, B, C and D using cut lines A-A', B-B', C-C' and D-D', respectively[128]*. Reprinted with permission from John Wiley and Sons.*

4.3.3. Quantitative Comparison of Single-, Double- and Quadruple-Fish Designs

To compare the effectiveness of various devices, the four key designs were considered including the single-fish device (Fig. 2-2)[129], the double-fish devices with modified traps (Design 3 in Fig. 4-1C) and the indirect flow assisted loading (Design 4 in Fig. 4-1D), as well as the quadruple-fish device with indirect flow loading (Design 5 in Fig. 4-4). Running 10 tests in each device resulted in sample sizes ranging from 10 to 40 fish (10 fish in the single, 20 in the double and 40 in the quadruple designs). The loading times per fish were 30±3.7 s, 28.9±3.7 s 26.9±2 s and 20.4±4.1 s for the four Designs, respectively (Fig. 4-9A), with no significant difference found between the loading times (Mann-Whitney U test, p-value > 0.05). Statistically similar loading efficiencies of 85±7.6%, 85±7.6% and 87.5±5.6% were obtained for Designs 3, 4 and 5, respectively (Mann-Whitney U test, p-value > 0.05) (Fig. 4-9B). Since, the same loading strategy and trap design was used in all three devices, similar loading times and efficiencies could be

expected. Comparing the orientation efficiencies clarified the advantage of Design 4 over 3, therefore, this design was used as the basis for Design 5, as mentioned previously. Using Design 4, we could achieve an orientation efficiency of 90±7.1% that was significantly higher than Design 3 (Mann-Whitney U test, p-value>0.05, p-value<0.05). Therefore, the same orientation technique used in Design 4, was employed in Design 5 to trap four zebrafish larvae.

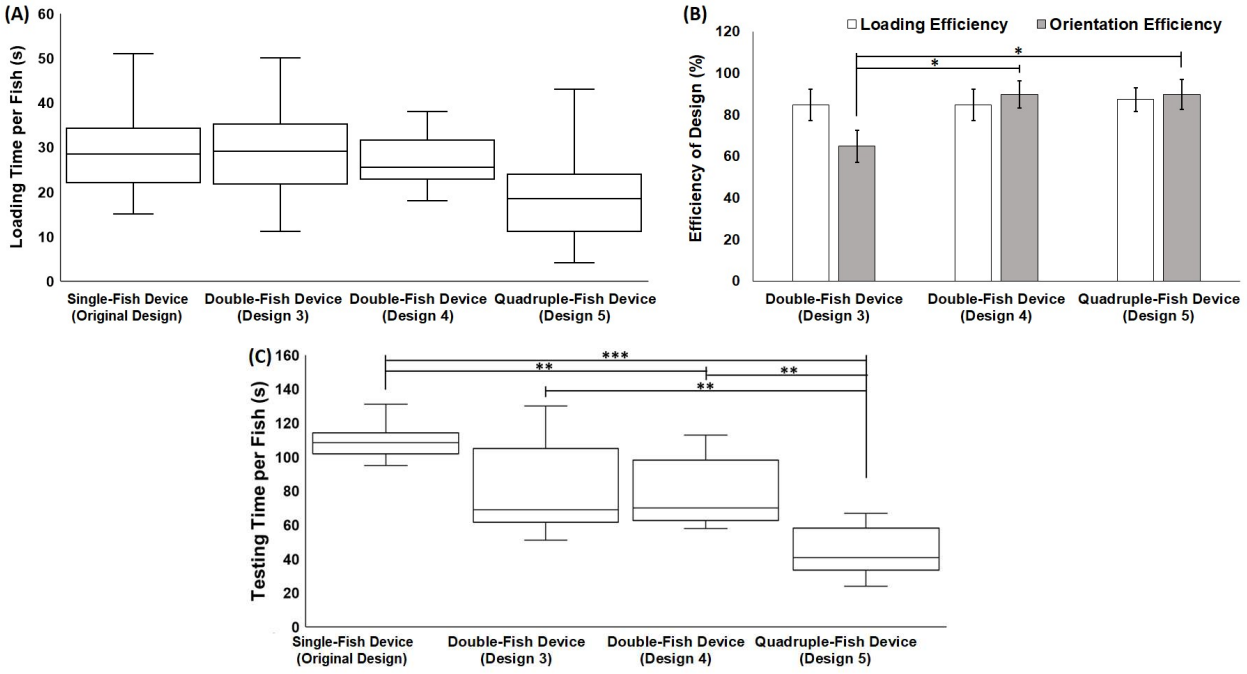

*Fig. 4-9. Performance comparison of single-, double- and quadruple-fish devices, showing the (A) loading time per fish, the (B) loading and orientation efficiencies and the (C) total testing time per fish. The lines within the boxes mark the median. Upper and lower boundaries are the 75th and 25th percentile and whiskers are the maximum and minimum. *: p<0.05, **: p<0.01, ***: p<0.001. N=10, 20, 40 for single-, double- and quadruple-fish devices, respectively*[128]*. Reprinted with permission from John Wiley and Sons.*

To assess the competitive value of quadruple-fish device over the other three devices, the total testing time per fish in each device was calculated and compared in Fig. 4-9C. Testing times of 110±3.7 s, 80.9±9.3 s, 78.9±6.7 s and 44.4±4.8 s were found for the single-, double- (Design 3 and

Design 4) and quadruple-fish devices, respectively. Fig. 4-9C shows a significant decrease in the testing time per fish as we move from single- to double-fish devices, as a result of the design alterations. The testing time was further reduced in the quadruple-fish device by approximately 60% compared to the single-fish device. This clearly demonstrates the advantage of Design 5 when aiming to facilitate larger sample sizes.

4.3.4. Locomotor Response in Single and Quadruple-Fish Devices

As the single-fish device has already been established[129], the RD and TBF of fish tested in the quadruple-fish device was compared with those in the single-fish device for validation purposes. The total electric current of 12 μA (3 μA per trap) obtained through the electric-field simulation in COMSOL was applied in the quadruple-fish device, while an electric current of 3 μA was used in the single-fish device, ensuring the larvae were exposed to a consistent stimulus in all traps in both devices. N=45 larvae in three trials were tested and the results in Fig. 4-10 indicate that no significant change was found in the electric-induced responses in the two devices. The RDs and TBFs were statistically similar among the devices, based on a Mann–Whitney U with p-value>0.05. Therefore, the final device enables testing of four fish simultaneously without altering the locomotor response while reducing the time of experiment significantly. As the stimulus must be applied only once to the four zebrafish larvae, the new platform facilitates larger sample sizes and offers a way to make screening more efficient. In addition to this, the final device offers a uniform testing environment, ensuring factors such as stimulus duration and magnitude are the same for all fish.

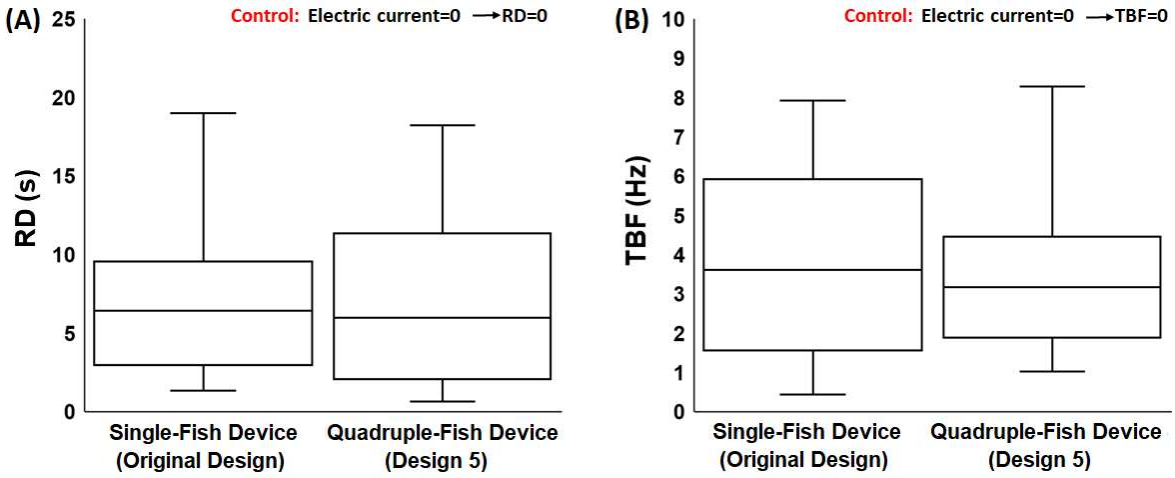

Fig. 4-10. Comparison of electric-induced locomotor response of zebrafish larvae trapped in the single- and quadruple-fish devices. (A) Response duration and (B) tail beat frequency of zebrafish larvae exposed to electric current of 3 μA inside the single-fish and the quadruple-fish devices. Control group RD and TBF were both zero. The lines within the boxes mark the median. Upper and lower boundaries are the 75th and 25th percentile and whiskers are the maximum and minimum. (N=45 larvae per experimental condition in three independent trials)[128]*. Reprinted with permission from John Wiley and Sons.*

4.4. Conclusion

An effective microfluidic device for decreasing the testing time of behavioural assays of 5-7 dpf zebrafish larvae was demonstrated. The device provided a convenient platform for manipulation, testing and imaging four zebrafish larvae simultaneously for tail movement screening. The first step in the design process involved correctly orienting and successfully trapping larvae for screening. Investigating various trap shapes and valve configurations, we ended up with the final rectangular cross-section dimensions to successfully hold the fish in a dorsal position within the traps. Different methods for longitudinal orientation of larvae were researched including using an orientation loop, direct flow and indirect flow. The final design's use of indirect

flow for loading provided the loading and trapping efficiencies of 87.5% and 90%, respectively and offered sufficient control for experiments.

Simulations were utilized to ensure that the device was suitable for behavioural screening. The numerical simulation of the electric field was used to find the required current stimulus and verify that a uniform electric field for each trap-screening pool configuration was obtained. Flow simulations providing the pressure drop across the trap and the shear stress matched the fish loading sequence seen during experiments and ensured that the maximum stress applied was below the threshold for damaging larvae. A viability test was conducted in addition to the numerical tests to ensure the fish are not injured. These results provided further evidence that the device was suitable for use. No difference in RD and TBF for the quadruple-fish device and single-fish device were found, while the testing time per fish was reduced by approximately 60%. The presented design is, therefore, ideal for future behavioral, genetic and chemical screening assays of multiple zebrafish larvae.

The demonstrated techniques and design will enable faster and more efficient screening, holding potential in the fields of phenotypic neurobehavioral research for drug discovery and toxicology.

Chapter 5**

5. Involvement of Dopaminergic Neurons in Electric-induced Movement Response of Zebrafish Larvae

Thus far, we introduced electrofluidic devices to screen behavioral responses of zebrafish larvae evoked by electrical stimuli (Obj. 1 and 3 of the thesis). We also demonstrated that this response was sensitive to electric current intensity, voltage drop across fish body and electric field direction and habituation of response occurred upon exposure to multiple electric stimuli (Obj. 2 of the thesis). In this chapter, our quadruple-fish device was used to investigate the potential involvement of dopaminergic pathway in modulation of electric-induced response (Obj. 4 of the thesis).

** The content of this chapter has been published in Khalili, E. van Wijngaarden, G. Zoidl, P. Rezai, "Dopaminergic signaling regulates zebrafish larvae's response to electricity", *Biotechnology J.,* 2100561, 2022. Permissions for the use of the text has been received from John Wiley and Sons.

5.1. Introduction

In humans, electrical stimulation of brain activities such as deep brain stimulation of PD patients or electrical stimulation in physical therapy have gained a lot of attention[160–162]. This cross-disciplinary interest raises important questions about the molecular and cellular mechanisms of how organisms respond to electrical stimulation.

Dopaminergic signaling modulates different behavior of mammals such as the motor activities[163,164]. Zebrafish larvae offer several advantages for locomotion studies applicable in examining and creating treatments to combat movement disorders. The structure of the dopaminergic nervous system in zebrafish brain is analogous to mammals and similar receptors can be identified for most of the mammalian subtypes and zebrafish[30,165,166]. Several studies have characterized the pharmacology of zebrafish dopaminergic system and investigated the effects of various compounds, that target the dopaminergic receptors of zebrafish larvae, on its locomotion behaviour[25,56,66,167–172]. This may make zebrafish an appropriate model for studying the role of dopaminergic system in locomotion induced by electricity.

Our quadruple-fish electrofluidic device can be used to perform fast and controllable assays on the molecular pathways involved in zebrafish response to electricity, which are still unknown. Since previous studies have identified a correlation between zebrafish general locomotion and dopaminergic signaling pathway[25,66,167–172], we hypothesized that this pathway is involved in the modulation of zebrafish electric-induced locomotion in our device. A specific question that was aimed to be addressed was whether D1- and/or D2-like dopaminergic receptors are involved in zebrafish response to electricity.

To test our hypothesis and answer the above research question, our quadruple-fish microfluidic device[128] was employed to characterize the acute effects of various dopamine compounds on the

electric-induced locomotion of zebrafish larvae for the first time. The electric response was analyzed using RD and TBF as quantitative phenotypes[129]. The electric-induced locomotor response of larvae exposed to dopamine antagonists were compared to those treated with dopamine agonists. We also examined whether the observed impairment in electric-induced movement due to dopamine antagonist exposure could be recovered through subsequent treatment with a dopamine agonist. Our findings elevate the present knowledge about the electric-induced behavior of zebrafish larvae and its potential regulation by the dopaminergic system in the context of a customizable assay platform for on-demand and quantitative behavioral studies.

5.2. Results

In this chapter, we demonstrated a novel application of our quadruple zebrafish microfluidic screening device introduced in chapter 4 and investigated the effects of several dopaminergic receptor compounds (Table 2-1) on zebrafish electric-induced locomotor response.

5.2.1. Effect of Dopamine Non-selective Antagonists and Agonists on Zebrafish Response to Electricity

Here, we investigated the effect of butaclamol and apomorphine (non-selective dopamine antagonists and agonists, respectively) on the electric-induced locomotor activity of larvae in our microfluidic device (Fig. 5-1A). Then, the larvae treated with butaclamol was post treated with apomorphine to examine the combined effect of the non-selective dopamine antagonist and agonist on zebrafish locomotor response, for the first time. As shown in Fig. 5-1B and 1C, the RD and TBF of zebrafish larvae obtained for the control and apomorphine-exposed groups were statistically similar (Mann-Whitney U test, p-value>0.05), showing that apomorphine treatment did not affect the electrically induced response of zebrafish larvae. However, zebrafish receiving

butaclamol exhibited 51% and 27% reduction in the average RD and TBF, respectively, which were both statistically significant. Post treatment with apomorphine rescued the electric-induced locomotor responses and resulted in a 71% increase in RD and 33% increase in TBF. There was no statistical difference between the control group and the post-treated larvae (Mann-Whitney U test, p-value>0.05), demonstrating an improvement of locomotor function under treatment of butaclamol-exposed zebrafish larvae with apomorphine due to an increase in dopamine concentration.

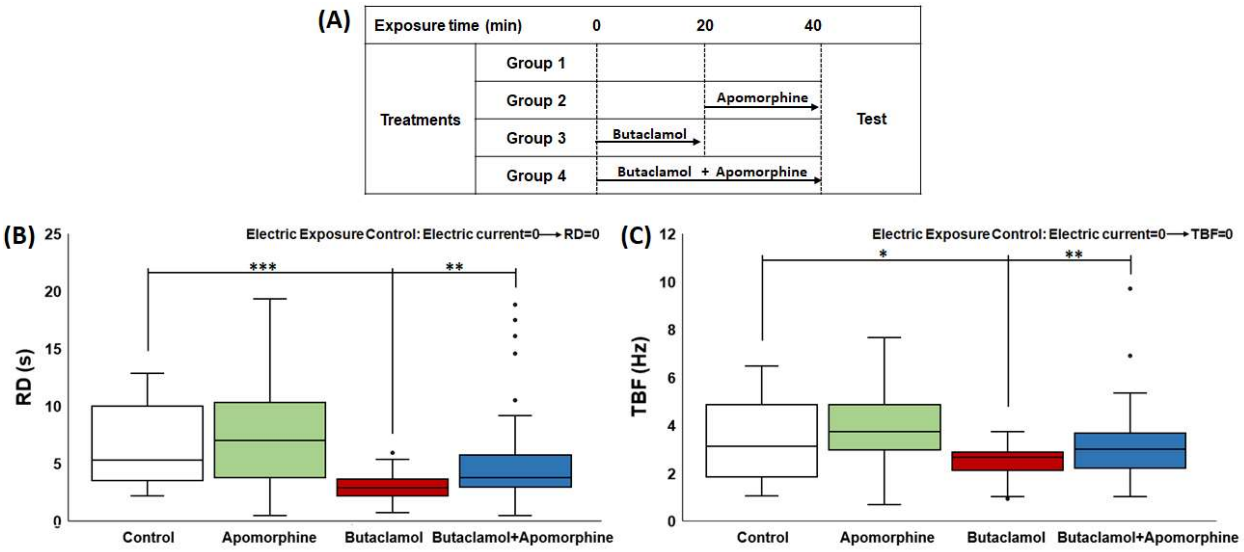

*Fig. 5-1. Effects of apomorphine and butaclamol on 6 dpf zebrafish larvae's electric response. (A) Exposure timeline of zebrafish larvae. Electric-induced (B) RD and (C) TBF of zebrafish larvae exposed to no chemical (control), 0.2 µM apomorphine, 16.7 µM butaclamol, and 0.2 µM apomorphine after exposure to 16.7 µM butaclamol. Control group RD and TBF were both zero. The lines within the boxes mark the median. Upper and lower boundaries are the 75th and 25th percentile and whiskers are the maximum and minimum. *: p<0.05, **: p<0.01, ***: p<0.001. (N=45 larvae per experimental condition in three independent trials)*[130]*. Reprinted with permission from John Wiley and Sons.*

5.2.2. Effect of D1- and D2-like Selective Dopamine Antagonists and Agonists on Zebrafish Response to Electricity

After showing the effect of non-selective dopamine compounds on the electric-induced response of zebrafish larvae, we assessed potential roles of specific dopamine receptors in regulating this response.

We first assessed the effect of SKF-81297 (a D1-like selective agonist) alone and observed no significant effect on the electric-induced RD and TBF of zebrafish larvae (Fig. 5-2.). In contrast, the response of larvae exposed to SCH-23390 (a D1-like selective antagonist) was marked by a shorter RD and TBF with values decreasing by 48% and 27%, respectively (Mann-Whitney U test, p-value<0.001 and 0.05, respectively). In zebrafish larvae exposed to SCH-23390, we observed no significant change upon post treatment with SKF-81297.

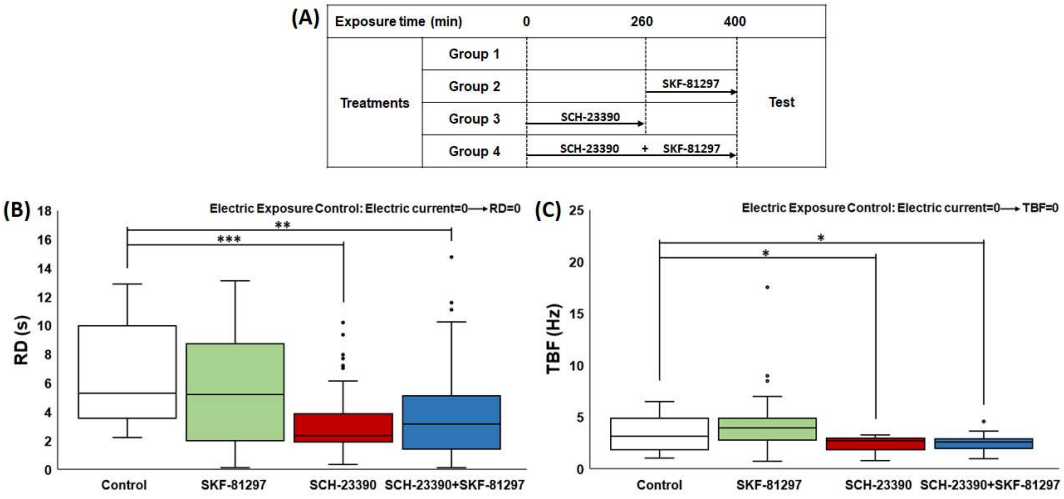

Fig. 5-2. Effect of SCH-23390 and SKF-81297 on 6 dpf zebrafish larvae's electric response. (A) Exposure timeline of zebrafish larvae. Electric-induced (B) RD and (C) TBF of zebrafish larvae exposed to no chemical (control), 50 µM SKF-81297, 0.6 µM SCH-23390, and SKF-81297 after exposure to 0.6 µM SCH-23390. Control group RD and TBF were both zero. The lines within the boxes mark the median. Upper and lower boundaries are the 75th and 25th percentile and whiskers are the maximum and

*minimum. *: p<0.05, **: p<0.01, ***: p<0.001. (N=45 larvae per experimental condition in three independent trials)*[130]*. Reprinted with permission from John Wiley and Sons.*

We then determined the effects of two D2-like selective compounds on zebrafish electric response (Fig. 5-3).

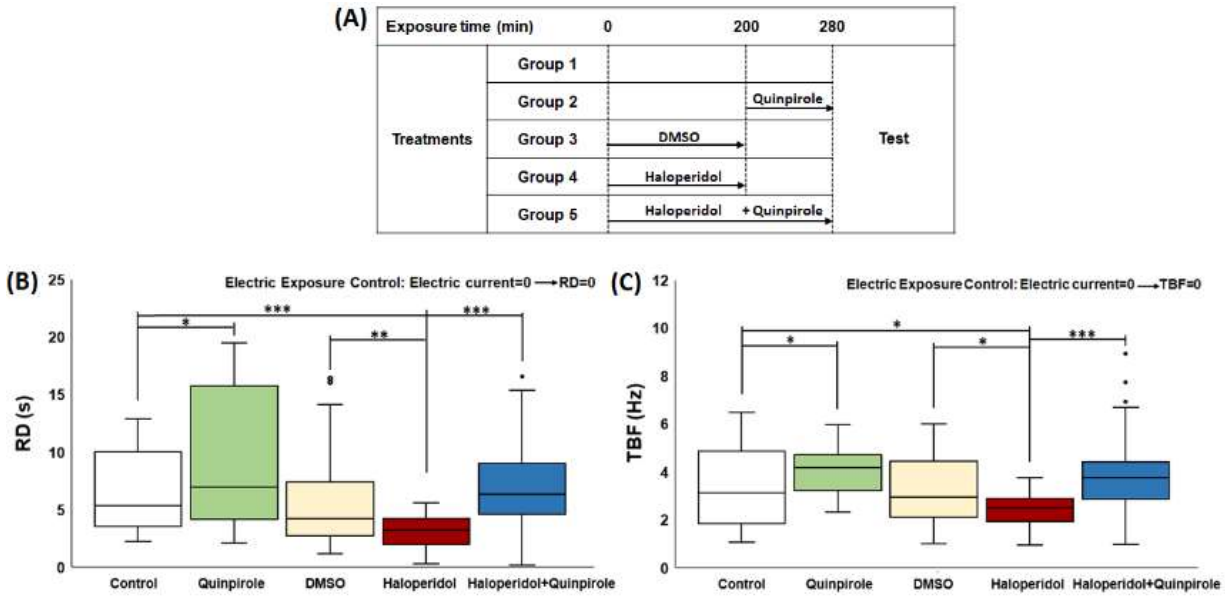

*Fig. 5-3. Effect of DMSO, haloperidol and quinpirole on 6 dpf zebrafish larvae's electric response. (A) Exposure timeline for zebrafish larvae. Electric-induced (B) RD and (C) TBF of zebrafish larvae exposed to no chemical (control), 16.7 µM quinpirole, DMSO (0.4%), 16.7 µM haloperidol and quinpirole after exposure to 16.7 µM haloperidol. Control group RD and TBF were both zero. The lines within the boxes mark the median. Upper and lower boundaries are the 75th and 25th percentile and whiskers are the maximum and minimum. *: p<0.05, **: p<0.01, ***: p<0.001. (N=45 larvae per experimental condition in three independent trials)*[130]*. Reprinted with permission from John Wiley and Sons.*

When larval electric-induced locomotor response was recorded after exposure to quinpirole (a D2-like selective agonist), increased activity was observed (Mann-Whitney U test, p-value<0.05). Treatment with quinpirole raised RD and TBF by 49% and 24%, respectively. DMSO vehicle did not alter zebrafish larvae locomotor activity from the control level, ensuring that DMSO can be

used as solvent for haloperidol in our assay. Haloperidol exposure decreased the RD and TBF by 49% and 33%, respectively and completely abolished the locomotor activities at 50 μM (Data not shown). Posttreatment with quinpirole caused a 55% increase in electric-induced RD and a 70% rise in TBF. No statistical difference was observed between the control group and the post-treated larvae (Mann-Whitney U test, p-value>0.05), verifying an improvement of locomotor activity under treatment of haloperidol-exposed zebrafish larvae with quinpirole due to an increase in dopamine concentration.

5.3. Discussion

Previous reports have established that zebrafish larvae display changes in their natural behavior (i.e., behaviour without external stimulation) following exposure to drugs that are known to act on dopamine receptors in mammals[42,56,66,170,172]. In our earlier works, we reported that the acute administration of neuroactive drugs that alter dopaminergic signaling (e.g., apomorphine, SKF-38393, quinpirole, 6-OHDA and levodopa) caused similar effects on electric-induced locomotor activity of zebrafish larvae[99,129]. Using our quadruple-fish microfluidic device, the involvement of the dopaminergic pathway in the electric-induced response of zebrafish larvae, and specifically the D1- and D2-receptors, were further investigated. Exposure to apomorphine, a non-selective dopamine agonist, had no impact on the electric-induced response. This may be either due to the drug affecting multiple different receptors[173] or possible saturation of the dopamine receptors after treatment with this specific dose[174,175]. In contrast, exposure to the non-selective antagonist butaclamol, resulted in a decrease in electric-induced movement, possibly because of suppression of the dopaminergic signalling[170], matching observations from the literature for 6 dpf zebrafish larvae[56] and mammals[176–178], suggesting the induction of analogous actions in zebrafish and mammals caused by dopamine receptor agents. For the first time, we showed that the hypoactivity

caused by butaclamol was reversed through subsequent treatment with apomorphine, restoring the electric locomotor response to match the behavior observed in the control group.

Exposure to D1 and D2-like selective dopamine antagonists of SCH-23390 and haloperidol caused lower general locomotor activity in 6 dpf zebrafish larvae[56] and rodents[66,178–180]. King et al also reported haloperidol having sedative effects on humans[181]. These results suggest a similar drug action mechanism for mammals and zebrafish triggered by the mentioned selective antagonists, possibly due to blockage of either D1- or D2-like receptors. SCH-23390 and haloperidol reduced electric-induced movement of zebrafish larvae in our microfluidic device, consistent with previous findings reported in the literature[56,66,178–181].

SKF-81297 (a D1-like selective dopamine agonist) induced no significant effects on general locomotor response when freely swimming 6 dpf zebrafish larvae were treated with the drug[182]. However, the resulting phenotypes for the D1 receptor-deficient mice were not uniform for all studies and did not align with expected observations of D1 receptor ligand treatment[183]. Some researchers reported an increase in general locomotor activity in rodents[184,185]. The effect was less prevalent in younger organisms such as 5-10 days old compared to weaned rats[186]. In contrast other researchers observed no significant difference in general movement of WT weaned mice[187] or Swiss Webster mice[188] when exposed to D1-like receptor agonists. Treatment with SKF-81297 resulted in no significant change in electric-induced locomotor response of zebrafish larvae, suggesting that D1- dopamine receptors might not be heavily involved in modulating zebrafish larvae's electric-induced response. The results obtained in our experiments match the previously reported results, showing no significant change in electric-induced locomotor response upon exposure to SKF-81297[182,187,188].

Researchers also reported that treatment with quinpirole (a D2-like selective dopamine agonist), not only stimulated general locomotor activity in zebrafish larvae[56,171], but in rodents as well[178,189]. Similarly, exposure to quinpirole significantly increased the electric-induced movement of larvae, revealing a dominant involvement of D2-like dopamine receptors in electric-induced response.

SKF-81297 and quinpirole (dopamine-selective agonists) were employed for the first time to ascertain whether they would restore the disrupted electric-induced RD and TBF of larvae pretreated with SCH-23390 and haloperidol (dopamine-selective antagonists), respectively. We demonstrated that posttreatment with quinpirole restored the electric-induced locomotor response, while posttreatment with SKF-81297 did not fully improve the larvae's activity. Performing assays with selective dopamine agonists and antagonists revealed a dominant involvement of D2-like dopamine receptors in regulating the electric-induced locomotor response of zebrafish larvae.

5.4. Conclusion

The presented screening technique provides researchers with a valuable investigative tool for studying the biological pathways in sensory-motor systems. This can be particularly useful in future work regarding systems that may be involved in zebrafish response to electricity along with examining larvae's locomotor response, on-demand genetic testing and in both toxicology and drug screening applications.

This study provided behavioral evidence that the dopaminergic signaling pathway is involved in the zebrafish electric-induced movement. The administration of drugs that target the dopaminergic receptors in mammals elicited similar impacts on electric-induced locomotor activity in zebrafish and showed the significant involvement of D2-like receptors. The results may introduce zebrafish electric-induced response as a useful measure in predicting behavioral

response to chemicals suspected to affect the dopaminergic system. Although present report matches mammalian reports of impacted movement as a result of induced changes to the dopaminergic system, further work is needed to eliminate the possibility of effects on other signaling pathways. The drugs tested have higher affinities for dopaminergic targets. However, they cannot be solely dopaminergic receptor ligands. Previous research has shown that these chemicals can also bind to adrenergic, cholinergic, histaminergic, and serotonergic receptors but with lower affinity[190–192]. Additional research is needed to determine the relative affinities for these receptors to fill this knowledge gap. The proposed studies will advance the understanding of electric-induced behaviors in a lower vertebrate model recognized for high-throughput and high-content analysis.

Chapter 6[††]

6. Application of Zebrafish Electric-Induced Response in Chemical Toxicity and Gene Screening Assays

Using the proposed electrofluidic devices, in previous chapters, we showed the electric-induced behavioral responses of larvae, its sensitivity to electric current intensity, voltage drop across fish body and field direction, and its potential regulation by dopaminergic signaling (Obj. 1-4 of the thesis). Here, our single-fish microfluidic device was used to evaluate the applicability of our device in chemical screening assays. The use of single-fish device was due to its availability as the experiments in this chapter were done mostly during year 2 of the PhD.

[††] Some content of this chapter has been published in Khalili, A. R. Peimani, N. Safarian, K. Youssef, G. Zoidl, P. Rezai, "Phenotypic Chemical and Mutant Screening of Zebrafish Larvae using an On-Demand Response to Electric Stimulation", *J. of Integrative Biology,* vol. 11, no. 10, pp. 373–383, 2019. Permissions for the use of the text has been received from Oxford University Press.

6.1. Introduction

There is a potential in utilizing the electric-induced responses and electrofluidic platforms for zebrafish behavioral assays. This may include assays involving screening for various neurotoxins, drugs, toxicology, environmental pollutants and genetic studies. Here, we aimed to investigate if our device is sensitive enough to detect the alteration in electric-induced behavioral responses of zebrafish larvae exposed to a neurotoxin that produces PD symptoms and a PD modifying compound.

PD is one of the most prevalent neurological disorders which affects about 1% of the world population over 60 years old[193]. PD which is characterized by difficulties in movement control, is caused by genetic mutations or exposure to environmental factors such as insecticides, neurotoxins or pesticides[194]. To better understand the pathological and physiological effects of PD and recognize therapeutic options, *in-vivo* experiments with animal models have been performed.

Researchers have used zebrafish to produce zebrafish PD model through exposure to various neurotoxins[41,195–197]. A variety of drugs such as levodopa, Minocycline, Sinemet, and Vitamin E have also been used to assess the feasibility of rescuing the neurobehavioral deficiencies induced in different zebrafish PD models[40,41,198]. Some of the toxins like paraquat, rotenone, 6-OHDA and MPTP which cause PD like symptoms in mammals, also result in dopamine loss in zebrafish[66,199]. Anichtchik et al.[43] used 6-OHDA and MPTP, two neurotoxins with different mechanisms of action, to investigate whether zebrafish show the neurochemical and behavioural alterations like those presented in rodents and humans. The results showed that single systemic injections of MPTP and 6-OHDA caused a remarkable decline in the noradrenaline and dopamine concentrations in zebrafish brain. Corresponding to these changes, the general locomotor activity decreased, and the swimming pattern changed from a circular pattern along the tank walls for

control group to disorganized patterns of swimming for neurotoxin-lesioned fish. Bretaud et al.[197] immersed larval zebrafish in pesticides paraquat and rotenone diluted in tank water and MPTP to study the effect of these neurotoxins on motor behavior. Exposure to MPTP at larval stages reduced locomotor activity in 7 dpf zebrafish and decreased the number of dopaminergic neurons at 5 dpf without any morphological change. Sublethal dose of rotenone and paraquat did not lead to striking effects on larvae; however, combining them at a medium dose resulted in cardiovascular defect. Lam et al.[200] co-treated zebrafish larvae exposed to MPTP with PD drug L-deprenyl/selegiline to prevent from the adverse effect on dopaminergic neurons, confirming the similarity of the mechanism of dopaminergic neuron toxicity induced by MPTP between mammals and zebrafish larvae. Feng et al.[41] treated zebrafish larvae at 2 dpf with different concentrations of 6-OHDA in the presence or absence of vitamin E, Sinemet and minocycline for 4 days in a multi-well plate. Their experiments demonstrated that all tested drugs were able to rescue the locomotor deficiency in zebrafish induced by 6-OHDA. Similarly, Cronin et al.[40] exposed zebrafish to 6-OHDA to investigate the neuro-restorative and neuroprotective capacity of different drugs. Exposure to 6-OHDA induced significant neuronal loss and locomotor deficits in 5-day-old larvae. Based on their results, L-DOPA (1 mM) could partially restore locomotor activity and isradipine (1 mM) did not reverse or prevent 6-OHDA-induced neuronal loss or locomotor deficiency. However, minocycline (10 mM) and rasagiline (1 mM) prevented neuronal loss and locomotor impairment resulted from three-days exposure to 6-OHDA and even reversed the locomotor deficit due to prior exposure to 6-OHDA. Therefore, the idea of employing zebrafish larvae as a desirable *in vivo* model for dopaminergic neuronal cell loss induced by different toxins is justified by these results.

The electric response of zebrafish larva may also involve functioning of different genes and proteins. If so, our method can be used to delineate the genetic basis of electric response, and to

phenotypically investigate the involved genes on-demand. For example, Panx1a is a vertebrate protein that plays a key role in oxidative stress, which is considered as one of the main contributors to the development of a variety of diseases such as stroke, cancer, heart failure, AD and PD[201–203]. Yet, the phenotypic effect of Panx1a on movement is not well understood. Systematic investigation of WT and Panx1a KO zebrafish larvae will help us understand if our technique can detect any alteration in sensing and responding to electrical stimulus due to Panx1a KO.

In chapter 3, we introduced a microfluidic device for on-demand electrical stimulation and phenotypic movement response assessment of 5-7 dpf semi-mobile zebrafish larvae. This opens broad areas of applications including on-demand behavioral investigations of chemical toxicity and gene functions using electric response as a versatile and on-demand readout.

In proof of concept studies for chemical screening, here, we examined zebrafish larvae's electric response after exposure to 6-OHDA, an established neurotoxin used for inducing PD symptoms[204–208]. We also investigated the effect of levodopa, a commonly-used neuroprotective agent for PD patients[209,210], on 6-OHDA exposed and unexposed zebrafish. we showed that 6-OHDA exposure adversely affected zebrafish's response to electricity. The electrical movement impairment due to 6-OHDA was interestingly recoverable using levodopa post-treatment.

For gene function studies, we compared the electric response of WT zebrafish larvae with that of a Panx1a KO model[211]. Using our technology and for the first time, we showed that Panx1a loss altered zebrafish's response to electricity. Then, we aimed to use the behavioral criteria to study the role of Panx1a channels for early stages of the development of Parkinson related disorders. This time, the electric-induced RD and TBF of WT and Panx1a KO zebrafish larvae in response to 6-OHDA, was studied to form a better view of Panx1a channels' involvement in the etiology of PD.

6.2. Results

The single-fish microfluidic device (Fig. 2-2) was used to investigate the application of zebrafish electric-induced response in chemical and gene screening assays.

6.2.1. Electric Movement Assay for Chemical Screening

Here, we aimed to study if our microfluidic technique could be used for behavioral screening of zebrafish PD models, using standard levodopa and 6-OHDA exposure assays. The effect of these chemicals and their concentration on the electric locomotor response of zebrafish larvae is not understood. Hence, electric current of 3 μA, which could induce the longest RD in zebrafish (Fig. 3-5), was used for evaluating the locomotor response alterations in zebrafish PD models.

First, we asked if 6-OHDA-induced neurodegeneration could affect the response of zebrafish larvae to electric signal. 45 zebrafish larvae per experimental condition in three independent trials were exposed to 0, 50, 100 and 250μM 6-OHDA, then incubated at 28°C from 2 to 5 dpf[40,41]. Five dpf larvae were then trapped in our microfluidic device as described in section 2.6.1. In the presence of 3μA electric current, the electric-induced tail movement of larvae trapped was monitored and recorded for chemically-exposed and unexposed control larvae. The locomotor response was then analysed in terms of RD and TBF as explained in section 2.8. Our electric-based behavioral assay demonstrated that exposure to 50 and 100 μM 6-OHDA could not alter the electric-induced locomotor response of zebrafish larvae (Mann-Whitney U test, p-value>0.05). However, 250 μM 6-OHDA decreased the electric-induced RD and TBF of zebrafish larvae by 50% and 70%, respectively (Fig. 6-1). The results were consistent with previous research indicating general locomotor deficiency after dopaminergic cell loss caused by exposure to 6-OHDA.

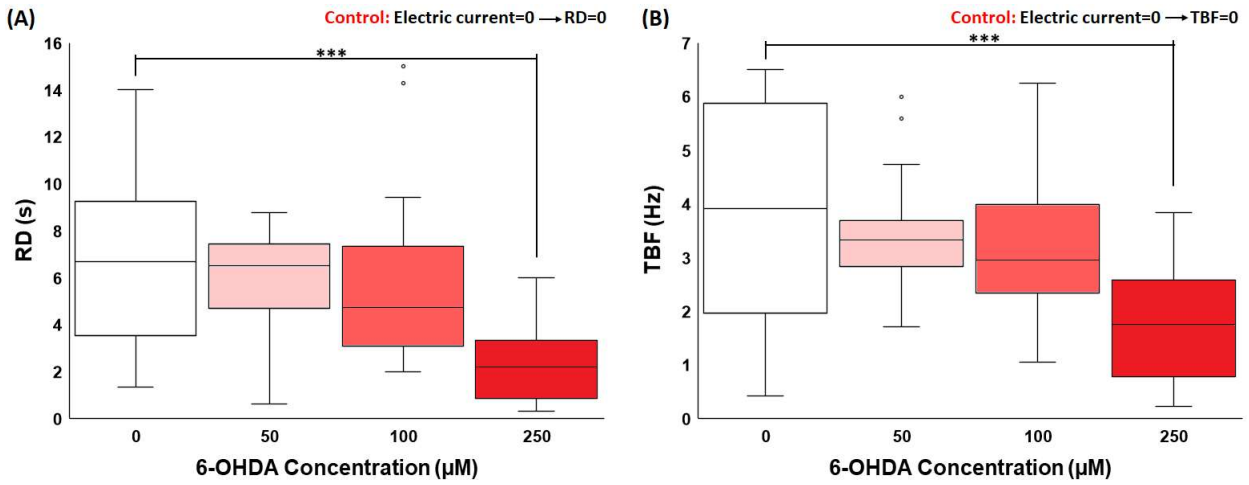

*Fig. 6-1. Electrically induced (A) RD and (B) TBF of WT zebrafish larvae exposed to 0, 50, 100 and 250μM 6-OHDA (I=3 μA). Control group RD and TBF were both zero. The lines within the boxes mark the median. Upper and lower boundaries are the 75th and 25th percentile and whiskers are the maximum and minimum. ***: p<0.001. (N=45 larvae per experimental condition in three independent trials)*[129]*. Reprinted with permission from Oxford University Press.*

Next, we examined the effect of levodopa on the electric-induced locomotor response of zebrafish larvae. By exposing 2 dpf zebrafish larvae to 1mM levodopa for 72 hrs (which is widely used in the literature[40,132,198]), our preliminary assays indicated that continuous exposure induces a reduction in RD and TBF, compared to the larvae that were exposed daily to the same replenished dose of levodopa and for the same duration of time (Fig. 6-2). Considering the 90 min half-life of levodopa[212], during the continuous exposure the augmented dopamine was potentially degraded into dopamine aldehyde (DOPAL) which is selectively toxic to neurons expressing the dopamine transporter[213]. The decrease in electrical RD and TBF in the continuous exposure assay is consistent with the previous research indicating general locomotor deficiency after dopaminergic cell loss[29,43]. Our daily exposure assay verified that renewing levodopa could compensate for this reduction in the dopamine concentration and generate behavioral phenotypes similar to the control group.

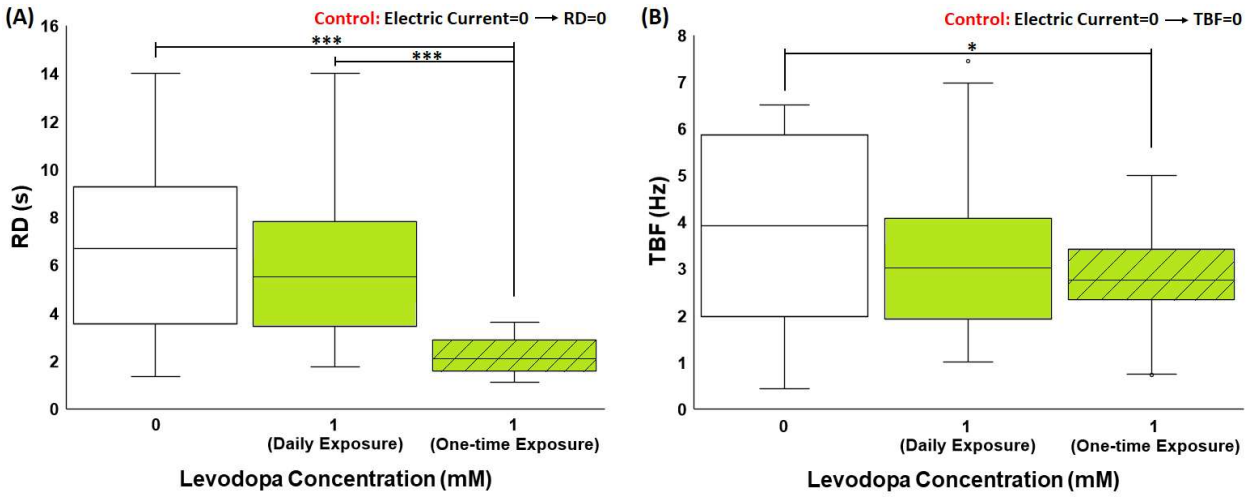

*Fig. 6-2. Electric-induced (A) RD and (B) TBF of 2 dpf zebrafish larvae exposed to 1 mM levodopa, with the drug being renewed daily (Daily Exposure) or administered only once at the beginning (One-time Exposure). Control group RD and TBF were both zero. The lines within the boxes mark the median. Upper and lower boundaries are the 75th and 25th percentile and whiskers are the maximum and minimum. *: p<0.05, ***: p<0.001. (N=45 larvae per experimental condition in three independent trials)*[129]*. Reprinted with permission from Oxford University Press.*

Experiments were then conducted to evaluate the capability of our device in detecting the dose-dependent effect of levodopa on zebrafish locomotion. We also aimed to determine the proper dose of levodopa for further investigations as a drug against 6-OHDA. A total of 45 zebrafish larvae per experimental condition were exposed to 0.5, 1 and 2mM levodopa, then incubated at 28^{o}C from 2 to 5 dpf, with daily levodopa renewal. Electrically-evoked tail movement of zebrafish larvae was monitored for levodopa-exposed and unexposed control larvae as shown in Fig. 6-3.

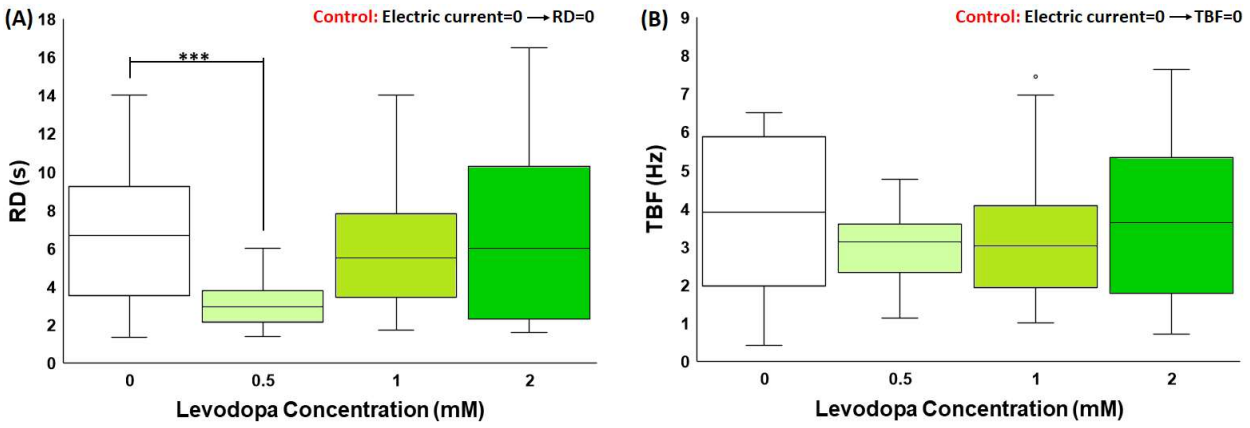

*Fig. 6-3. Electric-induced (A) RD and (B) TBF of zebrafish larvae exposed to 0.5, 1 and 2mM levodopa for 3 days, compared to unexposed larvae. Control group RD and TBF were both zero. The lines within the boxes mark the median. Upper and lower boundaries are the 75th and 25th percentile and whiskers are the maximum and minimum. ***: p<0.001. (N=45 larvae per experimental condition in three independent trials)*[129]*. Reprinted with permission from Oxford University Press.*

Exposure to 0.5 mM levodopa significantly reduced the larvae's RD by 53% (Mann-Whitney U test, p-value<0.001) while higher concentrations led to response revival to a normal level (Fig. 6-3A). Levodopa concentration had no significant effect on the TBF of the larvae although a slight reduction was observed at 0.5 mM levodopa (Fig. 6-3B) which is consistent with the other data reported for systemic administration of low doses of levodopa to other animals such as rats and mice[214,215]. Our results in Fig. 6-3 verified that the sensorimotor pathways involved in zebrafish response to electric current are affected by levodopa concentration. While this interesting result requires further investigations, we have found that the reduction in locomotor RD (as the more sensitive phenotype) is similar to the results reported for low doses of dopamine agonists. The mechanism by which low doses of dopamine agonists produce hypomotility has been suggested to be related to a decrease in dopamine synthesis, release and firing of dopaminergic neurons. It is reported that levodopa shares properties with other dopamine agonists in stimulating dopamine

autoreceptors that mediate the inhibition of dopamine synthesis and release, resulting in zebrafish locomotor impairment[42,195,214,215].

Further experiments in Fig. 6-4 were performed to investigate if the effect of 0.5 mM levodopa on electric-induced movement is exposure time dependent. Two dpf zebrafish larvae were exposed to 0.5 mM levodopa for 1, 3, 4 and 5 days. Our results demonstrated that exposure for 3 days caused a significant decrease in the RD, but further exposure time up to 5 days did not affect the RD much further. Moreover, TBF of the larvae was not affected by the exposure time to 0.5 mM levodopa.

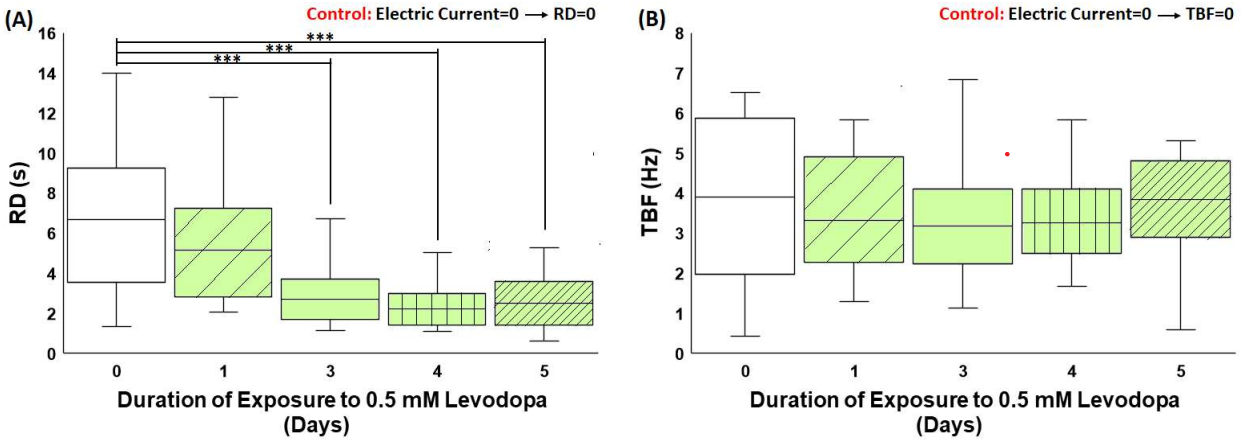

*Fig. 6-4. Electric-induced (A) RD and (B) TBF of zebrafish larvae exposed to 0.5 mM levodopa for 1, 3, 4 and 5 days. Control group RD and TBF were both zero. The lines within the boxes mark the median. Upper and lower boundaries are the 75th and 25th percentile and whiskers are the maximum and minimum. ***: p<0.001. (N=45 larvae per experimental condition in three independent trials)*[129]*. Reprinted with permission from Oxford University Press.*

Next, we examined if 6-OHDA affects the electric locomotion of zebrafish larvae and whether treatment with levodopa rescues this impairment, as observed in general locomotion assays[40,41,132,198]. We exposed 2 dpf zebrafish larvae to 250 µM 6-OHDA (selected based on preliminary concentration investigations[98] (Fig. 6-1)) for either 32 hrs or 72 hrs. Our results in Fig.

6-5 demonstrated that both exposure times led to the same and significant levels of deficits in locomotor activity, causing a reduction in RD and TBF of zebrafish larvae in comparison to the control group. Therefore, we used zebrafish larvae exposed to 250 µM 6-OHDA for 32 hrs as PD models to assess the functionality of levodopa as a drug for restoring the electric locomotor deficiencies induced by 6-OHDA. Post-treatment of zebrafish PD models with two concentrations of levodopa (0.5 mM and 1 mM) were investigated (Fig. 6-6A).

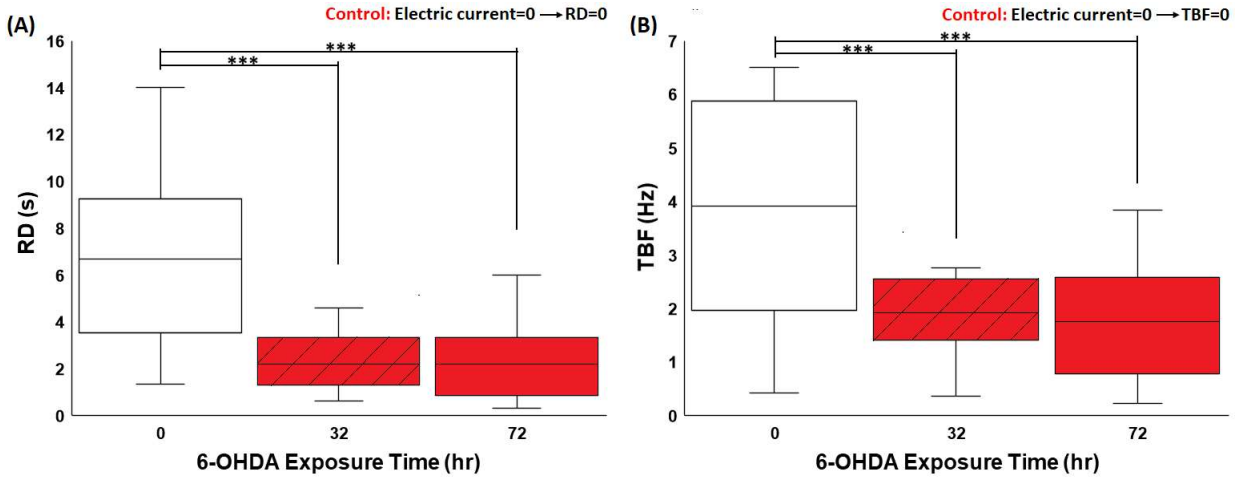

*Fig. 6-5. Electric-induced (A) RD and (B) TBF of 2dpf zebrafish larvae exposed to 250 µM 6-OHDA for 32 and 72 hrs, compared to unexposed control larvae. Control group RD and TBF were both zero. The lines within the boxes mark the median. Upper and lower boundaries are the 75th and 25th percentile and whiskers are the maximum and minimum. ***: p<0.001. (N=45 larvae per experimental condition in three independent trials)*[129]*. Reprinted with permission from Oxford University Press.*

As shown in Fig. 6-6B and 6C, 6-OHDA treatment resulted in 63% and 53% reduction in the average RD and TBF, respectively. Post-treatment of zebrafish larvae with 0.5 mM levodopa neither could improve the impairments resulted from exposure to 6-OHDA, nor had it an accumulative deteriorating effect over that of 6-OHDA, which was expected based on our levodopa assay in Fig. 6-3 and Fig. 6-4. However, post-treatment with 1 mM levodopa rescued the

electric-induced locomotor responses and resulted in a significant increase of 53% in RD and 40% in TBF when compared with 6-OHDA exposed larvae (Mann-Whitney U test, p-value<0.001 and p-value<0.01, respectively). There was no statistical difference between the post-treated larvae and the control group (Mann-Whitney U test, p-value> 0.05). This result is similar to those presented for the general locomotion of zebrafish larvae[40], demonstrating an improvement of locomotor function under treatment of 6-OHDA exposed zebrafish larvae with levodopa due to an increase in dopamine concentration.

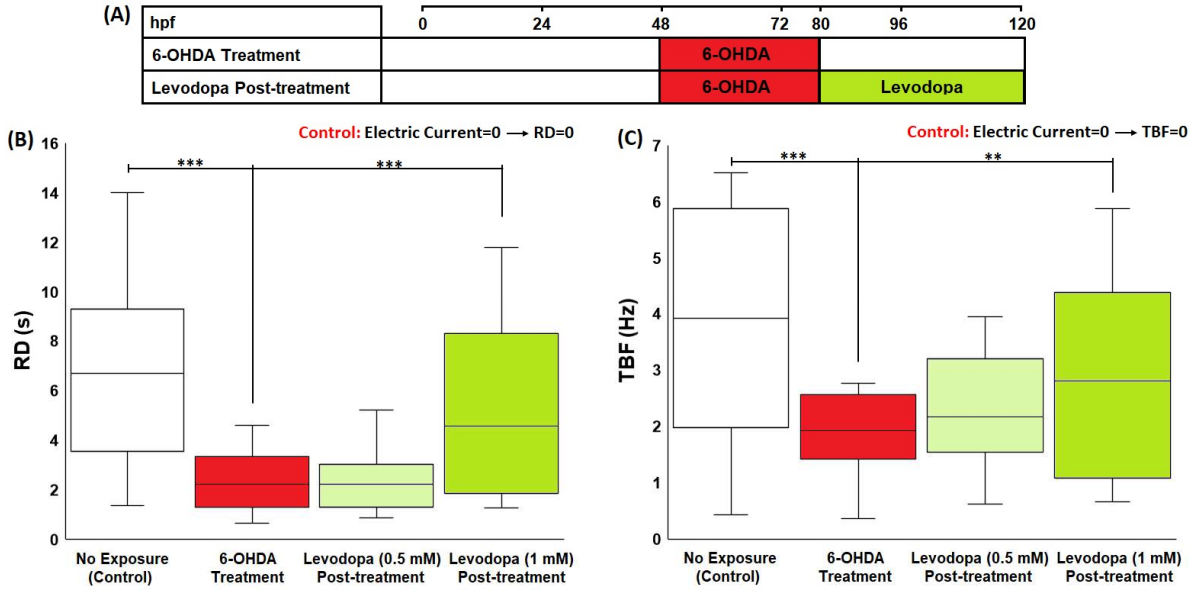

*Fig. 6-6. (A) Timeline for 6-OHDA and levodopa exposure during co-treatment and post-treatment assays. Electric-induced (B) RD and (C) TBF of zebrafish larvae exposed to no chemical (control), 250 µM 6-OHDA for 32h, 0.5 mM and 1 mM levodopa for 40 hrs after exposure to 250 µM 6-OHDA for 32hrs (post-treatment). Control group RD and TBF were both zero. The lines within the boxes mark the median. Upper and lower boundaries are the 75th and 25th percentile and whiskers are the maximum and minimum. **: p<0.01, ***: p<0.001. (N=45 larvae per experimental condition in three independent trials)*[129]*. Reprinted with permission from Oxford University Press.*

The results verified that our technique is applicable and sensitive enough to be used for drug screening while providing a tool with which zebrafish larvae's locomotion can be evoked on-demand and studied quantitatively with precision. Although, it is still not clear whether the electric-induced movement of zebrafish larvae is a reflexive or voluntarily response, but modulation of response with 6-OHDA and levodopa suggests the involvement of dopaminergic neurons in sensing the electric stimulus.

6.2.2. Electric Movement Assay for Gene Screening

Here, we interrogate if our technique can detect any alteration in sensing and responding to electrical stimulus due to Panx1a KO. Accordingly, we tested the electric-induced response of Panx1a KO larvae and compared it with the WT larvae at various electric currents.

In preliminary studies, we observed that the Panx1a KO larvae responded to electric current at 1 μA with >80% response rate, unlike the WT larvae that initiated a strong response at 0.5 μA. This shift in the electric-induced response threshold might be caused directly or indirectly by ablation of the Panx1a gene which requires further investigations in the future. The WT and Panx1a KO larvae displayed a robust locomotion in response to electric currents higher than 1 μA. Accordingly, we explored the electric-induced RD and TBF of Panx1a KO zebrafish larvae at 1-9 μA electric currents (Fig. 6-7). The RD and TBF for unexposed Panx1a KO larvae were both zero. For comparison of the results to WT larvae, please refer to Fig. 6-8.

The RD of Panx1a KO larvae at 1 and 9 μA were 0.6±0.1 and 1.1±0.1s, respectively, which were statistically shorter than those at 3 and 6 μA (Fig. 6-7A; Mann-Whitney U test, p-value<0.001 for 3 μA vs 1 and 9 μA, and 6 μA vs 1 and 9 μA). This appeared to follow the similar inverted U-shaped trend observed for the WT larvae (Fig. 3-5A); that is, electric-induced response lasted longer at the medium currents of 3 and 6 μA, and shorter at the low and high currents of 1 and 9

μA. Moreover, as shown in Fig. 6-8, at 1 and 3 μA, the Panx1a KO larvae tended to display a shorter electric-induced response than the WT larvae (Mann-Whitney U test, p-value<0.001), while no statistical differences were observed at the higher currents of 6 and 9 μA (Mann-Whitney U test, p-value>0.05).

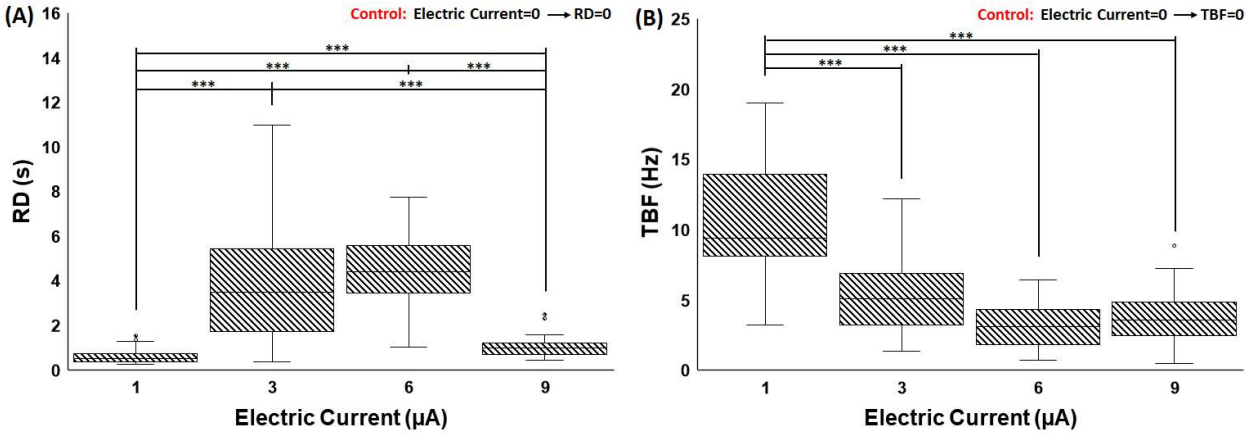

*Fig. 6-7. Electric-induced (A) RD and (B) TBF of Panx1a KO zebrafish larvae at different electric currents. Control group RD and TBF were both zero. The lines within the boxes mark the median. Upper and lower boundaries are the 75th and 25th percentile and whiskers are the maximum and minimum. ***: p<0.001. (N=45 larvae per experimental condition in three independent trials)*[129]*. Reprinted with permission from Oxford University Press.*

The TBF of the Panx1a KO zebrafish larvae was also assessed as presented in Fig. 6-7B. The highest TBF of the Panx1a KO larvae was 10.6±0.6 Hz at 1 μA which was significantly distinct from the rest of TBFs at higher currents (Mann-Whitney U test, p-value<0.001). At 3 μA and higher currents, a plateau trend was observed in the TBF of Panx1a KO larvae which is again similar to what was seen in WT larvae (Fig. 3-5B). Interestingly, it was observed that at low currents of 1 and 3 μA, the Panx1a KO larvae tended to respond with a higher TBF as compared to the WT larvae (Mann-Whitney U test, p-value<0.001 for both currents) as shown in Fig. 6-8.

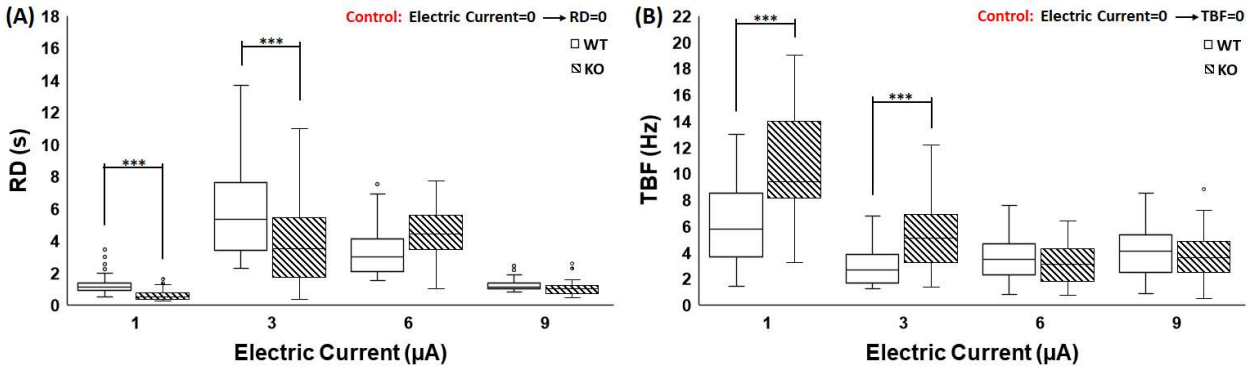

*Fig. 6-8. Electric-induced (a) RD and (b) TBF of WT and Panx1a KO zebrafish larvae at different electric currents. Control group RD and TBF were both zero. The lines within the boxes mark the median. Upper and lower boundaries are the 75th and 25th percentile and whiskers are the maximum and minimum. ***: p<0.001. (N=45 larvae per experimental condition in three independent trials)*[129]*. Reprinted with permission from Oxford University Press.*

Our microfluidic platform could induce on-demand locomotion in both WT and KO zebrafish larvae and detect an alteration in locomotion of KO zebrafish larvae as compared to WT. The results are consistent with the alteration reported in the movement activity of Panx1a KO mice when compare to the control mice[216]. It was concluded that the microfluidic platform has broad application potential for in-depth phenotyping characterization of gene-edited zebrafish like the Panx1a model.

6.2.3. Electric Movement Assay for Combined Chemical and Gene Screening

Here, we exposed 2 dpf WT and Panx1a KO larvae to 250 μM 6-OHDA for either 72 or 120 hrs to produce zebrafish PD models. Comparing The behavioral responses of WT and KO groups of zebrafish larvae exposed to 6-OHDA with the non-treated control groups may open opportunities for unravelling the connection of Panx1a and PD.

6.2.3.1. Panx1a Function Impacts Behavioural Changes Induced by 6-OHDA Treatment in 5 dpf Zebrafish Larvae

As shown in section 6.2.2, Panx1a KO larvae responded with shorter RD, but higher TBF compared to WT group, suggesting the potential involvement of Panx1a in zebrafish larvae electric-induced response. Here, the effect of 6-OHDA on locomotor activity was evaluated by examining the behavioral phenotypes of RD and TBF of larvae exposed to electrical stimulus (Fig. 6-9). Exposure to 6-OHDA for 72 hrs caused a 68% and 50% decrease in the RD and TBF of WT control larvae. Our results were consistent with previously published data, where 6-OHDA insult was associated to mobility deficits[217,218]. However, no significant changes in the locomotor activity of Panx1a KO larvae were detected after 6-OHDA treatment, verifying that 6-OHDA treatment does not induce locomotor deficits in 5 dpf larvae in the absence of Panx1a functions. This result suggests that Panx1 channels and 6-OHDA might function through similar signaling pathways, so that in the absence of Panx1 the 6-OHDA target is disrupted as well[219,220].

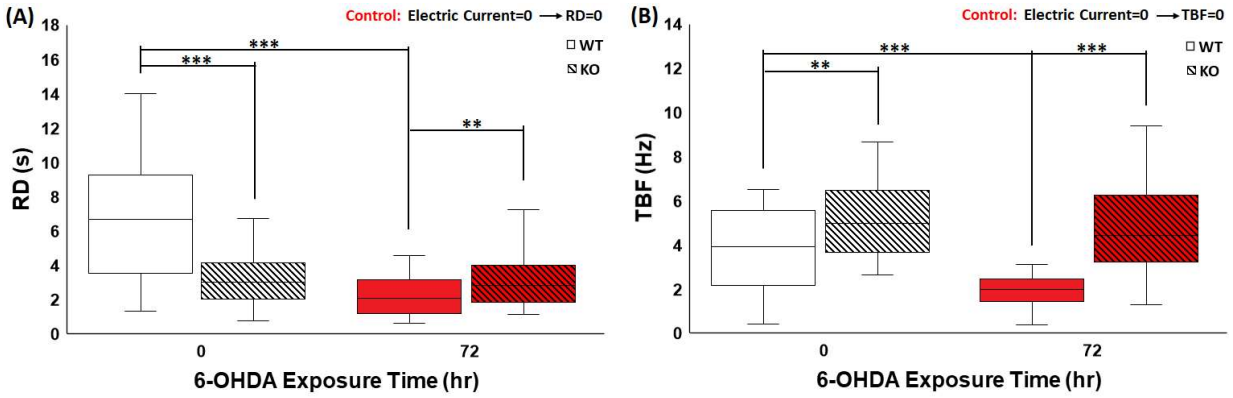

*Fig. 6-9. Electric-induced (A) RD and (B) TBF of 5 dpf WT and Panx1a KO zebrafish larvae exposed to 250 µM 6-OHDA for 0 and 72 hrs. Control group RD and TBF were both zero. The lines within the boxes mark the median. Upper and lower boundaries are the 75th and 25th percentile and whiskers are the maximum and minimum. **: p<0.01, ***: p<0.001. (N=45 larvae per experimental condition in three independent trials)*[129]*. Reprinted with permission from Oxford University Press.*

6.2.3.2. Dopaminergic Degeneration Minds the Duration of Exposure to 6-OHDA

The first week of zebrafish development is such vital that every day counts for some new events (signaling pathway) to come to the effect[220]. To assess the impact of age and treatment duration on the extent of injury, we repeated our experiments on 7 dpf larvae. We exposed 2 dpf WT and Panx1a KO larvae to 250 µM 6-OHDA for either 72 or 120 hrs and tested their performance at the age of 7 dpf (Fig. 6-10). After a 72 hrs treatment, the RD and TBF of 7dpf WT larvae were significantly reduced by 63% and 40%, respectively. The results were consistent with the data obtained for 5 dpf larvae in section 6.2.3.1. The electric-induced RD and TBF of 7 dpf Panx1a KO larvae were unchanged upon 72 hrs treatment with 6-OHDA, similar to the behavioral response of 5 dpf mutants.

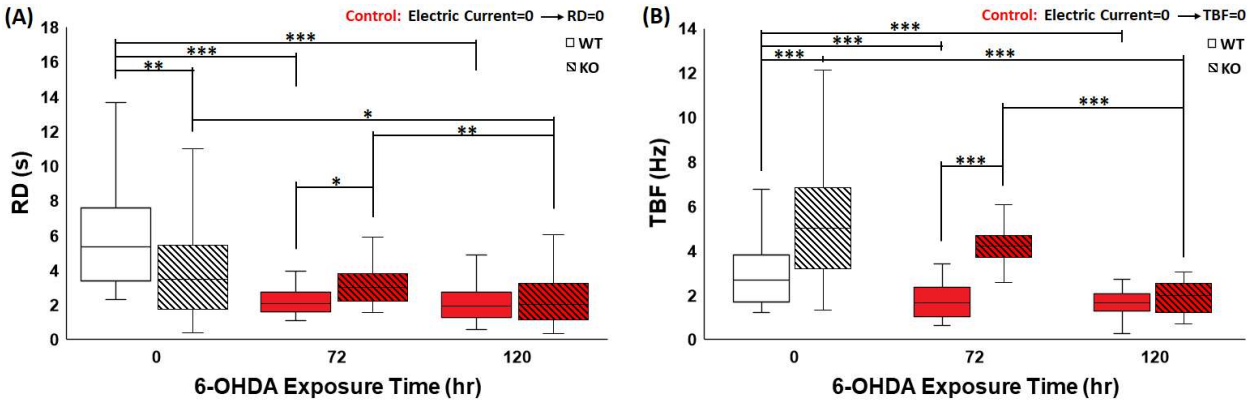

*Fig. 6-10. Electric-induced (A) RD and (B) TBF of 7 dpf WT and Panx1a KO zebrafish larvae exposed to 250 µM 6-OHDA for 0, 72 and 120 hrs. Control group RD and TBF were both zero. The lines within the boxes mark the median. Upper and lower boundaries are the 75th and 25th percentile and whiskers are the maximum and minimum. *: p<0.05, **: p<0.01, ***: p<0.001. (N=45 larvae per experimental condition in three independent trials)*[129]*. Reprinted with permission from Oxford University Press.*

Extending the treatment from 72 to 120 hrs had no effect on 7 dpf WT larvae, suggesting that both exposure times led to the same and significant levels of motor deficiency and dopaminergic

cell death. The results confirmed that WT larvae showed the greatest sensitivity to the neurotoxin within the first 5 days of development. In contrast, 7 dpf Panx1a KO larvae exhibited marked declines of 24% in RD and 52% in TBF when the 6-OHDA exposure time was extended from 72 to 120 hrs, which confirms that the susceptibility of mutants to the neurotoxin depends on duration of exposure. The deregulations of the dopaminergic pathway in Panx1a KO larvae shown previously[221] is the probable cause of the 6-OHDA susceptibility at 7 dpf. We concluded that the absence of functional Panx1a channels compromised dopaminergic signaling in 6-OHDA treated zebrafish larvae.

6.3. Conclusion

The goal of this study was to show the application of our novel microfluidic platform, in which the recently-introduced movement response of zebrafish larvae to electrical stimulation could be examined on-demand and phenotypically, in chemical screening and gene function studies. Employing the proposed platform, the effect of 6-OHDA neurotoxin, levodopa neuroprotective chemical, and Panx1a gene KO on electric locomotor behavior of zebrafish larvae was studied.

Independent 6-OHDA and levodopa treatments resulted in dose-dependent alterations in locomotion of zebrafish, suggesting a possible link between zebrafish's electric-induced movement and the dopaminergic pathway. Post-treating 6-OHDA exposed zebrafish PD models with 1 mM levodopa could rescue the impairment further supporting the above claim, while verifying that our technique is applicable and sensitive to be used for chemical screening.

In our gene KO studies and at 1 and 3 μA, Panx1a KO larvae responded with shorter RD, but higher TBF compared to WT, suggesting the potential involvement of Panx1a in electric-induced response of zebrafish larvae.

Gaining mechanistic insight into the pathophysiology of PD, which currently has no cure, is a timely objective. One of the many steps to find a cure is to develop investigative platforms with the potential to accelerate this process. Our chemical and gene screening results opened up opportunities for studying the connection of Panx1a as a novel risk factor in the etiology of PD. Here, we used our microfluidic platform which enables reliable stimulation and recording of behavioral outputs using the well characterized 6-OHDA-induced PD protocol. Taking a step further, we demonstrated how this platform could be combined with gene-editing zebrafish serving as animal models of human PD. This cross-disciplinary combination enables the quantification of behavioral and molecular responses in vivo, which is exemplified by testing Panx1a KO zebrafish larvae. In this process our research sheds some light on the association of Panx1a with the etiology of PD. The important finding is that the loss of Panx1a delays behavioral responses in response to 6-OHDA by two days. This is a significant delay suggesting that targeting Panx1a could temporally protect the brain from neurodegeneration. The microfluidic device and protocol used in this study will allow the phenotypic screening during a future drug-discovery process which evaluates whether targeting Panx1 can affect the onset or progression of PD.

Chapter 7

7. Thesis Summary and Prospect

7.1. Thesis Summary

Zebrafish is an established model organism for studying the genetic, neuronal and behavioral bases of diseases and for toxicity and drug screening. The embryonic and larval stages of zebrafish have been used extensively in fundamental and applied research due to advantages offered such as body transparency, small size, low cost of cultivation and high genetic homology with humans. However, the conventional experimental methods used for handling and investigating this organism are limited due to their low throughput, labor intensiveness and inaccuracy in delivering external stimuli to the zebrafish while quantifying various neuronal and behavioral responses. Microfluidic and lab-on-a-chip devices have emerged as ideal technologies to overcome these challenges and provide appropriate platforms for precise manipulation, stimulation and behavioral screening. In this thesis, we provided an overview of the microfluidic methods used to manipulate

(deliver and orient), immobilize and expose zebrafish larvae, followed by quantification of their behavioral responses.

Very recently, it was shown that zebrafish larvae execute an oriented movement toward the positive electrode of an electric field along a microchannel[99]. Phenotypic characterization of this response was not feasible due to larva's rapid movement along the channel. To overcome this challenge, we introduced a microfluidic device to partially immobilize the larva's head while leaving its mid-body and tail unrestrained in a chamber to image motor behaviors in response to electric stimulation, hence achieving quantitative phenotyping of the electrically evoked movement in zebrafish larvae using two quantifying parameters of RD and TBF. The effect of electric current, voltage and field direction on the RD and TBF of 5–7 dpf zebrafish larvae was studied. For a larva with a fixed head and a moving tail, we observed that the response to electric current in the range of 1 to 9 μA depended on the current magnitude; that is, the longest RD was evoked at intermediate currents of 3 and 6 μA and the highest TBF was induced at the lowest current of 1 μA with a decreased plateau trend at higher currents, potentially resulted from paralysis in the larvae, and in line with previously published literature. We then assessed larvae's response to electric current direction and voltage magnitude (at 3 μA). Changing the current direction significantly altered the RD and TBF with long and low-frequency responses seen when the anode was positioned at the larvae's tail. The electric voltage drop across fish body had a significant effect on larvae's locomotion with long RD and low TBF observed at 5.6 V in the range of 1.3-9 V. We also demonstrated that the zebrafish locomotor response to repeated 3 μA current pulses diminished with dependency on the interstimulus interval. However, the diminished response was fully recovered after a 5-min resting period or introduction of a novel light stimulus

(i.e., habituation-dishabituation strategy). Therefore, electric response suppression in zebrafish was attributed to the habituation as a form of non-associative learning.

We then introduced a platform for heart activity screening and behavioral studies of zebrafish larvae. Using the developed multi-phenotypic microfluidic platform, we detected a temporary increase in zebrafish heartrate upon exposure to electric stimulation that was diminished after removing the electrical stimuli.

One of the remaining challenges for the broad use of microfluidic devices is their limited throughput, especially in behavioural assays. To address this challenge, a microfluidic device with enhanced control of experimentation with multiple larvae was designed, which features a design to immobilize four zebrafish larvae in parallel and expose them to electric current that induces tail locomotion. The new design decreased the testing time per larva by approximately 60% when compared to our previously developed single-fish device. Critical behavioural parameters such as RD and TBF were similar in both single- and quadruple-fish devices. The developed microfluidic device has significant advantages for greater throughput and efficiency when behavioral phenotyping is required in various applications, including chemical testing in toxicology and gene screening.

In proof-of-concept studies for chemical screening and to shed some light on the signaling molecular mechanisms involved in zebrafish response to electricity, we asked if changes to dopaminergic signaling pathways can affect their electrically-evoked locomotion. To answer this question, the effects of multiple selective and non-selective dopamine compounds on the electric response of zebrafish larvae was investigated. The electric-induced RD and TBF of 6 dpf larvae was monitored to discern the effect of non-lethal concentrations of dopaminergic agonists (apomorphine, SKF-81297, and quinpirole), and antagonists (butaclamol, SCH-23390, and

haloperidol). All dopamine antagonists decreased locomotor activity, while dopamine agonists did not induce similar behaviours in larvae. The D2- like selective dopamine agonist quinpirole enhanced movement. However, exposure to non-selective and D1-selective dopamine agonists apomorphine and SKF-81297 caused no significant change in the electric response. Exposing larvae that were pre-treated with butaclamol and haloperidol to apomorphine and quinpirole, respectively, restored electric locomotion. This study demonstrated that electric-induced zebrafish larvae locomotion could be altered by dopamine receptor antagonists and agonists and these chemicals generally had opposite effects. In other words, the results revealed a correlation between electric response and the dopamine signalling pathway. We propose that the electrofluidic assay has profound application potential for fundamental electric-induced response research, neurodegenerative disease and brain disorder studies especially those related to the dopamine imbalance and as a chemical screening method when investigating biological pathways and behaviors.

Investigations were also performed on zebrafish exposed to neurotoxin 6-OHDA (an established neurotoxin used for inducing PD symptoms), levodopa (a commonly used neuroprotective agent for PD patients) and larvae carrying a Panx1a gene KO, as a proof of principle applications to demonstrate on-demand movement behavior screening in chemical and mutant assays. We demonstrated for the first time that 6-OHDA leads to electric response impairment, levodopa treatment rescues the response and Panx1a is involved in the electrically evoked movement of zebrafish larvae. Our device was also employed to gain insight into the role of Panx1a-based channel activity in PD. 6-OHDA was used to cause a Parkinsonian phenotype in WT and Panx1a KO zebrafish larvae. Our findings showed that the absence of Panx1a channels compromised dopaminergic signaling in the 6-OHDA model of PD and delayed the onset of the

locomotor deficiency by two days. Taken together, our results demonstrated a microfluidic platform in which a controlled electrical stimulus paradigm offers opportunities to investigate the roles of Panx1a and other candidate genes in PD.

7.2. Thesis Prospects

In our research, we studied zebrafish larvae electric-induced behavioral response inside single- and quadruple-fish microfluidic devices. Despite advantages offered by the proposed devices and methods in this thesis, several complementary studies can be conducted in the future. Some of them will be discussed in the following sections.

7.2.1. Limitations and Challenges associated with the Proposed Platforms

Despite different advantages offered by the microfluidic devices developed and the experimental methods discussed in this thesis, we acknowledge that they may not be completely ready to serve as a replacement for the conventional techniques used by biologists and scientists. Here, we discuss some limitations of our presented devices that need to be tackled to make them more suitable and applicable for end-users without any engineering background.

The proposed technologies need to be adapted and integrated with facilities used in the biology laboratories. For that, devices must be compatible with the current pipetting-based fluid handling and multi well plate-based screening techniques. The integration process may require design modifications. For now, adaptation of this technology by small laboratories which test few larvae at a time might be more realistic than by larger-scale labs with high-content screening capabilities.

The manual loading, screening and unloading procedure still is not simple enough to be performed by minimally trained personnel. Automation of all these procedures would make it easier for the operators to work with these platforms.

The proposed microfluidic devices have been designed and fabricated with cost-efficiency consideration. However, more robust fabrication techniques (e.g., metal-deposition for gold electrode to avoid the copper electrodes degradation over time) can be used to offer more efficient and durable devices.

Tail tracking with Kinovea software and data analysis was also a time-consuming procedure that could be facilitated by developing a custom-written MATLAB software for automated tail tracking.

Throughput of our enhanced throughput device is now limited to four larvae per trial which does not meet the demands for high throughput screening yet. In future, the throughput can be increased by parallelizing more traps upon access to either a microscope with larger FOV or a motorized stage enabling consecutive imaging process.

7.2.2. Future Technological Research Direction

We designed our first microfluidic device to partially immobilize zebrafish larva in the lateral direction while its tail was free to move inside the screening pool. We could evoke and quantify zebrafish electric-induced locomotor response and explore the effect of various electrical stimulation levels as well as different electric field directions. A challenge is the image processing of the recorded videos that takes a long time to be analyzed. A custom-written image processing software can be developed for each device to track zebrafish tail movement. Development of this software can automate the data analysis process and decrease human error probability.

A thorough investigation of the recorded videos and quantitative analysis of zebrafish's motor patterns can result in identification of well-established motor patterns. We also anticipate using machine-learning techniques to train our software on identifying different zebrafish movement patterns.

We proposed a multi-phenotypic microfluidic device for bidirectional imaging of heart and tail activities. The presented design is expected to contribute to a wide range of microfluidic applications such as multi-organ imaging on a chip and multi-phenotypic chemical screening assays. In the future, our device can be modified to improve the resolution of the dual-imaging and expanding the device capabilities to monitor multiple larvae in parallel and a more extensive range of phenotypes such as fin and mouth movement.

To enhance the throughput of the behavioral screening platform, we replicated the TR and developed a proof-of-concept microfluidic device. Further modifications to the device, dependent on the microscopy capabilities such as the FOV, could increase the number of fish tested simultaneously to further reduce the testing time and enhance the throughput of behavioral assays with the proposed technology. Additional features such as on chip chemical exposure could likewise expand the applications and range of the design presented. Although the results obtained in our quadruple-fish device provided a promising perspective for increasing the test throughput, more experiments are needed to control the loading process and the orientation of the larvae to ensure that most of larvae are loaded tail first. Also, the modifications have not met the demands for high throughput screening yet, but our effort can be considered as the first step towards increasing the throughput of our technique in the future. Automation of loading, stimulating, image acquisition and analysis can also be performed to enhance the throughput of our assays and make the device more appealing for biologists and other scientists. A motorized stage would also add great potential to the system and facilitate the imaging process.

Further research opportunities may involve experiments with larvae expressing genetically encoded calcium indicators to conduct neural studies within specific neuronal pathways in live zebrafish larvae. Since the larva is partially immobilized and its brain is visually accessible for

imaging purposes, the neural activities of the zebrafish larvae evoked by the electrical stimuli can be monitored. A simultaneous study of the behavioral and neural electric-induced responses is also achievable by designing an appropriate imaging setup and using our devices.

7.2.3. Future Biological Research Direction

The electric-induced behavioral response was examined on-demand and phenotypically for applications in chemical screening and gene function studies. In combination with loss-of-function and gain-of-function zebrafish models, the versatile platform reported in this thesis will be instrumental for correlating the mechanism of electric-induced responses with the behavioral phenotypes.

Taking a step further, we demonstrated how this platform can be combined with gene-editing zebrafish serving as animal models of human PD. This cross-disciplinary combination shed some light on the association of Panx1a with the etiology of PD. In the future, the microfluidic device and protocol used in this study can be employed in the phenotypic screening during a drug-discovery process which evaluates whether targeting Panx1 can affect the onset or progression of PD.

In this thesis, we showed the application of our technique in PD pathology studies. However, the same assays can be performed for AD and Huntington's disease (HD), as most of the neurodegenerative diseases have common disease pathogenesis. Recently different natural antiparkinsonian compounds such as passion flower and ginseng that demonstrated PD therapeutic effects in other organisms. However, no information has been provided on the ability of these compounds to revitalize the electrically-induced response deficiency induced in zebrafish PD models. Our techniques can be used to determine the sublethal toxic doses of these compounds and monitor their effect on the electric-induced response of larvae.

We demonstrated the diminishment of zebrafish locomotor response to repeated 3μA current pulses with dependency on the interstimulus which was attributed to the habituation as a form of non-associative learning. In the future, our technique can be applied to characterize the molecular, cellular, and physiological underpinnings of habituation to repeated electric stimuli.

We have screened the effect of a few chemicals with a limited concentration range and one gene on zebrafish electric-induced response. One can employ our devices to investigate how a broader range of chemicals at a wider dose range can influence zebrafish electric-induced response. In terms of microplastics toxicity, several potential applications can be considered using our quadruple-fish device. The toxicity effect of different types of microplastics such as polystyrene, polyethylene, polypropylene, and polyvinyl chloride with various shapes and sizes on behavioral responses and heartrate of zebrafish larvae can also be tested. Our microfluidic platform can also be used to monitor the effect of heavy metals such as cadmium and zinc on the electrically-induced behavioural responses of zebrafish larvae and determine the sublethal concentration of these chemicals for ecotoxicity screening.

Our quadruple-fish device was then utilized for chemical screening and provided behavioral evidence that the dopaminergic signalling pathway might be involved in modulation of zebrafish electric-induced movement. The results may support the claim that zebrafish electric-induced response can be considered as a useful measure in predicting mammalian behavioral response to chemicals suspected to affect the dopaminergic system. Although present report matches mammalian reports of impacted movement as a result of induced changes to the dopaminergic system, further work is needed to eliminate the possibility of effects on other signaling pathways. The drugs tested have higher affinities for dopaminergic targets. However, they cannot be solely

dopaminergic receptor ligands. Previous research has shown that these chemicals can also bind to adrenergic, cholinergic, histaminergic, and serotonergic receptors but with lower affinity[190–192]. Additional research is needed to determine the relative affinities for these receptors to fill this knowledge gap.

References

1. Dooley, K. & Zon, L. I. Zebrafish: a model system for the study of human disease. *Curr. Opin. Genet. Dev.* **10**, 252–256 (2000).

2. Webb, D. R. Animal models of human disease: Inflammation. *Biochem. Pharmacol.* **87**, 121–130 (2014).

3. Ruggeri, B. A., Camp, F. & Miknyoczki, S. Animal models of disease: Pre-clinical animal models of cancer and their applications and utility in drug discovery. *Biochem. Pharmacol.* **87**, 150–161 (2014).

4. Mullane, K. & Williams, M. Animal models of asthma: Reprise or reboot? *Biochem. Pharmacol.* **87**, 131–139 (2014).

5. McGonigle, P. Animal models of CNS disorders. *Biochem. Pharmacol.* **87**, 140–149 (2014).

6. Pandey, U. B. & Nichols, C. D. Human Disease Models in Drosophila melanogaster and the Role of the Fly in Therapeutic Drug Discovery. *Drug Deliv.* **63**, 411–436 (2011).

7. Lieschke, G. J. & Currie, P. D. Animal models of human disease: Zebrafish swim into view. *Nat. Rev. Genet.* **8**, 353–367 (2007).

8. Giacomotto, J. & Ségalat, L. High-throughput screening and small animal models, where are we? *Br. J. Pharmacol.* **160**, 204–216 (2010).

9. Szabo, M. *et al.* Cell and small animal models for phenotypic drug discovery. *Drug Des. Devel. Ther.* **11**, 1957–1967 (2017).

10. Bhatia, S., Daschkey, S., Lang, F., Borkhardt, A. & Hauer, J. Mouse models for pre-clinical drug testing in leukemia. *Expert Opin. Drug Discov.* **11**, 1081–1091 (2016).

11. Bugel, S. M., Tanguay, R. L. & Planchart, A. Zebrafish: A Marvel of High-Throughput Biology for 21st Century Toxicology. *Curr. Environ. Heal. Reports* **1**, 341–352 (2014).

12. Parasuraman, S. Toxicological screening. *J. Pharmacol. Pharmacother.* **2**, 74–79 (2011).

13. Helke, K. L. & Swindle, M. M. Animal models of toxicology testing: the role of pigs. *Expert Opin. Drug Metab. Toxicol.* **9**, 127–139 (2013).

14. Leung, M. C. K. *et al.* Caenorhabditis elegans: An emerging model in biomedical and environmental toxicology. *Toxicol. Sci.* **106**, 5–28 (2008).

15. Dengg, M. & Van Meel, J. C. A. Caenorhabditis elegans as model system for rapid toxicity assessment of pharmaceutical compounds. *J. Pharmacol. Toxicol. Methods* **50**, 209–214 (2004).

16. Diard, M. *et al.* Caenorhabditis elegans as a simple model to study phenotypic and genetic virulence determinants of extraintestinal pathogenic Escherichia coli. *Microbes Infect.* **9**, 214–223 (2007).

17. Santalla, M., Portiansky, E. & Ferrero, P. Drosophila Melanogaster, an Emerging Animal

Model for the Study of Human Cardiac Diseases. *Argentine J. Cardiol.* **84**, 424–430 (2016).

18. Navarro, J. A. *et al.* Analysis of dopaminergic neuronal dysfunction in genetic and toxin-induced models of Parkinson's disease in Drosophila. *J. Neurochem.* **131**, 369–382 (2014).

19. Jennings, B. H. Drosophila-a versatile model in biology & medicine. *Mater. Today* **14**, 190–195 (2011).

20. Yu, X. & Li, Y. V. Zebrafish as an alternative model for hypoxic-ischemic brain damage. *Int J Physiol Pathophysiol Pharmacol* **3**, 88–96 (2011).

21. Gallo, G. R. & Bellipanni, G. New Insight in Melanoma Studies From the Zebrafish Animal Model. *World Cancer Res. J.* **4**, 1–7 (2017).

22. Parker, T. *et al.* A multi-endpoint in vivo larval zebrafish (Danio rerio) model for the assessment of integrated cardiovascular function. *J. Pharmacol. Toxicol. Methods* **69**, 30–38 (2014).

23. Avila, D., Helmcke, K. & Aschner, M. The Caenorhabiditis elegans model as a reliable tool in neurotoxicology. *Hum. Exp. Toxicol.* **31**, 236–243 (2012).

24. Rand, M. D. NIH Public Access. **32**, 1–19 (2011).

25. Kokel, D. & Peterson, R. T. Chemobehavioural phenomics and behaviour-based psychiatric drug discovery in the zebrafish. *Briefings Funct. Genomics Proteomics* **7**, 483–490 (2008).

26. Auluck, P. K. Chaperone Suppression of alpha -Synuclein Toxicity in a Drosophila Model for Parkinson's Disease. *Science (80-.).* **295**, 865–868 (2002).

27. Bier, E. & Mcginnis, W. 3 Model Organisms in the Study of Development and Disease Model Organisms: Advantages and Limitations of the Various Systems. *Oxford Monograohs Med. Genet.* 25–45 (2004).

28. Hsu, C. H., Wen, Z. H., Lin, C. S. & Chakraborty, C. The zebrafish model: use in studying cellular mechanisms for a spectrum of clinical disease entities. *Curr Neurovasc Res* **4**, 111–120 (2007).

29. Xi, Y., Noble, S. & Ekker, M. Modeling neurodegeneration in zebrafish. *Curr. Neurol. Neurosci. Rep.* **11**, 274–282 (2011).

30. Erickstad, M., Hale, L. A., Chalasani, S. H. & Groisman, A. A microfluidic system for studying the behavior of zebrafish larvae under acute hypoxia. *Lab Chip* **15**, 857–866 (2015).

31. Huiting, L. N., Laroche, F. & Feng, H. The Zebrafish as a Tool to Cancer Drug Discovery. *Austin J. Pharmacol. Ther.* **3**, 1069 (2015).

32. Levraud, J. P., Palha, N., Langevin, C. & Boudinot, P. Through the looking glass: Witnessing host-virus interplay in zebrafish. *Trends Microbiol.* **22**, 490–497 (2014).

33. Moore, J. *et al.* Life spans and senescent phenotypes in two strains of Zebrafish (Danio rerio) Life spans and senescent phenotypes in two strains of Zebrafish (Danio rerio). **5565**, 1055–1068 (2002).

34. Parichy, D. M., Elizondo, M. R., Mills, M. G., Gordon, T. N. & Engeszer, E. NIH Public Access. **238**, 2975–3015 (2011).

35. Ali, S., Champagne, D. L., Spaink, H. P. & Richardson, M. K. Zebrafish embryos and larvae: A new generation of disease models and drug screens. *Birth Defects Res. Part C - Embryo Today Rev.* **93**, 115–133 (2011).

36. Chen, C. Y. & Cheng, C. M. Microfluidics expands the zebrafish potentials in pharmaceutically relevant screening. *Adv. Healthc. Mater.* **3**, 940–945 (2014).

37. Rihel, J. *et al.* Zebrafish behavioral profiling links drugs to biological targets and rest/wake regulation. *Science (80-.).* **327**, 348–351 (2010).

38. Kokel, D. *et al.* Rapid Behaviour-Based Identification of neuractive small Molecules in the Zebrafish. *Nat. Chem. Biol.* **6**, 231–237 (2010).

39. Maves, L. Recent advances using zebrafish animal models for muscle disease drug discovery. *Expert Opin. Drug Discov.* **9**, 1033–1045 (2015).

40. Cronin, A. & Grealy, M. Neuroprotective and Neuro-restorative Effects of Minocycline and Rasagiline in a Zebrafish 6-Hydroxydopamine Model of Parkinson's Disease. *Neuroscience* **367**, 34–46 (2017).

41. Feng, C.-W. *et al.* Effects of 6-Hydroxydopamine Exposure on Motor Activity and Biochemical Expression in Zebrafish (*Danio Rerio*) Larvae. *Zebrafish* **11**, 227–239 (2014).

42. Ek, F. *et al.* Behavioral Analysis of Dopaminergic Activation in Zebrafish and Rats Reveals Similar Phenotypes. *ACS Chem. Neurosci.* **7**, 633–646 (2016).

43. Anichtchik, O. *et al.* Loss of PINK1 Function Affects Development and Results in Neurodegeneration in Zebrafish. *J. Neurosci.* **28**, 8199–8207 (2008).

44. Xu, X., Weber, D., Burge, R. & VanAmberg, K. Neurobehavioral impairments produced by developmental lead exposure persisted for generations in zebrafish (Danio rerio). *Neurotoxicology* **52**, 176–185 (2016).

45. Avallone, B. *et al.* Structural and functional changes in the zebrafish (Danio rerio) skeletal muscle after cadmium exposure. *Cell Biol. Toxicol.* **31**, 273–283 (2015).

46. Zhu, B. *et al.* Effect of combined exposure to lead and decabromodiphenyl ether on neurodevelopment of zebrafish larvae. *Chemosphere* **144**, 1646–1654 (2016).

47. Jin, Y. *et al.* Embryonic exposure to cadmium (II) and chromium (VI) induce behavioral alterations, oxidative stress and immunotoxicity in zebrafish (Danio rerio). *Neurotoxicol. Teratol.* **48**, 9–17 (2015).

48. Ansari, S. & Ansari, B. A. Effects of Heavy Metals on the Embryo and Larvae of Zebrafish, Danio rerio (Cyprinidae). *Sch. Acad. J. Biosci.* **3**, 52–56 (2015).

49. Hill, A. J., Teraoka, H., Heideman, W. & Peterson, R. E. Zebrafish as a model vertebrate for investigating chemical toxicity. *Toxicol. Sci.* **86**, 6–19 (2005).

50. Souza, J. P., Baretta, J. F., Santos, F., Paino, I. M. M. & Zucolotto, V. Toxicological effects of graphene oxide on adult zebrafish (Danio rerio). *Aquat. Toxicol.* **186**, 11–18 (2017).

51. Kovrižnych, J. A. *et al.* Acute toxicity of 31 different nanoparticles to zebrafish (Danio rerio) tested in adulthood and in early life stages - Comparative study. *Interdiscip. Toxicol.* **6**, 67–73 (2013).

52. Panula, P. *et al.* The comparative neuroanatomy and neurochemistry of zebrafish CNS systems of relevance to human neuropsychiatric diseases. *Neurobiol. Dis.* **40**, 46–57 (2010).

53. Rink, E. & Wullimann, M. F. Connections of the ventral telencephalon and tyrosine hydroxylase distribution in the zebrafish brain (Danio rerio) lead to identification of an ascending dopaminergic system in a teleost. *Brain Res. Bull.* **57**, 385–387 (2002).

54. Colwill, R. M. & Creton, R. Locomotor behaviors in zebrafish (Danio rerio) larvae. *Behav. Processes* **86**, 222–229 (2011).

55. Stewart, A. M., Braubach, O., Spitsbergen, J., Gerlai, R. & Kalueff, A. V. Zebrafish models for translational neuroscience research: from tank to bedside. *Trends Neurosci* **37**, 264–278 (2014).

56. Irons, T. D. D. *et al.* Acute Administration of Dopaminergic Drugs has Differential Effects on Locomotion in Larval Zebrafish. *Pharmacol. Biochem. Behav.* **103**, 792–813 (2013).

57. Irons, T. D., MacPhail, R. C., Hunter, D. L. & Padilla, S. Acute neuroactive drug exposures alter locomotor activity in larval zebrafish. *Neurotoxicol. Teratol.* **32**, 84–90 (2010).

58. Fajardo, O., Zhu, P. & Friedrich, R. W. Control of a specific motor program by a small brain area in zebrafish. *Front. Neural Circuits* **7**, 67 (2013).

59. Mu, Y., Li, X., Zhang, B. & Du, J. Article Visual Input Modulates Audiomotor Function via Hypothalamic Dopaminergic Neurons through a Cooperative Mechanism. *Neuron* **75**, 688–699 (2012).

60. Lu, Z. & Desmidt, A. A. Early development of hearing in zebrafish. *JARO - J. Assoc. Res. Otolaryngol.* (2013) doi:10.1007/s10162-013-0386-z.

61. Bianco, I. H., Kampff, A. R. & Engert, F. Prey Capture Behavior Evoked by Simple Visual Stimuli in Larval Zebrafish. *Front. Syst. Neurosci.* **5**, 1–13 (2011).

62. Monesson-olson, B. D., Browning-kamins, J., Aziz-bose, R. & Kreines, F. Optical Stimulation of Zebrafish Hair Cells Expressing. **9**, 1–8 (2014).

63. Steenbergen, P. J. Response of zebrafish larvae to mild electrical stimuli: A 96-well setup for behavioural screening. *J. Neurosci. Methods* **301**, 52–61 (2018).

64. Chan, P. K., Lin, C. C. & Cheng, S. H. Noninvasive technique for measurement of

heartbeat regularity in zebrafish (Danio rerio) embryos. *BMC Biotechnol.* **9**, 1–10 (2009).

65. Cianciolo Cosentino, C. *et al.* Intravenous Microinjections of Zebrafish Larvae to Study Acute Kidney Injury. *J. Vis. Exp.* 2–5 (2010) doi:10.3791/2079.

66. Giacomini, N. J., Rose, B., Kobayashi, K. & Guo, S. Antipsychotics produce locomotor impairment in larval zebrafish. *Neurotoxicol. Teratol.* **28**, 245–250 (2006).

67. Youssef, K., Peimani, A. R., Bayat, P., Dibaji, S. & Rezai, P. Miniaturized Sensors and Actuators for Biological Studies on Small Model Organisms of Disease. in *Environmental, Chemical and Medical Sensors* 199–225 (Springer, Singapore, 2018). doi:10.1007/978-981-10-7751-7_9.

68. Khoshmanesh, K. *et al.* New rationale for large metazoan embryo manipulations on chip-based devices. *Biomicrofluidics* **6**, 1–14 (2012).

69. Au, A. K., Lee, W. & Folch, A. HHS Public Access. **14**, 1294–1301 (2015).

70. Waldbaur, A., Rapp, H., Länge, K. & Rapp, B. E. Let there be chip - Towards rapid prototyping of microfluidic devices: One-step manufacturing processes. *Anal. Methods* **3**, 2681–2716 (2011).

71. Wlodkowic, D., Faley, S., Skommer, J., McGuinness, D. & Cooper, J. M. Biological implications of polymeric microdevices for live cell assays. *Anal. Chem.* **81**, 9828–9833 (2009).

72. Rogers, C. I., Qaderi, K., Woolley, A. T. & Nordin, G. P. 3D printed microfluidic devices with integrated valves. *Biomicrofluidics* **9**, 1–9 (2015).

73. Tseng, P., Murray, C., Kim, D. & Di Carlo, D. Research highlights: Printing the future of microfabrication. *Lab Chip* **14**, 1491–1495 (2014).

74. Wang, W., Liu, X., Gelinas, D., Ciruna, B. & Sun, Y. A fully automated robotic system for microinjection of zebrafish embryos. *PLoS One* **2**, (2007).

75. Noori, A., Selvaganapathy, P. R. & Wilson, J. Microinjection in a microfluidic format using flexible and compliant channels and electroosmotic dosage control. *Lab Chip* **9**, 3202–3211 (2009).

76. Miura, S., Teshima, T., Tomoike, F. & Takeuchi, S. Glass-capillary-accessible dynamic microarray for microinjection of zebrafish embryos. *17th Int. Conf. Miniaturized Syst. Chem. Life Sci. MicroTAS 2013* **1**, 452–454 (2013).

77. Zhu, F. *et al.* Three-dimensional printed millifluidic devices for zebrafish embryo tests. *Biomicrofluidics* **9**, 1–10 (2015).

78. Yang, F. *et al.* An integrated microfluidic array system for evaluating toxicity and teratogenicity of drugs on embryonic zebrafish developmental dynamics. *Biomicrofluidics* **5**, (2011).

79. Wielhouwer, E. M. *et al.* Zebrafish embryo development in a microfluidic flow-through system. *Lab Chip* **11**, 1815–1824 (2011).

80. van Noort, S. *et al.* Fish and chips: A microfluidic perfusion platform for monitoring zebrafish development. *Lab Chip* **12**, 892–900 (2012).

81. Li, Y. *et al.* Zebrafish on a chip: A novel platform for real-time monitoring of drug-induced developmental toxicity. *PLoS One* **9**, (2014).

82. Huang, S. H., Huang, K. S. & Liou, Y. M. Simultaneous monitoring of oxygen consumption and acidification rates of a single zebrafish embryo during embryonic development within a microfluidic device. *Microfluid. Nanofluidics* **21**, (2017).

83. Zheng, C. *et al.* Fish in chips: An automated microfluidic device to study drug dynamics

in vivo using zebrafish embryos. *Chem. Commun.* **50**, 981–984 (2014).

84. Shen, Y.-C. *et al.* A Student Team in a University of Michigan Biomedical Engineering Design Course Constructs a Microfluidic Bioreactor for Studies of Zebrafish Development. *Zebrafish* **6**, 201–213 (2009).

85. Akagi, J. *et al.* Fish on chips: Automated microfluidic living embryo arrays. *Procedia Eng.* **47**, 84–87 (2012).

86. Akagi, J. *et al.* Fish on chips: Microfluidic living embryo array for accelerated in vivo angiogenesis assays. *Sensors Actuators, B Chem.* **189**, 11–20 (2013).

87. Huang, S. H., Yu, C. H. & Chien, Y. L. Light-addressable measurement of in vivo tissue oxygenation in an unanesthetized Zebrafish embryo via phase-based phosphorescence lifetime detection. *Sensors* **15**, 8146–8162 (2015).

88. Popova, A. A. *et al.* Fish-Microarray: A Miniaturized Platform for Single-Embryo High-Throughput Screenings. *Adv. Funct. Mater.* **28**, 1–12 (2018).

89. Akagi, J. *et al.* Dynamic analysis of angiogenesis in transgenic zebrafish embryos using a 3D multilayer chip-based technology. *Proc. SPIE - Int. Soc. Opt. Eng.* **v 8615**, 86151B (2013).

90. Zhu, F. *et al.* Automated Lab-on-a-Chip Technology for Fish Embryo Toxicity Tests Performed under Continuous Microperfusion (μFET). *Environ. Sci. Technol.* **49**, 14570–14578 (2015).

91. Akagi, J. *et al.* Miniaturized embryo array for automated trapping, immobilization and microperfusion of zebrafish embryos. *PLoS One* **7**, 12–15 (2012).

92. Wang, K. I. K. *et al.* Toward embedded laboratory automation for smart lab-on-a-chip embryo arrays. *Biosens. Bioelectron.* **48**, 188–196 (2013).

93. Bischel, L. L., Mader, B. R., Green, J. M., Huttenlocher, A. & Beebe, D. J. Zebrafish Entrapment by Restriction Array (ZEBRA) device: A low-cost, agarose-free zebrafish mounting technique for automated imaging. *Lab Chip* **13**, 1732–1736 (2013).

94. Lin, X. *et al.* High-throughput mapping of brain-wide activity in awake and drug-responsive vertebrates. *Lab Chip* **15**, 680–689 (2015).

95. Lin, X. *et al.* Autonomous system for cross-organ investigation of ethanol-induced acute response in behaving larval zebrafish. *Biomicrofluidics* **10**, 024123–1 (2016).

96. Hong, S. G., Lee, P., Baraban, S. C. & Lee, L. P. A Novel Long-term, Multi-Channel and Non-invasive Electrophysiology Platform for Zebrafish. *Sci. Rep.* **6**, 1–10 (2016).

97. Nady, A., Peimani, A. R., Zoidl, G. & Rezai, P. A microfluidic device for partial immobilization, chemical exposure and behavioural screening of zebrafish larvae. *Lab Chip* **17**, 4048–4058 (2017).

98. Khalili, A., Youssef, K., Zoidl, G. & Rezai, P. Neurotoxin-Induced Impairment and Neuroprotective-Based Recovery of Electrotactic Locomotion in Zebrafish Larvae as a Model for Neurobehavioral Studies in Parkinson's Disease. in *International Conference on Miniaturized Systems for Chemistry and Life Sciences (μTAS 2018)* 1553–1556 (2018).

99. Peimani, A. R., Zoidl, G. & Rezai, P. A microfluidic device to study electrotaxis and dopaminergic system of zebrafish larvae. *Biomicrofluidics* **12**, 014113–1 (2018).

100. Fuad, N. M., Kaslin, J. & Wlodkowic, D. Lab-on-a-Chip imaging micro-echocardiography (iμEC) for rapid assessment of cardiovascular activity in zebrafish larvae. *Sensors Actuators, B Chem.* **256**, 1131–1141 (2018).

101. Candelier, R. *et al.* A microfluidic device to study neuronal and motor responses to acute chemical stimuli in zebrafish. *Sci. Rep.* **5**, 1–10 (2015).

102. Chen, C. Y., Chang Chien, T. C., Mani, K. & Tsai, H. Y. Axial orientation control of zebrafish larvae using artificial cilia. *Microfluid. Nanofluidics* **20**, 1–9 (2016).

103. Mondal, S., Ahlawat, S. & Koushika, S. P. Simple Microfluidic Devices for in vivo Imaging of C. elegans, Drosophila and Zebrafish. *J. Vis. Exp.* 1–9 (2012) doi:10.3791/3780.

104. Akagi, J. *et al.* Microfluidic device for a rapid immobilization of Zebrafish larvae in environmental scanning electron microscopy. *Cytom. Part A* **87**, 190–194 (2015).

105. Akagi, J., Hall, C. J., Crosier, K. E., Crosier, P. S. & Wlodkowic, D. Immobilization of zebrafish larvae on a chip-based device for environmental scanning electron microscopy (ESEM) imaging. **892346**, 892346 (2013).

106. Huemer, K. *et al.* Long-term Live Imaging Device for Improved Experimental Manipulation of Zebrafish Larvae. *J. Vis. Exp.* 1–12 (2017) doi:10.3791/56340.

107. Zhang, G. *et al.* An integrated microfluidic system for zebrafish larva organs injection. *Proc. IECON 2017 - 43rd Annu. Conf. IEEE Ind. Electron. Soc.* **2017-Janua**, 8563–8566 (2017).

108. Ellett, F. & Irimia, D. Microstructured Devices for Optimized Microinjection and Imaging of Zebrafish Larvae. *J. Vis. Exp.* (2017) doi:10.3791/56498.

109. Chen, C. A non-invasive acoustic-trapping of zebrafish microfluidics A non-invasive acoustic-trapping of zebrafish microfluidics. **014109**, (2021).

110. Lee, Y., Seo, H. W., Lee, K. J., Jang, J. & Kim, S. A Microfluidic System for Stable and Continuous EEG Monitoring from Multiple Larval Zebrafish. 14–17 (2020).

111. Cho, S. J., Kang, Y. J. & Kim, S. High-throughput zebrafish intramuscular recording

assay. *Sensors Actuators, B Chem.* **304**, 127332 (2020).

112. Wang, Y. F., Chen, I. W., Subendran, S. & Kang, C. W. Edible additive effects on zebrafish cardiovascular functionality with hydrodynamic assessment. *Sci. Rep.* 1–8 (2020) doi:10.1038/s41598-020-73455-9.

113. Zhang, G. *et al.* Zebrafish Larva Orientation and Smooth Aspiration Control for Microinjection. *IEEE Trans. Biomed. Eng.* **68**, 47–55 (2021).

114. Kwon, H. J. *et al.* Design of a microfluidic device with a non-traditional flow profile for on-chip damage to zebrafish sensory cells. *J. Micromechanics Microengineering* **24**, (2014).

115. Peimani, A. R., Zoidl, G. & Rezai, P. A microfluidic device for quantitative investigation of zebrafish larvae's rheotaxis. *Biomed. Microdevices* **19**, 1–6 (2017).

116. Rezai, P., Siddiqui, A., Selvaganapathy, P. R. & Gupta, B. P. Electrotaxis of Caenorhabditis elegans in a microfluidic environment. *Lab Chip* **10**, 220–226 (2010).

117. Rezai, P., Salam, S., Selvaganapathy, P. R. & Gupta, B. P. Effect of pulse direct current signals on electrotactic movement of nematodes Caenorhabditis elegans and Caenorhabditis briggsae. *Biomicrofluidics* **5**, (2011).

118. Rezai, P., Siddiqui, A., Selvaganapathy, P. R. & Gupta, B. P. Behavior of Caenorhabditis elegans in alternating electric field and its application to their localization and control. *Appl. Phys. Lett.* **96**, 1–4 (2010).

119. Mani, K., Hsieh, Y. C., Panigrahi, B. & Chen, C. Y. A noninvasive light driven technique integrated microfluidics for zebrafish larvae transportation. *Biomicrofluidics* **12**, 1–12 (2018).

120. Panigrahi, B. & Chen, C. Microfluidic Transportation Control of Larval Zebrafish through

Optomotor Regulations under a Pressure-Driven Flow. (2019).

121. Subendran, S., Kang, C. W. & Chen, C. Y. Comprehensive hydrodynamic investigation of zebrafish tail beats in a microfluidic device with a shape memory alloy. *Micromachines* **12**, 1–10 (2021).

122. Peimani, A. R., Zoidl, G. & Rezai, P. A microfluidic device to study electrotaxis and dopaminergic system of zebrafish larvae. *Biomicrofluidics* **12**, 1–15 (2018).

123. Khalili, A. & Rezai, P. Microfluidic devices for embryonic and larval zebrafish studies. *Briefings Funct. Genomics,* **18**, 419–432 (2019).

124. Tabor, K. M. *et al.* Direct activation of the Mauthner cell by electric field pulses drives ultrarapid escape responses. *J. Neurophysiol.* **112**, 834–844 (2014).

125. Zabihihesari, A., Hilliker, A. J. & Rezai, P. Localized microinjection of intact: Drosophila melanogaster larva to investigate the effect of serotonin on heart rate. *Lab Chip* **20**, 343–355 (2020).

126. Khalili, A., Wijngaarden, E. van, Zoidl, G. R. & Rezai, P. Multi-phenotypic and bi-directional behavioral screening of zebrafish larvae. *Integr. Biol.* **12**, 211–220 (2020).

127. Khalili, A., van Wijngaarden, E., Zoidl, G. R. & Rezai, P. Zebrafish Larva's Response to Electric Signal: Effects of Voltage, Current and Pulsation for Habituation Studies. *Sensors Actuators A. Phys.* **332**, (2021).

128. Khalili, A., van Wijngaarden, E., Youssef, K., Zoidl, G. & Rezai, P. Designing microfluidic devices for behavioral screening of multiple zebrafish larvae. *Biotechnol. J.* **17**, 2100076 (2022).

129. Khalili, A. *et al.* Phenotypic chemical and mutant screening of zebrafish larvae using an on-demand response to electric stimulation. *Integr. Biol.* **11**, 373–383 (2019).

130. Khalili, A., van Wijngaarden, E., Zoidl, G. R. & Rezai, P. Dopaminergic signaling regulates zebrafish larvae's response to electricity. *Biotechnol. J.* (2022).

131. Bedell, V. M. *et al.* In vivo Genome Editing Using High Efficieny TALENs. *Nature* **491**, 114–118 (2012).

132. Sheng, D. *et al.* Deletion of the WD40 domain of LRRK2 in zebrafish causes parkinsonism-like loss of neurons and locomotive defect. *PLoS Genet.* **6**, (2010).

133. Kazama, Y., Carlen, E. T., van den Berg, A. & Hibara, A. Top-and-side dual-view microfluidic device with embedded prism. *Sensors Actuators, B Chem.* **248**, 753–760 (2017).

134. Reed, B. & Jennings, M. *Guidance on the housing and care of Zebrafish Danio rerio*. *Research Animals Department, Science Group, RSPCA* (2011).

135. Gerhart, A. K. & Janz, D. M. Toxicity of aqueous L-selenomethionine and tert-butyl hydroperoxide exposure to zebrafish (Danio rerio) embryos following tert-butyl hydroquinone treatment. *Toxics* **7**, (2019).

136. Pardo-Martin, C. *et al.* High-throughput cellular-resolution in vivo vertebrate screening. *Nat Methods* **7**, 634–636 (2010).

137. Bartolini, T., Mwaffo, V., Butail, S. & Porfiri, M. Effect of acute ethanol administration on zebrafish tail-beat motion. *Alcohol* **49**, 721–725 (2015).

138. Patterson, B. W., Abraham, A. O., MacIver, M. A. & McLean, D. L. Visually guided gradation of prey capture movements in larval zebrafish. *J. Exp. Biol.* **216**, 3071–83 (2013).

139. Featherstone, D., Drewes, C. D. & Coats, J. R. Short Communication: Noninvasive Detection of Electrical Events During the Startle Response in Larval Medaka. *J. Exp. Biol.*

158, 583–589 (1991).

140. Prugh, J. I., Kimmel, C. B. & Metcalfe, W. K. Noninvasive recording of the Mauthner neurone action potential in larval zebrafish. *J. Exp. Biol.* **101**, 83–92 (1982).

141. Pradel, G., Schachner, M. & Schmidt, R. Inhibition of memory consolidation by antibodies against cell adhesion molecules after active avoidance conditioning in zebrafish. *J. Neurobiol.* **39**, 197–206 (1999).

142. Valente, A., Huang, K. H., Portugues, R. & Engert, F. Ontogeny of classical and operant learning behaviors in zebrafish. *Learn. Mem.* **19**, 170–177 (2012).

143. Gao, X. *et al.* Improved electrical conductivity of PDMS/SCF composite sheets with bolting cloth prepared by a spatial confining forced network assembly method. *RSC Adv.* **7**, 14761–14768 (2017).

144. Aleström, P. *et al.* Zebrafish: Housing and husbandry recommendations. *Lab. Anim.* **54**, 213–224 (2020).

145. Best, J. D. *et al.* Non-associative learning in larval zebrafish. *Neuropsychopharmacology* **33**, 1206–1215 (2008).

146. Easter Jr, S. S. & Nicola, G. N. The development of vision in the zebrafish. *Dev. Biol.* **180**, 646–663 (1996).

147. Rankin, C. H. *et al.* Habituation revisited: An updated and revised description of the behavioral characteristics of habituation. *Neurobiol. Learn. Mem.* **92**, 135–138 (2009).

148. Sampurna, B. P., Audira, G., Juniardi, S., Lai, Y. H. & Hsiao, C. Der. A simple ImageJ-based method to measure cardiac rhythm in zebrafish embryos. *Inventions* **3**, 1–11 (2018).

149. Schwerte, T., Voigt, S. & Pelster, B. Epigenetic variations in early cardiovascular

performance and hematopoiesis can be explained by maternal and clutch effects in developing zebrafish (Danio rerio). *Comp. Biochem. Physiol. - A Mol. Integr. Physiol.* **141**, 200–209 (2005).

150. Kopp, R., Schwerte, T. & Pelster, B. Cardiac performance in the zebrafish breakdance mutant. *J. Exp. Biol.* **208**, 2123–2134 (2005).

151. Wolman, M. A., Jain, R. A., Liss, L. & Granato, M. Chemical modulation of memory formation in larval zebrafish. *Proc. Natl. Acad. Sci. U. S. A.* **108**, 15468–15473 (2011).

152. Nelson, J. C. *et al.* Acute regulation of habituation learning via posttranslational palmitoylation. *Curr. Biol.* **30**, 2729-2738.e4 (2020).

153. Roberts, A. C. *et al.* Long-term habituation of the C-start escape response in zebrafish larvae. *Neurobiol. Learn. Mem.* **134**, 360–368 (2016).

154. Firoz, C. K. *et al.* An overview on the correlation of neurological disorders with cardiovascular disease. *Saudi J. Biol. Sci.* **22**, 19–23 (2015).

155. Malek, N. *et al.* Vascular disease and vascular risk factors in relation to motor features and cognition in early Parkinson's disease. *Mov. Disord.* **31**, 1518–1526 (2016).

156. Thompson, R. F. Habituation: A history. *Neurobiol. Learn. Mem.* **92**, 127–134 (2009).

157. Brown, G. D. Nonassociative learning processes affecting swimming probability in the seaslug Tritonia diomedea: Habituation, sensitization and inhibition. *Behav. Brain Res.* **95**, 151–165 (1998).

158. Morgan, R. P., Ulanowicz, R. E., Rasin, V. J., Noe, L. A. & Gray, G. B. Effects of Shear on Eggs and Larvae of Striped Bass, Morone saxatilis, and White Perch, M. americana. *Trans. Am. Fish. Soc.* **105**, 149–154 (1976).

159. Ulanowicz, R. E. The mechanical effects of water flow on fish eggs and larvae. *Fish. energy Prod. a Symp.* **1**, 77–87 (1976).

160. Sui, Y. *et al.* Deep Brain Stimulation Initiative: Toward Innovative Technology, New Disease Indications, and Approaches to Current and Future Clinical Challenges in Neuromodulation Therapy. *Front. Neurol.* **11**, 597451 (2021).

161. Lozano, A. M. *et al.* Deep brain stimulation: current challenges and future directions. *Nat. Rev. Neurol.* **15**, 148–160 (2019).

162. Nussbaum, E. L. *et al.* Neuromuscular electrical stimulation for treatment of muscle impairment: Critical review and recommendations for clinical practice. *Physiother. Canada* **69**, 1–76 (2017).

163. Ungerstedt, U. 6-Hydroxydopamine-Induced Degeneration of the Nigrostriatal Dopamine Pathway: The Turning Syndrome. *Pharmacol Ther B* **2**, 37–40 (1976).

164. Oberlander, C., Euvrard, C., Dumont, C. & Boissier, J. R. Circling Behaviour Induced by Dopamine Releasers and/or Uptake Inhibitors During Degeneration of the Nigrostriatal Pathway. *Eur. J. Pharmacol.* **60**, 163–170 (1979).

165. Boehmier, W. *et al.* Evolution and expression of D2 and D3 dopamine receptor genes in zebrafish. *Dev. Dyn. an Off. Publ. Am. Assoc. Anat.* **230**, 481–493 (2004).

166. Maximino, C. & Herculano, A. M. A review of monoaminergic neuropsychopharmacology in zebrafish. *Zebrafish* **7**, 359–378 (2010).

167. Souza, B. R., Romano-Silva, M. A. & Tropepe, V. Dopamine D2 receptor activity modulates Akt signaling and alters GABAergic neuron development and motor behavior in zebrafish larvae. *J. Neurosci.* **31**, 5512–5525 (2011).

168. Seibt, K. J. *et al.* Antipsychotic drugs reverse MK-801-induced cognitive and social

interaction deficits in zebrafish (Danio rerio). *Behav. Brain Res.* **224**, 135–139 (2011).

169. Savio, L. E. B., Vuaden, F. C., Piato, A. L., Bonan, C. D. & Wyse, A. T. S. Behavioral changes induced by long-term proline exposure are reversed by antipsychotics in zebrafish. *Prog. Neuropsychopharmacol. Biol. Psychiatry* **36**, 258–263 (2012).

170. Farrell, T. C. *et al.* Evaluation of spontaneous propulsive movement as a screening tool to detect rescue of Parkinsonism phenotypes in zebrafish models. *Neurobiol. Dis.* **44**, 9–18 (2011).

171. Boehmler, W. *et al.* D4 Dopamine receptor genes of zebrafish and effects of the antipsychotic clozapine on larval swimming behaviour. *Genes. Brain. Behav.* **6**, 155–166 (2007).

172. Burgess, H. A. & Granato, M. Modulation of locomotor activity in larval zebrafish during light adaptation. *J. Exp. Biol.* **210**, 2526–2539 (2007).

173. Outeiro, T. F. & Ferreira, J. J. Zebrafish as an Animal Model for Drug Discovery in Parkinson ' s Disease and Other Movement Disorders : A Systematic Review. *Front. Neurol.* **9**, 347 (2018).

174. Jauhar, S. *et al.* Regulation of dopaminergic function : an [18 F] -DOPA PET apomorphine challenge study in humans . *Transl. Psychiatry* e1027 (2017) doi:10.1038/tp.2016.270.

175. Nyberg, S., Chou, Y. & Halldin, C. Saturation of striatal D 2 dopamine receptors by clozapine. *Int. J. Neuropsychopharmacol.* **5**, 11–16 (2002).

176. Voith, K. & Herr, F. The behavioral pharmacology of butaclamol hydrochloride (AY-23,028), a new potent neuroleptic drug. *Psychopharmacologia* **42**, 11–20 (1975).

177. Bergman, J., Madras, B. K. & Spealman, R. D. Behavioral effects of D1 and D2 dopamine

receptor antagonists in squirrel monkeys. *J. Pharmacol. Exp. Ther.* **258**, 910–917 (1991).

178. Beninger, R. J., Mazurski, E. J. & Hoffman, D. C. Receptor subtype-specific dopaminergic agents and unconditioned behavior. *Pol. J. Pharmacol. Pharm.* **43**, 507–528 (1991).

179. Morato, G. S., Lemos, T. & Takahashi, R. N. Acute exposure to maneb alters some behavioral functions in the mouse. *Neurotoxicol. Teratol.* **11**, 421–425 (1989).

180. Choi, W. Y., Morvan, C., Balsam, P. D. & Horvitz, J. C. Dopamine D1 and D2 antagonist effects on response likelihood and duration. *Behav. Neurosci.* **123**, 1279–1287 (2009).

181. King, D. J., Lucas, M. B. & Lucas, R. A. Antipsychotic Drug-Induced Dysphoria. *Br. J. Psychiatry* **167**, 480–482 (1995).

182. Spulber, S. *et al.* PFOS induces behavioral alterations, including spontaneous hyperactivity that is corrected by dexamfetamine in zebrafish larvae. *PLoS One* **9**, e94227 (2014).

183. Dracheva, S. *et al.* Paradoxical locomotor behavior of dopamine d1 receptor transgenic mice. *Exp. Neurol.* **157**, 169–179 (1999).

184. Xu, M. *et al.* Dopamine Dl Receptor Mutant Mice Are Deficient in Striatal Expression of Dynorphin and in Dopami ! lie-Mediated Behavioral Responses. **79**, 729–742 (1994).

185. White, N. M., Packard, M. G. & Hiroi, N. Place conditioning with dopamine D1 and D2 agonists injected peripherally or into nucleus accumbens. *Psychopharmacology (Berl).* **103**, 271–276 (1991).

186. Shieh, G. J. & Walters, D. E. Stimulating dopamine D1 receprors increases the locomotor activity of developing rats. *Eur. J. Pharmacol.* **311**, 103–107 (1996).

187. Scott, L., Forssberg, H., Aperia, A. & Diaz-heijtz, R. Locomotor Effects of a D1R Agonist Are DARPP-32 Dependent in Adult but not Weanling Mice. **58**, 779–783 (2005).

188. Chausmer, A. L. & Katz, J. L. Comparison of interactions of D1-like agonists, SKF 81297, SKF 82958 and A-77636, with cocaine: Locomotor activity and drug discrimination studies in rodents. *Psychopharmacology (Berl).* **159**, 145–153 (2002).

189. Sobrian, S. K., Jones, B. L., Varghese, S. & Holson, R. R. Behavioral response profiles following drug challenge with dopamine receptor subtype agonists and antagonists in developing rat. *Neurotoxicol. Teratol.* **25**, 311–328 (2003).

190. Millan, M. J. *et al.* Differential actions of antiparkinson agents at multiple classes of monoaminergic receptor. I. A multivariate analysis of the binding profiles of 14 drugs at 21 native and cloned human receptor subtypes. *J. Pharmacol. Exp. Ther.* **303**, 791–804 (2002).

191. Hyttel, J. SCH 23390 - the first selective dopamine D-1 antagonist. *Eur. J. Pharmacol.* **91**, 153–154 (1983).

192. Bymaster, F. P. *et al.* Radioreceptor binding profile of the atypical antipsychotic olanzapine. *Neuropsychopharmacol. Off. Publ. Am. Coll. Neuropsychopharmacol.* **14**, 87–96 (1996).

193. Tysnes, O. B. & Storstein, A. Epidemiology of Parkinson's disease. *J. Neural Transm.* **124**, 901–905 (2017).

194. Verstraeten, A., Theuns, J. & Van Broeckhoven, C. Progress in unraveling the genetic etiology of Parkinson disease in a genomic era. *Trends Genet.* **31**, 140–149 (2015).

195. Anichtchik, O. V, Kaslin, J., Peitsaro, N., Scheininà, M. & Panula, P. Neurochemical and behavioural changes in zebrafish Danio rerio after systemic administration of 6-

hydroxydopamine and 1-methyl-4-phenyl-1,2,3,6-tetrahydropyridine. *J. Neurochem* **88**, 443–453 (2004).

196. Matsui, H. *et al.* A chemical neurotoxin, MPTP induces Parkinson's disease like phenotype, movement disorders and persistent loss of dopamine neurons in medaka fish. *Neurosci. Res.* **65**, 263–271 (2009).

197. Bretaud, S., Lee, S. & Guo, S. Sensitivity of zebrafish to environmental toxins implicated in Parkinson's disease. *Neurotoxicol. Teratol.* **26**, 857–864 (2004).

198. Stednitz, S. J. *et al.* Selective toxicity of L-DOPA to dopamine transporter-expressing neurons and locomotor behavior in zebrafish larvae. *Neurotoxicol. Teratol.* **52**, 51–56 (2015).

199. Flinn, L. *et al.* Complex i deficiency and dopaminergic neuronal cell loss in parkin-deficient zebrafish (Danio rerio). *Brain* **132**, 1613–1623 (2009).

200. Lam, C. S., Korzh, V. & Strahle, U. Zebrafish embryos are susceptible to the dopaminergic neurotoxin MPTP. *Eur. J. Neurosci.* (2005) doi:10.1111/j.1460-9568.2005.03988.x.

201. Xu, J., Chen, L. & Li, L. Pannexin hemichannels: A novel promising therapy target for oxidative stress related diseases. *J. Cell. Physiol.* **233**, 2075–2090 (2018).

202. Maritim, A. C., Sanders, R. A. & Watkins, J. B. Diabetes, oxidative stress, and antioxidants: A review. *J. Biochem. Mol. Toxicol.* **17**, 24–38 (2003).

203. Andersen, J. K. Oxidative stress in neurodegeneration: Cause or consequence? *Nat. Rev. Neurosci.* **10**, S18 (2004).

204. Zhang, C., Cagliero, C., Pierson, S. A. & Anderson, J. L. Rapid and sensitive analysis of polychlorinated biphenyls and acrylamide in food samples using ionic liquid-based in situ

dispersive liquid-liquid microextraction coupled to headspace gas chromatography. *J. Chromatogr. A* **1481**, 1–11 (2017).

205. Zuch, C. L. *et al.* Time course of degenerative alterations in nigral dopaminergic neurons following a 6-hydroxydopamine lesion. *J. Comp. Neurol.* **427**, 440–454 (2000).

206. Blandini, F., Armentero, M. T., Fancellu, R., Blaugrund, E. & Nappi, G. Neuroprotective effect of rasagiline in a rodent model of Parkinson's disease. *Exp. Neurol.* **187**, 455–459 (2004).

207. Glinka, Y., Tipton, K. F. & Youdim, M. B. H. Mechanism of inhibition of mitochondrial respiratory complex I by 6- hydroxydopamine and its prevention by desferrioxamine. *Eur. J. Pharmacol.* **351**, 121–129 (1998).

208. Parng, C., Roy, N. M., Ton, C., Lin, Y. & McGrath, P. Neurotoxicity assessment using zebrafish. *J. Pharmacol. Toxicol. Methods* **55**, 103–112 (2007).

209. Birkmayer, W. & Hornykiewicz, O. The L-3,4-dioxyphenylalanine (DOPA)-effect in Parkinson-akinesia. *Wien Kin Wochenschr* **10**, 787–788 (1961).

210. Cotzias, G. C. Levodopa in the Treatment of Parkinsonism. *J. Am. Med. Assoc.* **218**, 1903–1908 (1971).

211. Safaraian, N. *et al.* The phenotype of Panx1a knock out zebrafish reveals a novel role in sensory-motor gating. *Submitted* (2017).

212. Hauser, R. A. Levodopa: Past, present, and future. *Eur. Neurol.* **62**, 1–8 (2009).

213. Lipski, J. *et al.* L-DOPA: A scapegoat for accelerated neurodegeneration in Parkinson's disease? *Prog. Neurobiol.* **94**, 389–407 (2011).

214. Bunney, B. S., Aghajanian, G. K. & Roth, R. H. Comparison of Effects of L-Dopa,

Amphetamine and Apomorphine on Firing Rate of rat Dopaminergic Neurons. *Nat. New Biol.* **245**, 123–125 (1973).

215. Paalzow, G. H. M. & Paalzow, L. K. L- Dopa, how it may exacerbate parkinsonian symptoms. 15–19 (1986).

216. Kovalzon, V. M., Latyshkova, A. A., Komarova, A. D. & Panchin, Y. V. Sleep-wake cycle and experimental models of Panx1 mutations. *Zhurnal Nevrol. i psikhiatrii im. S.S. Korsakova* **118**, 61 (2018).

217. Ryczko, D. & Dubuc, R. Dopamine and the brainstem locomotor networks: From lamprey to human. *Frontiers in Neuroscience* (2017) doi:10.3389/fnins.2017.00295.

218. Carlsson, A. On the neuronal circuitries and neurotransmitters involved in the control of locomotor activity. in *Journal of Neural Transmission, Supplement* (1993).

219. Ahmadian, E., Eftekhari, A., Samiei, M., Maleki Dizaj, S. & Vinken, M. The role and therapeutic potential of connexins, pannexins and their channels in Parkinson's disease. *Cell. Signal.* **58**, 111–118 (2019).

220. Crespo Yanguas, S. *et al.* Pannexin1 as mediator of inflammation and cell death. *Biochim. Biophys. Acta - Mol. Cell Res.* **1864**, 51–61 (2017).

221. Safarian, N., Whyte-Fagundes, P., Zoidl, C., Grigull, J. & Zoidl, G. Visuomotor deficiency in panx1a knockout zebrafish is linked to dopaminergic signaling. *Sci. Rep.* **10**, 9538 (2020).

Author Contributions during PhD

Journal Papers:

1. A. Khalili, N. Safarian, E. van Wijngaarden, G. R. Zoidl, P. Rezai, “A Microfluidic-Based Study Uncovers a Delayed Onset of a Parkinson-like Phenotype in the Panx1a Knockout Zebrafish Model”, (Under Preparation).
2. A. Khalili, E. van Wijngaarden, G. R. Zoidl, P. Rezai, “Simultaneous Screening of Zebrafish Larvae Cardiac and Respiratory Functions: A Microfluidic Multi-phenotypic Approach”, (Under Review).
3. A. Khalili, E. van Wijngaarden, G. Zoidl, P. Rezai, “Dopaminergic signaling regulates zebrafish larvae's response to electricity”, *Biotechnology J.,* 2100561, 2022.
4. A. Khalili, E. van Wijngaarden, Kh. Youssef, G. Zoidl, P. Rezai, “Designing Microfluidic Devices for Behavioral Screening of Multiple Zebrafish Larvae”, *Biotechnology J.,* e2100076, 2021.

5. A. Khalili, E. van Wijngaarden, G. Zoidl, P. Rezai, "Zebrafish Larva's Response to Electric Signal: Effects of Voltage, Current and Pulsation for Habituation Studies", *J. of Sensors and Actuators: A. Physical,* vol. 332, 113070, 2021.
6. A. Zabihihesari, A. Khalili, A. J. Hilliker, P. Rezai "Open Access Tool and Microfluidic Devices for Phenotypic Quantification of Heart Function of Intact Fruit Fly and Zebrafish Larvae", *J. of Computers in Biology and Medicine*, 104314, 2021.
7. A. Khalili, E. van Wijngaarden, G. Zoidl, P. Rezai, "Multi-Phenotypic and Bi-Directional Behavioral Screening of Zebrafish Larvae", *J. of Integrative Biology,* vol. 12, no. 8, pp. 211–220, 2020.
8. A. Khalili, A. R. Peimani, N. Safarian, Kh. Youssef, G. Zoidl, P. Rezai, "Phenotypic Chemical and Mutant Screening of Zebrafish Larvae using an On-Demand Response to Electric Stimulation", *J. of Integrative Biology,* vol. 11, no. 10, pp. 373–383, 2019.
9. A. Khalili, and P. Rezai, "Microfluidic Devices for Embryonic and Larval Zebrafish Studies," *J. of Briefings in Functional Genomics*, vol. 18, no. 6, pp. 419-432, 2019.

Conference Papers:

1. A. Khalili, E. van Wijngaarden, G. Zoidl and P. Rezai, "Simultaneous Screening of Zebrafish Larva Locomotor and Cardiac Functions: A Microfluidic Multi-Phenotypic Approach", Canadian Society for Mechanical Engineering International Congress (CSME 2022), June 2022, University of Alberta, Edmonton, Canada.
2. A. Khalili, E. van Wijngaarden, G. Zoidl and P. Rezai, "Electrically Induced Movement Patterns in Zebrafish Using Microfluidics and Computer-Aided Analysis", 25th

International Conference on Miniaturized Systems for Chemistry and Life Sciences (μTAS 2021), Oct. 2021, pp. 383-384.

3. A. Khalili, E. van Wijngaarden, Kh. Youssef, G. Zoidl and P. Rezai, "Microfluidic Device to Screen the Electric Induced Behavioral Response of Multiple Zebrafish Larvae", 24th International Conference on Miniaturized Systems for Chemistry and Life Sciences (μTAS 2020), Oct. 2020, pp. 897-898.
4. A. Khalili, E. van Wijngaarden, G. Zoidl and P. Rezai, "Habituation of Zebrafish Larvae to Electrical Stimulus", 24th International Conference on Miniaturized Systems for Chemistry and Life Sciences (μTAS 2020), Oct. 2020, pp. 915-916.
5. A. Khalili, E. van Wijngaarden, G. Zoidl and P. Rezai, "Multi-Phenotypic Movement and Cardiac Screening of Zebrafish Larvae Using Bidirectional Imaging in a Microfluidic Device", 23rd International Conference on Miniaturized Systems for Chemistry and Life Sciences (μTAS 2019), Basel, Switzerland, Oct. 2019, pp. 386-387.
6. A. Khalili, E. van Wijngaarden, G. Zoidl and P. Rezai, "A Microfluidic Device to Phenotypically Study Zebrafish Larvae's Electric-Induced Response", Zebrafish for Personalized/Precision Medicine Conference, Toronto, Canada, Sept. 2019.
7. A. Khalili, Kh. Youssef, G. Zoidl, and P. Rezai, "Neurotoxin-Induced Impairment and Neuroprotective-Based Recovery of Electrotactic Locomotion in Zebrafish Larvae as a Model for Neurobehavioral Studies in Parkinson's Disease", In Proc. the 22nd International Conference on Miniaturized Systems for Chemistry and Life Sciences (μTAS 2018), Kaohsiung, Taiwan, Nov. 2018, pp.1553-1556.
8. A. Khalili, Kh. Youssef, G. Zoidl, and P. Rezai, "Towards a Model for Parkinson's Disease: Neurodegeneration in Zebrafish Larvae Detected by a Microfluidic Electrotaxis

Assay", presented at 2018 Joint Ontario-on-a-Chip and TOeP Symposium, University of Toronto, Toronto, Canada, May 2018.

Other Publications outside the Scope of the Thesis:

1. A. Khalili, A. Zabihihesari, M. J. Farshchi-Heydari, A. Eilaghi, P. Rezai, "Developing a low-cost double-bridge microfluidic device for microplastics identification using electrical resistance measurements", (Under Preparation).